SIMULTANEOUS TRANSMISSION MODE

FOR THE   POLARIMETRIC WSR-88D

STATISTICAL BIASES AND STANDARD DEVIATIONS
OF POLARIMETRIC VARIABLES

Valery M. Melnikov

with contributions by **Dusan S. Zrnić**

**Cooperative Institute for Mesoscale Meteorological Studies,
University of Oklahoma. 1313 Haley Circle, Norman, OK, 73069**

June 2004

TABLE OF CONTENTS

Preamble

Over the years NSSL has been providing technical information to the National Weather Service. This exchange had many forms, from formal reports and algorithms to consultation and supply of radar data in real time to the Weather Services Forecast Office. After the decision to evolve its network of WSR-88Ds to keep pace with emerging knowledge and technology the NWS provided a spare WSR-88D to NSSL. Hence, NSSL became the principal NOAA Laboratory for evolutionary and revolutionary enhancements of weather radar science and technology. At that time (mid nineties) Doppler Radar and Remote Sensing Research group committed to document in report form all significant innovations, changes, and results deemed of special value for operational applications regardless whether such writing was formally required. This is the sixteenth report in the series since 1997. It deals with estimation of polarimetric variables. Although the formalism for developing statistical properties of these estimates is known, the results in literature are incomplete or not available for many aspect of simultaneous transmission and reception of horizontally and vertically (SHV) polarized waves. NSSL recommended this SHV mode of polarimetric diversity be implemented on the network. Hence the main goal herein is to present a complete statistical analysis of all the variables that will be available in the polarimetric WSR-88D (SHV mode). Further, means to rid some variables from noise bias are suggested and improvements in sensitivity are discussed. The later is desirable because it could bring back the sensitivity lost per channel due to power splitting.

The NWS's Office of Science and Technology provided funds which supported this work but did not require a formal write-up. Thus the report represents our continuous commitment to NWS and the evolution of WSR-88D science and technology.

May 2004 in Norman
Dusan S. Zrnic

Introduction

Simultaneous transmission and reception of electromagnetic waves with horizontal and vertical polarizations has been chosen as a main mode for polarimetric prototype for the WSR-88D networking weather radar (Doviak et al. 2000). We will refer to this mode as **SHV** , i.e., **S**imultaneous transmission and reception of **H**orizontally and **V**ertically polarized waves. In the mode, six basic radar moments are measured in each radar resolution volume: reflectivity (Z), Doppler velocity (v), spectrum width (σ_v), differential reflectivity (Z_{DR}), the differential phase (φ_{dp}), and the modulus of the copolar correlation coefficient (ρ_{co}). The first three values are the base radar moments in terms of products of the WSR-88D, the latter three are base polarimetric moments. An additional polarimetric variable, the specific differential phase (K_{dp}), is used in rainfall measurements and hail recognition and is calculated from φ_{dp}.

Radar signals reflected from weather objects are random. The estimates of the radar moments are calculated on a pulse train consisting of a given number of samples M. The statistical errors of the estimates are characterized with bias and standard deviations. Main properties of the base radar estimates are well known (Doviak and Zrnic 1993). The standard deviations of the polarimetric variables in SHV mode for strong signal-to-noise ratios are known also (see, e.g., Bringi and Chandrasekar, 2001). Here we consider noise influence on the radar moments and calculate biases of polarimetric variables. We also consider some new algorithms to calculate polarimetric moments that have no noise dependent bias.

Statistical nature of scattered radar signals and limited number of radar samples in estimations of the moments bias the estimates. Further the estimates are characterized with the standard deviations. Thus significant issues in polarimetric measurements are values of bias and standard deviation. Considering dependence of differential reflectivity on drop size distribution Sachidananda and Zrnic, 1985 concluded that Z_{DR} should be measured with an accuracy of 0.1 dB. Ryzhkov and Zrnic 1998a,b have found that the same accuracy is needed to distinguish between water droplets and snowflakes or crystals. We will consider 0.1 dB as a desired level of bias of the estimation of differential reflectivity. The standard deviation of 0.2 dB will be assumed for desired uncertainty for the estimate. This uncertainty can be reduced with additional spatial averaging. In contrast to the standard deviation, bias can not be reduced with spatial averaging so that it should be kept as low as possible. Using the relation between reflectivity in the H-channel, differential reflectivity, and the rain rate (R), proposed by Chandrasekar and Bringi 1988, i.e., $R = 2.397 \ 10^{-3} Z^{0.94} Z_{dr}^{-1.08}$, where R is in mm h^{-1}, Z is in mm^6 m^{-3} and Z_{dr} is in linear units, we can estimate the error in the rain rate ΔR when differential reflectivity is measured with the uncertainty of ΔZ_{dr} : $|\Delta R|=1.08 \ R \ |\Delta Z_{dr}|/ \ Z_{dr}$. For light and moderate rain with Z about 30 dBZ, $R = 10$ to 30 mm h^{-1}, $Z_{DR} = 1$ dB, and $\Delta Z_{DR} = 0.1$ dB, uncertainty of the rain rate is 10 to 30%. Illingworth (2004) has come to a similar conclusion that to measure light and moderate rain with the accuracy 10 to 15%, Z_{DR} should be measured within 0.1 dB.

Desired uncertainties of the differential phase measurements can be estimated from a relation between the rain rate and K_{dp} . Doviak and Zrnic, 1993 (Eq. (8.31a)) give the following dependence: $R = 37.5 K_{dp}^{0.866}$, where R is in mm h^{-1} and K_{dp} is in deg km^{-1}, and the wavelength is 10 cm. From the latter, the fractional errors are:

$\Delta R / R = 0.866 \Delta K_{dp} / K_{dp}$. For moderate rain of 30 mm h^{-1}, the accuracy of the rain rate estimate of 10%, and $L = 2$ km, using relation (3.7) in this report we obtain needed uncertainty of the differential phase: $\Delta \varphi_{dp} = 2^{\circ}$. We consider this uncertainty as a desired level for the standard deviation of the measurements. Bias of the estimate should be less than half of this error, i.e., 1°.

Desired level of errors in the modulus of the correlation coefficient, ρ_{co}, measurements we set at 0.01. Simulations for different parameters of drop size distribution show that for rain, ρ_{co} is larger than 0.99 (Sachidananda and Zrnic, 1985). Less value can be measured in the presence of snowflakes, hail, or graupel, therefore we consider 0.01 as a desired level for the standard deviation of the ρ_{co} estimate. Bias of the estimate should be twice as low, i.e., 0.05. Desired levels of biases and the standard deviations (SD) of the polarimetric moments are presented in Table 1.

Table 1. Desired biases and standard deviations of estimations
of the polarimetric variables.

Z_{DR}		φ_{dp}		ρ_{co}	
Bias dB	SD dB	Bias deg	SD deg	Bias	SD
0.1	0.2	1	2	0.005	0.01

This report considers the following. a) The SHV mode with two receivers each of which has different noise levels. b) Measurement biases. c) Possibilities to utilize polarimetric observations, increase of radar sensitivity, improvements to the Doppler velocity estimates using estimates from the two polarimetric channels, and some schemes to reduce the effects of white noise on estimates. d) Effects of additional thermal noise that comes to radar from precipitation and the ground.

For convenience and completeness, we present here all expressions used in calculations of biases and the standard deviations of the estimates. Cumbersome expressions are placed in the appendixes.

1. Sources of statistical uncertainties of the estimates

For a given radar volume a radar signal processor produces the complex voltage $e(t_m)$ at time t_m corresponding to m^{th} received sample and $m = 1, 2,.. M$. All radar moments are calculated using these voltages in H and V channels, i.e., $e_m^{(h)}$ and $e_m^{(v)}$, where m designates the time moment. These voltages consist of weather signal and noise:

$$e_m^{(h)} = e_m^{(hs)} + e_m^{(hn)} \quad , \tag{1.1a}$$

$$e_m^{(v)} = e_m^{(vs)} + e_m^{(vn)} \quad , \tag{1.1b}$$

where superscripts n and s denote noise and signal. In the SHV mode, the polarimetric moments are calculated using the estimates of the powers in the channels and the copolar cross correlation function:

$$\hat{P}_h = \frac{1}{M} \sum_{m=1}^{M} e_m^{(h)} e_m^{(h)*} ,$$ (1.2a)

$$\hat{P}_v = \frac{1}{M} \sum_{m=1}^{M} e_m^{(v)} e_m^{(v)*} ,$$ (1.2b)

$$\hat{R}_{co} = \frac{1}{M} \sum_{m=1}^{M} e_m^{(h)} e_m^{(v)*} ,$$ (1.2c)

where ^ denotes M-sample estimate and * designates complex conjugate. It follows from (1.2) that statistical fluctuations of signals and noise are two sources of measurement errors.

The mean powers P_h and P_v and the mean correlation R_{co} in the channels are

$$P_h =< \hat{P}_h >= \frac{1}{M} \sum_{m=1}^{M} < e_m^{(h)} e_m^{(h)*} >= S_h + N_h ,$$ (1.3a)

$$P_v =< \hat{P}_v >= \frac{1}{M} \sum_{m=1}^{M} < e_m^{(v)} e_m^{(v)*} >= S_v + N_v ,$$ (1.3b)

$$R_{co} =< \hat{R}_{co} >= \frac{1}{M} \sum_{m=1}^{M} < e_m^{(h)} e_m^{(v)*} > ,$$ (1.3c)

where S_h , S_v and N_h , N_v are mean signal powers and noise powers in the channels and angular brackets denote ensemble average. In (1.3), we assumed that weather signals and noise in either channel are uncorrelated processes and noise samples in the H and V channels are not correlated. The powers S_h and S_v of weather signals are estimated as

$$\hat{S}_h = \hat{P}_h - N_h ,$$ (1.4a)
$$\hat{S}_v = \hat{P}_v - N_v .$$ (1.4b)

Mean noise power is usually calculated before data collection and from a much larger number of samples than available during the dwell time. That's why uncertainties in measurements of S_h and S_v depend on (a) statistical fluctuations of weather signals and (b) deviation of the estimate of noise powers from theirs mean values. Statistical fluctuations of radar signal produce variances of the estimates. Because the polarimetric parameters are calculated from nonlinear relations, these fluctuations produce biases of estimates as well. Additional bias and variances are caused by white noise and these contributions increase with decreasing of signal-to-noise ratio.

The following three functions are required for estimating polarimetric variables. The correlation functions in H and V channels and the temporal cross correlation function. Using the notations by Doviak and Zrnic (1993) we write

$$R_h(mT) = S_h \rho^{(h)}(mT) \exp(j\pi v_h m / v_a) + N_h \delta_{m0},$$ (1.5a)

$$R_v(mT) = S_v \rho^{(v)}(mT) \exp(j\pi v_v m / v_a) + N_v \delta_{m0},$$ (1.5b)

$$R_{co}(mT) = (S_h S_v)^{1/2} \rho_{co} \, \rho^{(hv)}(mT) \exp(j\pi v_{hv} m / v_a + j\varphi_{dp}),$$ (1.5c)

where the superscripts h, v, and hv mean that the parameters are calculated using the pulse train in H, V, or both H&V channels, δ_{mn} is 1 for $m = n$, and 0 otherwise, T is the pulse repetition interval ($T = 1/\text{PRF}$), v_a is the unambiguous velocity ($v_a = \lambda/4T$, where λ is the wavelength), ρ_{co} is the copolar correlation coefficient between H and V waves at same time, φ_{dp} is the differential phase, $\rho(mT)$ is the temporal correlation coefficient, m $=1,2,...M$, and j is imaginary one. Here we use ρ_{co} for the modulus of the copolar coefficient (as in e.g., Bringi and Chandrasekar 2001) instead of ρ_{hv} used in many publications to avoid confusion with calculations of the coefficient using H and V samples. The modulus of the copolar correlation coefficient ρ_{co} can be determined from (1.5c):

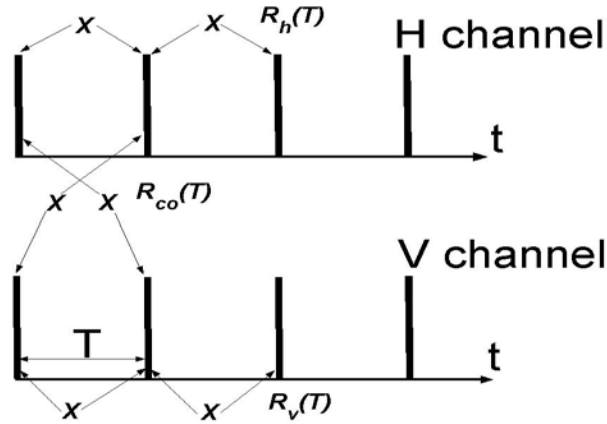$$\rho_{co} = |R_{co}(0)| / (S_h S_v)^{1/2}.$$ (1.5d)

Fig. 1.1. Pulse trains in the H and V channels and pulse pairs used in the calculations of the correlation functions in either channel and using both channels.

Fig. 1.1 shows a scheme for calculations of the correlation functions in H and V channels, i.e., $R_h(T)$ and $R_v(T)$ and also how H and V samples are used to calculate $R_{co}(T)$. Note that the number of samples in calculations for the single channel is M-1 whereas the number of samples in $R_{co}(T)$ calculations is $2(M-1)$.

Generally, the Doppler velocities v_h, v_v, v_{hv}, and the correlation coefficients $\rho^{(h)}(mT)$, $\rho^{(v)}(mT)$, and $\rho^{(hv)}(mT)$ could be different but if they are, the differences between them are very small and can be ignored in calculations of the statistical properties of estimates (Sachidanada and Zrnic 1985, 1986; Unal et al. 2001; Bringi and Chandrasekar 2001). Here we assume the velocities and the temporal correlation coefficients to be equal, i.e., $v = v_h = v_v = v_{hv}$ and $\rho(mT) = \rho^{(h)}(mT) = \rho^{(v)}(mT) = \rho^{(hv)}(mT)$.

For Gaussian spectra $\rho(mT)$ is given by

$$\rho(mT) = \exp[-(\pi\sigma_v m / v_a)^2 / 2]. \tag{1.6a}$$

It is convenient to normalize the spectrum width to v_a (note that Doviak and Zrnic 1993, normalize the spectrum width to $2\,v_a$) so that (1.6a) can be written using normalized spectrum width as:

$$\rho(m) = \exp[-(\pi\sigma_{vn} m)^2 / 2], \tag{1.6b}$$

$$\sigma_{vn} = \sigma_v / v_a, \qquad 0 \le \sigma_{vn} \le 1. \tag{1.6c}$$

$$v_n = v / v_a, \qquad -1 \le v_n \le 1. \tag{1.6c}$$

In equations (1.3) and (1.4), the noise levels are considered to be constant. In reality, noise depends on the temperature of the receivers and external noise which in turn depends on antenna elevation and precipitation along the radar beam. We consider three sources of changes in noise: a) additional thermal radiation that comes from the ground and precipitation, b) nonthermal radiation that comes from electrically active clouds, and c) fluctuations of the system gain.

It is well known, that heavy precipitation contributes additional thermal noise to the antenna. At low elevations, the antenna intercepts thermal radiation from the ground which contributes to noise. The net effect of all these factors is that standard procedures for estimating noise level are inadequate for instantaneous bias compensation in the 0,1-lag PPL estimator at low and moderate SNR. On the WSR-88D, noise is measured at highest elevations where radiation contribution from precipitation and ground is insignificant. Then the measured noise power is applied to low elevation observations where weather echo noise exists and the antenna intercepts thermal noise of the ground. Additional noise at lower elevations will bias the polarimetric parameters unless it is correctly estimated which is hard to do.

Fig. 1.2 shows noise as a function of the elevation angle in clear air. We see that the worm ground contributes to noise at low elevations. The total increase of noise is about 0.8 dB. We can estimate maximal increase of thermal noise for the WSR-88D with the system noise power of P_{sys} = -112.5 dBm (KOUN, measured on February 11, 2004),

i.e., $P_{sys} = 5.6 \ 10^{-15}$ W. System noise includes noise generated by the system itself plus environmental noise that comes to the antenna at the antenna park position, i.e., when the elevation is 22°. For S-band radar sounding heavy precipitation, the differential phase can exceed 200° in which case attenuation is over 8 dB (e.g., Ryzhkov and Zrnic 1995). In terms of temperature, this is 0.84 times the physical temperature of precipitation T_p. For $T_p = 290^o$ K (17° C) and the same ground temperature, the environmental power contribution is $P_e = $ k $(0.84 \ T_p)\Delta$f, where k is Boltzmann's constant (k $= 1.38 \ 10^{-23}$ J/K) and Δf is the receiver's bandwidth. For the short pulse mode of the WSR-88D, Δf $= 6.0 \ 10^5$ Hz. Using these parameters we obtain $P_e = 2.0 \ 10^{-15}$ W, i.e., $P_e/P_{sys} = 0.36$. For the data in Fig. 1.2, $P_e/P_{sys} = 0.2$. In our calculations of thermal noise influences we will consider this ratio to be in the interval 0 to 0.4. For more sensitive radar receivers, this ratio can be larger. Variations of P_e/P_{sys} for X-band radars can be found in Fabry 2001.
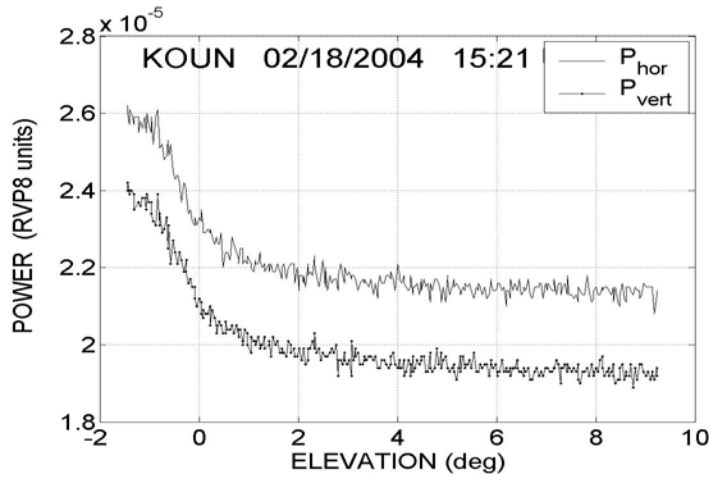

Fig.1.2. Elevation dependence of system noise in clear air
  for the horizontal and vertical channels of the WSR-88D
  KOUN.

In the presence of additional noise N_a, equations (1.4) are changed. If P_h is still the power of weather signal and internal apparatus noise, i.e., $P_h = S_h + N_h$, then the biased total powers in the channels are measured and the estimates of the power of weather signal are

$$\hat{S}_h = \hat{P}_h - N_h + N_a ,$$ (1.7a)

$$\hat{S}_v = \hat{P}_v - N_v + N_a .$$ (1.7b)

which are biased by additional thermal noise.

In general, additional noise in H and V channels can be different because the additional thermal radiation for the two channels may be different. For our assessment, we will consider N_a equal in the H and V channels.

Now we consider noise that comes to a radar antenna from electrically active clouds. Thunderstorms emit radiation in a broad frequency band including S-band. This

radiation can be intercepted by the antenna and results in excessive noise. Fig. 1.3 presents two consecutive reflectivity profiles through heavy thunderstorm where the noise skirt has not been removed by thresholding. Time interval between beginnings of the records is 263 ms. The number of samples in reflectivity calculation is 256 and noise is observed beyond 90 km. One can see a jump of about 10 dB of the noise level. Fig. 1.4 presents data when the transmitter was off and only noise was collected. Again, we see a jump of about 10 dB in the noise level due to lightning discharges. Such large noise jumps are less frequent than smaller ones. This noise is not thermal but because of its broad band it can be considered as white noise for a radar receiver. We will see in the next sections that a small increase of 1 dB in noise has significant impact on estimates of differential reflectivity and correlation coefficient.
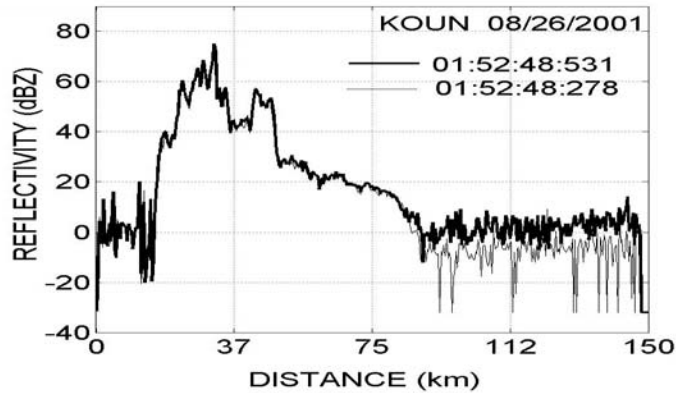

Fig. 1.3. Reflectivity along a radial. Azimuth is 35.2^o and the elevation is 8.6^o. UTC time is shown in a format of hour:minute:second:millisecond of the beginning of the records and the date is Aug 26, 2001. The data was obtained with the RVP7 processor.
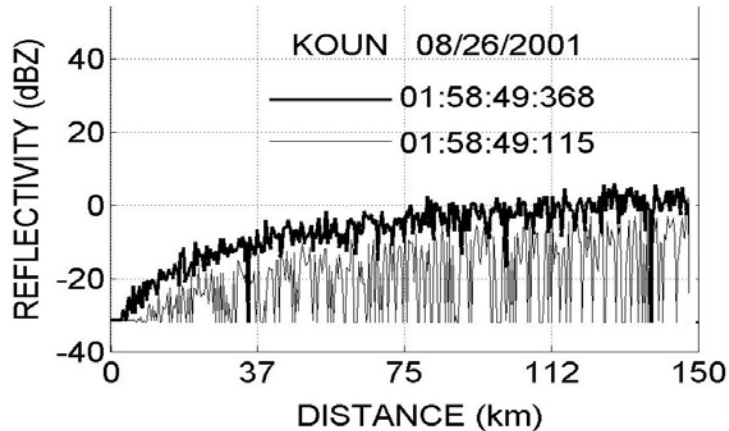

Fig. 1.4. Noise profiles along a radial. Azimuth is 35.2^o and the elevation is 10.1^o. The radar transmitter was off so that only noise was recorded. Noise increase over distance is due to multiplication with range squared which is used in reflectivity calculations. The data was recorded with the RVP7 processor.

10

Sometimes on WSR-88D KOUN, noise power exhibits instability as seen in Fig. 1.5. These power estimates were obtained from 400 range gates (bins) simultaneously using 128 samples at any one bin. The antenna was in the park position. The 400 bins were split into four parts with 100 bins in each. The mean power was calculated using 100 bins and 128 samples so that four estimates were obtained. This procedure was conducted over time during approximately 50 seconds to generate four curves in Fig 1.5. For random signals there would be no resemblance between these four curves and that is seen in the figure for the V channel. In contrast, the four curves for the H-channel exhibit temporary correlation which suggests some artifact. The time scale of this instability in the H channel is of few seconds. Because this change is within 1 dB of the correct mean noise power it is not usually recognized as malfunction by the radar monitoring systems.
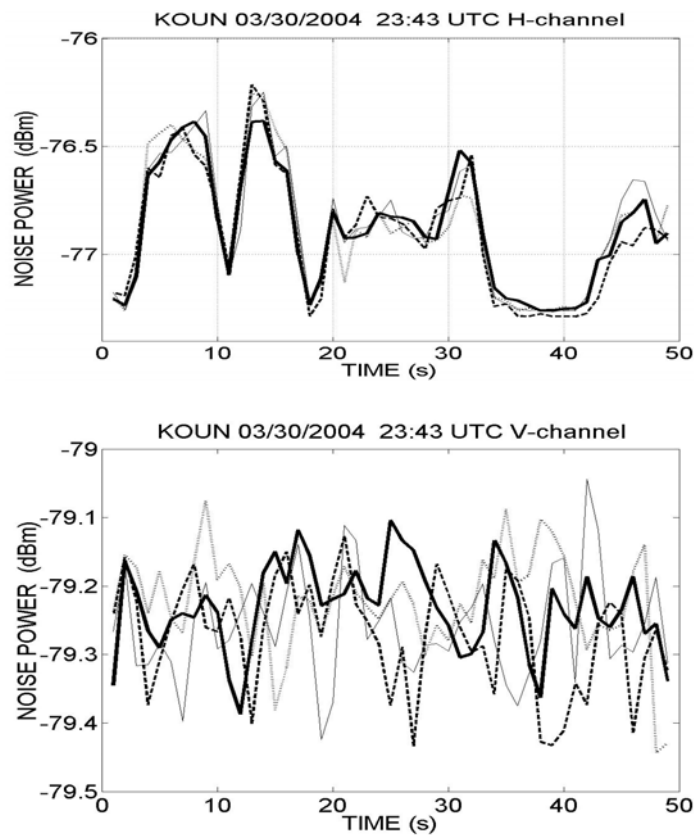

Fig. 1.5. Noise power records in the H (top) and V (bottom) channels on KOUN. The four curves correspond to the mean powers estimated in 100 consecutive bins along a radial. The total number of bins is 400. The data was obtained with the RVP8 processor.

In the next three sections, we present biases and variances for three main polarimetric variables calculated for the SHV mode: differential reflectivity, differential phase, and the copolar correlation coefficient. We do not consider here effects of wave propagation; we focus on uncertainties that do not depend on a length of propagation

path. Considerations of the propagation effects for S-band radar can be found in e.g., Bringi and Chandrasekar 2001, Sachidananda and Zrnic 1985, Doviak et. al. 2000, Torlaschi and Zawadzki 2003. The SHV mode has also some intrinsic errors of measurements due to coupling of the H and V signals, i.e., due to depolarization when some portion of energy at incident horizontal polarization couples into vertically polarized wave and vice versa (Doviak et. al. 2000).

2. Differential reflectivity Z_{DR}

The estimation of differential reflectivity in the SHV mode is calculated as logarithm of power ratio of weather signals at H and V polarizations:

$$\hat{Z}_{DR} = 10 \log \left(\frac{\hat{P}_h - N_h}{\hat{P}_v - N_v} \right). \tag{2.1}$$

The base of logarithm is 10. The estimates of powers in the H and V channels are calculated and then differential reflectivity in dB is obtained according to (2.1). On radars with logarithmic receivers, differential reflectivity is estimated differently and corresponding statistics can be found in Chandrasekar et al. 1986. To calculate bias and the variance of (2.1), we consider the ratio Z_{dr} of the powers which is in the parentheses in (2.1), i.e.,

$$\hat{Z}_{dr} = \frac{\hat{P}_h - N_h}{\hat{P}_v - N_v}. \tag{2.2}$$

Assuming small perturbations, i.e., $|\delta P_h| \ll P_h$, and $|\delta P_v| \ll P_v$, bias and the variance of differential reflectivity can be calculated (see, e.g., Bringi and Chandrasekar 2001, Appendix 5). The perturbations of power in the H and V channel can be written as

$$\hat{\delta P_h} = \hat{P}_h - P_h, \tag{2.3a}$$

$$\hat{\delta P_v} = \hat{P}_v - P_v. \tag{2.3b}$$

2.1. Bias

It is shown in the introduction, that it is desirable to have bias of differential reflectivity below 0.1 dB. As a rule, the standard deviations of the estimate will exceed this threshold, but it will be statistical fluctuations and can be reduced by additional spatial averaging. Bias cannot be reduced with additional smoothing so that it should be kept as low as possible. Assuming small deviations of the power estimates and substituting (2.3) into (2.2) we obtain the following bias

$$BIAS(Z_{dr}) = <\hat{Z}_{dr} - Z_{dr}> = <\frac{S_h + \delta\hat{P}_h}{S_v + \delta\hat{P}_v}> - \frac{S_h}{S_v} = Z_{dr}\left[\frac{<\delta\hat{P}_v^2>}{S_v^2} - \frac{<\delta\hat{P}_h\delta\hat{P}_v>}{S_h S_v}\right]. \qquad (2.4)$$

where Z_{dr} is the mean differential reflectivity. The variance of the power perturbations and the covariance of the perturbations are calculated in Appendix A. Using (A8) and (A12) we obtain

$$\frac{1}{Z_{dr}}BIAS(Z_{dr}) = \frac{1 + 2SNR_v}{M\ SNR_v^2} + \frac{1 - \rho_{co}^2}{M_I}, \qquad (2.5)$$

where $SNR_v = S_v / N_v$ is signal-to-noise ratio in the vertical channel, M_I is the number of independent samples (see (A7) in Appendix A). It is seen from (2.5) that the bias is positive and consists of two contributions: the first one depends on noise in the vertical channel and the second contribution depends on the spectrum width of weather signal and ρ_{co}. From (2.5), we can write bias of Z_{DR} expressed in dB as

$$BIAS(Z_{DR}) = <10\log(\hat{Z}_{dr}) - 10\log(Z_{dr})> = 10\log\left(\frac{Z_{dr} + \delta\hat{Z}_{dr}}{<Z_{dr}>}\right) =$$

$$10\log\left(1 + \frac{1}{Z_{dr}}BIAS(Z_{dr})\right) = 10\log\left(1 + \frac{1 + 2SNR_v}{M\ SNR_v^2} + \frac{1 - \rho_{co}^2}{M_I}\right).$$

A sum of the second and third terms in the parenthesis of the latter expression is small in comparison with 1, so that we can write

$$BIAS(Z_{DR}) = \frac{10}{\ln 10}\left(\frac{1 + 2SNR_v}{M\ SNR_v^2} + \frac{1 - \rho_{co}^2}{M_I}\right). \qquad (2.6)$$

We will consider signal-to-noise ratios to be more than one, i.e., more than 0 dB. The noise contribution to the bias is shown in Fig. 2.1 for the number of samples of 32, 48, and 64. Desired accuracy of Z_{DR} measurements is 0.1 dB. From the figure, we see that noise dependent bias is less than 0.1 dB if $SNR_v \geq 4$ dB and $M \geq 48$. Using approximation (A10) for the independent number of samples, (2.6) can be presented in a form that clearly shows its dependence on the total number of samples, SNR_v, ρ_{co}, and spectrum width σ_v:

$$BIAS(Z_{DR}) = \frac{10}{M\ln 10}\left(\frac{1 + 2SNR_v}{SNR_v^2} + \frac{0.56(1 - \rho_{co}^2)}{\sigma_{vn}}\right) \qquad (2.7)$$

$$0.04 \leq \sigma_{vn} \leq 0.60.$$

The latter inequality determines the limits where M_I is proportional to the spectrum width (see Appendix A).

The second contribution to the bias depends on ρ_{co} and the spectrum width. Fig. 2.2 shows this contribution, i.e., $(10/\ln 10)1.13(1-\rho_{co}^2)/M\,\sigma_{vn}$ for $M = 64$. For rain, ρ_{co} is usually more than 0.95. We see that bias less than 0.1 dB can be achieved if the spectrum width is wider than 1 m s^{-1}, i.e., almost for all weather cases. For lower ρ_{co} (for instance in the melting layer or in regions with hail), this bias may exceed the desired level of 0.1 dB.

The total bias of differential reflectivity is shown in Fig. 2.3 for two signal-to-noise ratios and three correlation coefficients. One can see that bias less than 0.1 dB can be achieved in rain ($\rho_{co} \geq 0.99$) for spectrum widths wider than 1 m s^{-1}. The number of samples 17 as in the bottom Fig. 2.3 corresponds to the surveillance scan of the WSR-88D (PRF = 321 Hz).
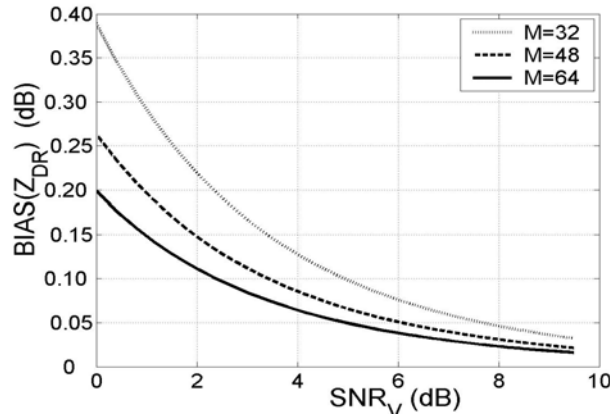

Fig.2.1. Noise dependent bias vs. signal-to-noise ratio
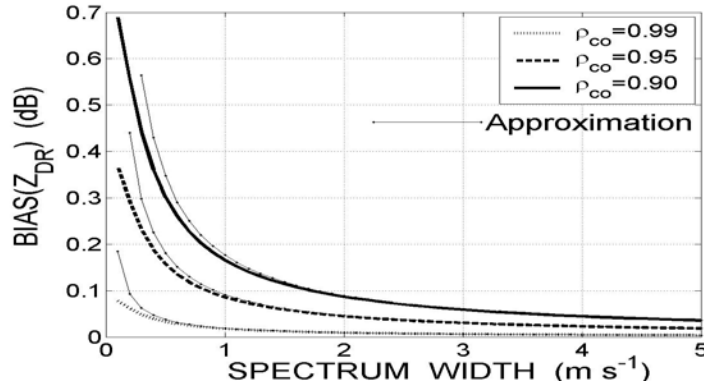in the V channel, i.e., the first term in (2.6).

Fig. 2.2. Spectrum width dependent bias of differential reflectivity.
$M = 64$. Approximation (2.7) is shown with the dots
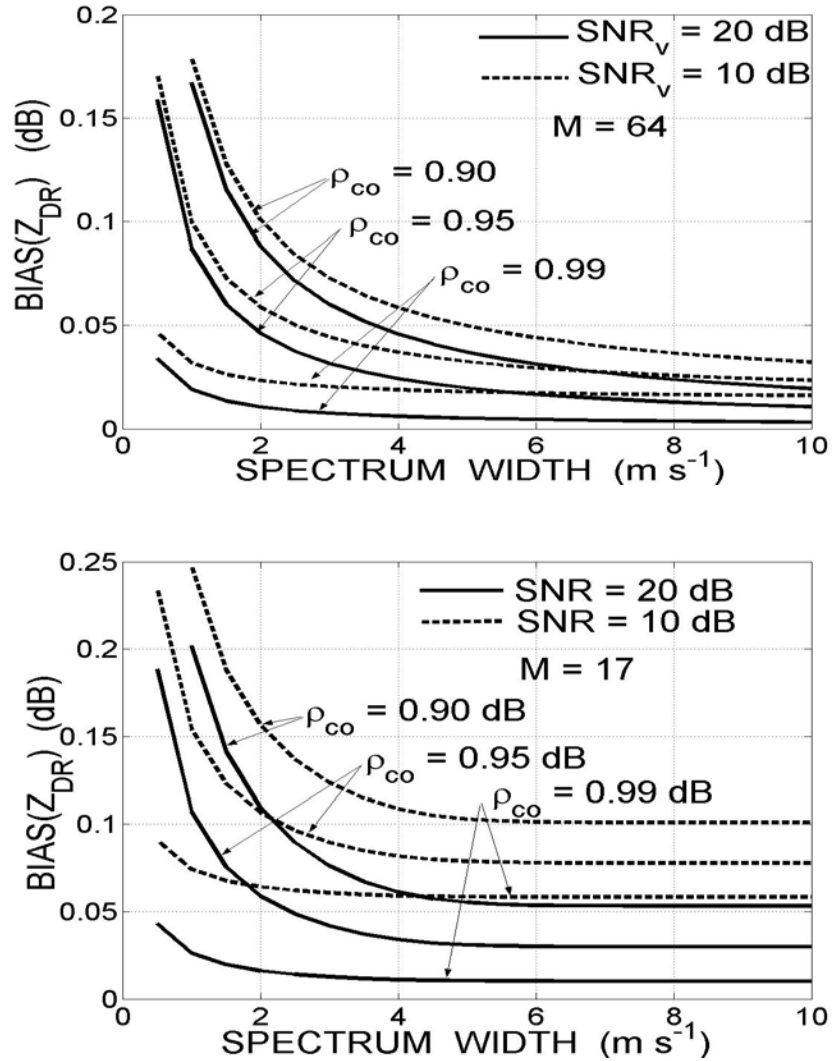connected with the thin solid lines.

14

Fig. 2.3. Bias of differential reflectivity as a function of the spectrum with for two SNR and ρ_{co} indicated. M=64, PRF = 1000 Hz (top figure) and M=17, PRF = 321 HZ (bottom).

Now consider bias that originates from additional thermal noise N_a (see (1.7) and discussions following that equation). Measured differential reflectivity in presence of the additional noise is

$$Z'_{DR} = 10\log\left(\frac{S_h + N_a}{S_v + N_a}\right),$$

whereas the actual differential reflectivity is $Z_{DR} = 10\log(S_h/S_v)$. Assuming for evaluation purposes that the additional noise is same in H and V radar channels, corresponding bias is

$$Bias\ (Z^{'}_{DR}) = Z^{'}_{DR} - Z_{DR} = 10\ \log\left(\frac{1 + N_a / S_h}{1 + N_a / S_v}\right) = 10\ \log\left(\frac{1 + N_a / N_h SNR_h}{1 + N_a / N_v SNR_v}\right) =$$

$$= 10\log\left(\frac{1 + N_a / N_h Z_{dr} SNR_v}{1 + N_a / N_v SNR_v}\right). \tag{2.8}$$

In Fig. 2.4, this bias is shown as a function of SNR_v for two noise ratios N_a / N. For sufficient large SNR, equation (2.8) simplifies to

$$Bias(Z^{'}_{DR}) \approx -\frac{10}{\ln 10}\frac{N_a}{N}\frac{1}{SNR_v}\frac{Z_{dr} - 1}{Z_{dr}}(dB).$$

For $Z_{dr} > 1$ this bias is negative and proportional to the additional noise. One can see from Fig. 2.4 that if N_a/N is 0.4 this bias is less than 0.1 dB only for SNR more than 13 dB.
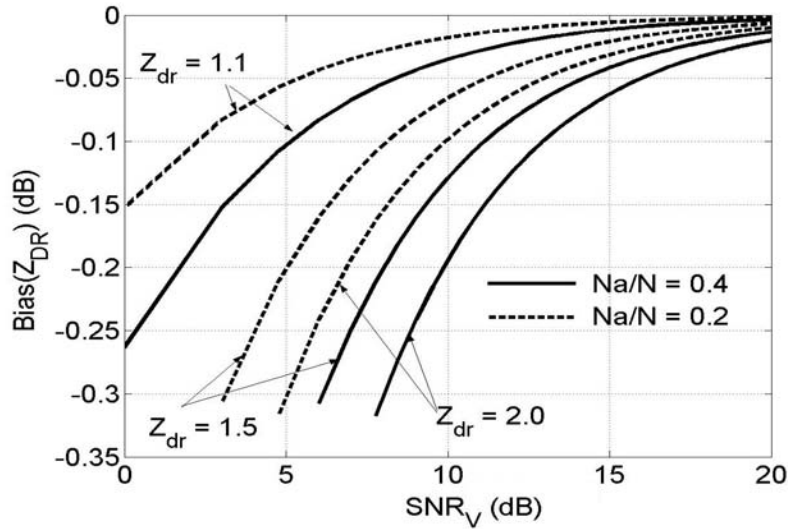

Fig. 2.4. Bias of the Z_{DR} estimates from additional thermal noise for two N_a/N ratios and Z_{dr} indicated.

Because additional thermal noise decreases signal-to-noise ratios in the channels there is statistical positive bias that was considered in the section earlier (see (2.6)), but for $Na/N < 0.5$ this bias is much less than bias (2.8). Thus, additional white noise biases the estimate as described in (2.8).

2.2. *Standard deviation*

For alternate polarization of transmitted pulses, statistics of the differential reflectivity has been studied by Bringi et al. 1983, Chandrasekar and Bringi 1988, Bringi and Chandrasekar 2001. For the SHV mode, the standard deviation of the Z_{DR} estimates has been studied by Sachidananda and Zrnic (1985).

In the SHV mode, the estimation of differential reflectivity expressed as a ratio of the powers is represented by (2.2) which can be represented using (2.3) as

$$\hat{Z}_{dr} = \frac{S_h + \delta\hat{P}_h}{S_v + \delta\hat{P}_v} \approx \frac{S_h}{S_v}\left(1 + \frac{\delta\hat{P}_h}{S_h} - \frac{\delta\hat{P}_v}{S_v}\right).$$

The perturbation of the estimate is

$$\delta\hat{Z}_{dr} = \hat{Z}_{dr} - Z_{dr} \approx \frac{S_h}{S_v}\left(\frac{\delta\hat{P}_h}{S_h} - \frac{\delta\hat{P}_v}{S_v}\right).$$

The variance of this perturbation is

$$<\delta^2\hat{Z}_{dr}> \approx \frac{S_h^2}{S_v^2}\left(\frac{<\delta\hat{P}_h^2>}{S_h^2} + \frac{<\delta\hat{P}_v^2>}{S_v^2} - \frac{2<\delta\hat{P}_h\delta\hat{P}_v>}{S_h S_v}\right). \tag{2.9}$$

Using equations (A8) and (A12) from the Appendix A, we obtain

$$\frac{<\delta^2 Z_{dr}>}{Z_{dr}^{\ 2}} = \frac{1 + 2SNR_h}{M\ SNR_h^2} + \frac{1 + 2SNR_v}{M\ SNR_v^2} + \frac{2(1 - \rho_{co}^2)}{M_I}. \tag{2.10}$$

We see the fractional variance consists of two terms: the noise contribution, i.e., the first two addends in (2.10) and the spectrum width contribution, i.e., the third addend in (2.10). Equation (2.10) is in accord with equation (7) by Sachidananda and Zrnic (1985) if in (7) we set $N_c = 0$, where the latter is some noise which is common to the H and V channels. In the SHV mode of the WSR-88D, radar has two separate receivers in the channels so that the common noise is absent. For high *SNR*, (2.10) is in accord with equation (6.141) by Bringi and Chandrasekar (2001).

The perturbation of Z_{DR} expressed in dB is obtained as

$$\delta\hat{Z}_{DR} = \hat{Z}_{DR} - Z_{DR} = 10\log\frac{\hat{Z}_{dr}}{Z_{dr}} = 10\log\frac{Z_{dr} + \delta\hat{Z}_{dr}}{Z_{dr}} = 10\log\left(1 + \frac{\delta\hat{Z}_{dr}}{Z_{dr}}\right)$$

So the standard deviation of the estimate can be written as

17

$$SD(Z_{DR}) \approx 10 \log\left(1 + \frac{<|\delta\hat{Z}_{dr}|>}{Z_{dr}}\right) \approx \frac{10}{\ln 10} \frac{<|\delta\hat{Z}_{dr}|>}{Z_{dr}} \text{ (dB)}$$

In the latter equation, we can use (2.10) for the modulus of the deviation, then

$$SD(Z_{DR}) = \frac{10}{\ln 10}\left[\frac{1 + 2SNR_h}{M \ SNR_h^2} + \frac{1 + 2SNR_v}{M \ SNR_v^2} + \frac{2(1 - \rho_{co}^2)}{M_I}\right]^{1/2} \text{ (dB)}. \qquad (2.11)$$

Using approximation (A9) for M_I, we obtain a simple expression for the standard deviation showing explicit dependence on SNR, M, ρ_{co}, and σ_v :

$$SD(Z_{DR}) = \frac{10}{M^{1/2} \ln 10}\left[\frac{1 + 2SNR_h}{SNR_h^2} + \frac{1 + 2SNR_v}{SNR_v^2} + \frac{1.13(1 - \rho_{co}^2)}{\sigma_{vn}}\right]^{1/2} \text{ (dB)}. \ (2.12)$$

$$0.04 \leq \sigma_{vn} \leq 0.60$$

It should be noted that for equal noise levels in the channels, the SNR_h and SNR_v are different due to differential reflectivity. For instance for positive Z_{DR} , weather signal in the V channel is lower than in the H channel and SNR_h is larger than SNR_v. In Fig 2.4, the noise contribution to the standard deviation is shown for equal noise levels in the channels and Z_{DR} of 0 and 3 dB. We see that the desired level of 0.2 dB accuracy can be achieved only for SNR > 15 dB.
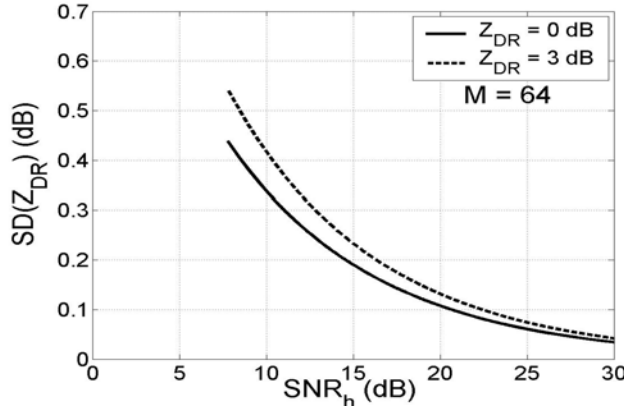

Fig. 2.4. Noise contribution to the standard deviation of Z_{DR}
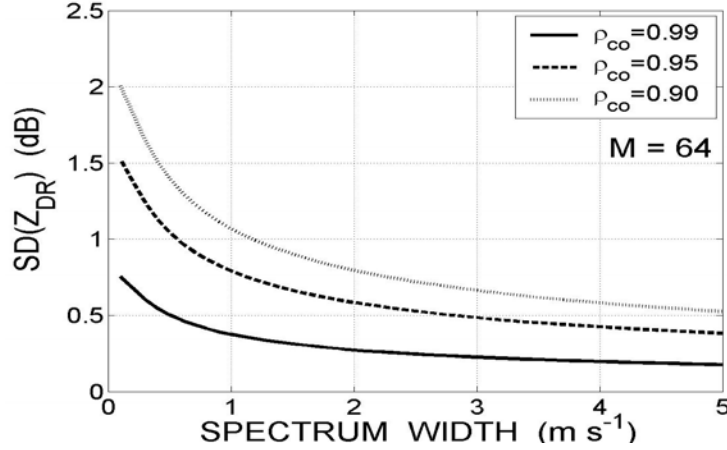for Z_{DR} indicated and $M = 64$.

Fig. 2.5. Spectrum width contribution to the standard deviation
of Z_{DR} for indicated ρ_{co}.

The spectrum width contribution to the standard deviation of Z_{DR} i.e., the third addend in the square brackets in (2.11) or (2.12) is shown in Fig. 2.5. We see that for $\rho_{co} = 0.99$ the statistical uncertainties of measurements are higher than the desired level of 0.2 dB. For usual spectral widths 2 to 6 m s^{-1}, the standard deviation is between 0.2 and 0.3 dB. For lower ρ_{co} the statistical uncertainties are larger.

For the SHV mode in absence of noise, Bringi and Chandrasekar (2001, section 6.52) give the following expression for the standard deviation of Z_{DR}

$$SD(Z_{DR}) = 10 \log \left\{ 1 + \left[\frac{2(1 - \rho_{co}^2)}{M_I} \right]^{1/2} \right\}.$$

which equals to (2.11) if the noise terms in (2.11) are omitted and $\log(1 + x)$ is replaced with $x/\ln 10$ for small x.

Fig. 2.6 presents total statistical uncertainties of Z_{DR} measurements for $Z_{DR} = 3$ dB. We see that it is hard to achieve accuracy of 0.2 dB even for strong signals with SNR > 20 dB and the usual spectral widths of 1 to 6 m s^{-1} ($\rho_{co} \geq 0.99$).

To analyze the influence of the additional thermal noise (1.7) on the standard deviations of the Z_{DR} estimates, we can use (2.11) or (2.12) with N_h and N_v substituted with $N_h + N_a$ and $N_v + N_a$ correspondingly. The standard deviations of the estimated are shown in Fig. 2.7 for two values of N_a: $N_a = 0$ and $N_a/N = 0.4$. One can see that this influence is small for signal-to-noise ratios more than 10 dB.
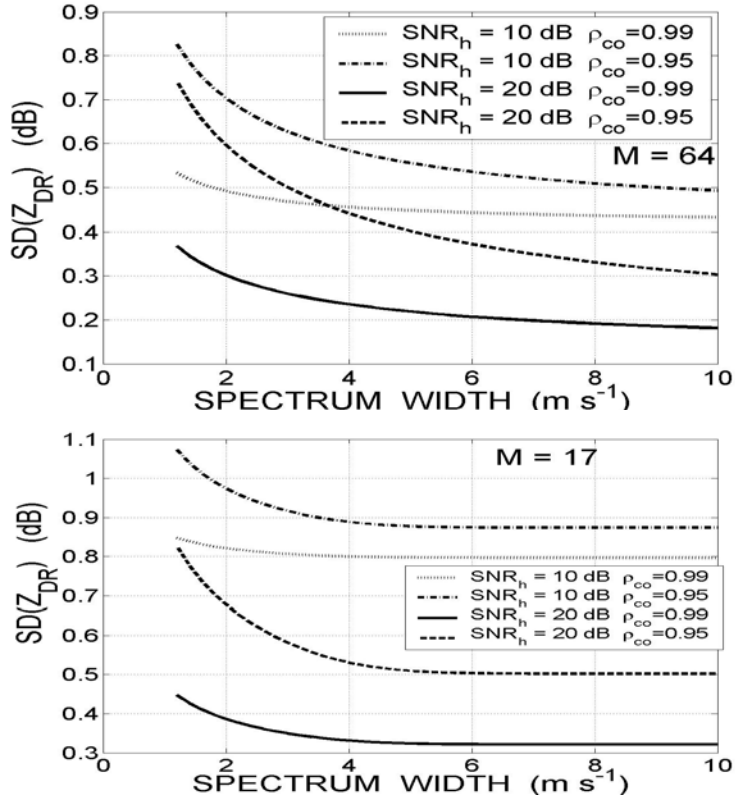
19

Fig. 2.6. Standard deviations of Z_{DR} for SNR_h of 10 and 20 dB, $Z_{DR} = 3$ dB and for indicated ρ_{co} . $M = 64$, PRF $= 1000$ Hz (top) and M $= 17$, PRF $= 321$ Hz (bottom).
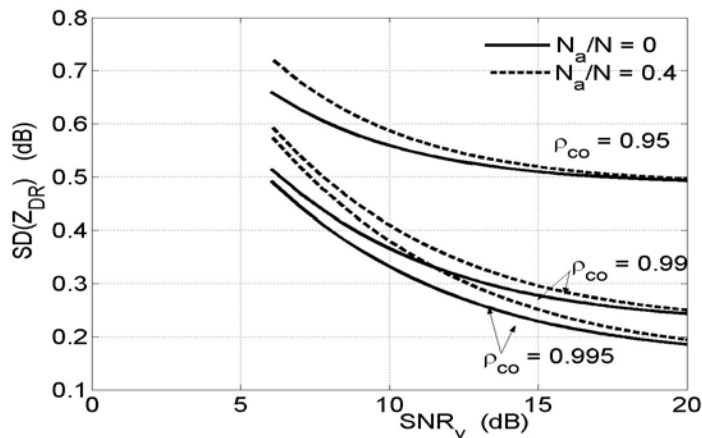

Fig. 2.7. Standard deviation of Z_{DR} due to additional thermal noise N_a for S-band radar, $\sigma_v = 3$ m s^{-1}, $Z_{DR} = 3$ dB, and $M = 64$.

20

The perturbation analysis exploded in the calculations has limits of applicability. Differential reflectivity is expressed as a ratio of powers, i.e., as a nonlinear relation and the perturbation analysis was applied to calculate the biases and the standard deviations. Conditions of applicability of the analysis can be expressed as

$$\begin{aligned} &\triangleleft |\delta P_h| \triangleright / S_h \ll 1, \\ &\triangleleft |\delta P_v| \triangleright / S_v \ll 1, \\ &\triangleleft |\delta P_h \delta P_v| \triangleright / (S_h S_v)^{1/2} \ll 1. \end{aligned} \tag{2.13}$$

The ratios on the right hand sides of (2.13) were used in Z_{dr} calculations (2.10) so that these conditions can be replaced with the following one:

$$SD(Z_{dr})/Z_{dr} \ll 1.$$

For practical use, we have to replace the "much less" inequalities with more definite ones. The perturbation analysis is based on series expansions which are acceptable approximations when a next term is 0.1 of a previous one. So we can apply the perturbation approximation when

$$SD(Z_{dr})/Z_{dr} \le 0.1. \tag{2.14}$$

Substitution of (2.10) and (A10) into (2.14) yields

$$\left[\frac{1 + 2SNR_h}{M \ SNR_h^2} + \frac{1 + 2SNR_v}{M \ SNR_v^2} + \frac{1.13(1 - \rho_{co}^2)}{M\sigma_{vn}} \right]^{1/2} \le 0.1 . \tag{2.15}$$

For radar in SHV mode, the H and V channels are usually close at technical characteristics so that for assessment purposes we can assume noise level to be equal in the channels. But due to differential reflectivity the signal-to-noise ratios are different in the channels: $SNR_h = Z_{dr} \ SNR_v$, so that (2.15) can be written as

$$\left[\frac{1 + 2Z_{dr} SNR_v}{Z_{dr}^2 SNR_v^2} + \frac{1 + 2SNR_v}{SNR_v^2} + \frac{1.13(1 - \rho_{co}^2)}{\sigma_{vn}} \right]^{1/2} \le 0.1M^{1/2} . \tag{2.16}$$

For SNR > 10 dB, the noise terms in (2.16) can be omitted and the condition becomes

$$\sigma_v \ge \frac{113(1 - \rho_{co}^2)v_a}{M} . \tag{2.17}$$

For instance for a S-band radar with $PRF = 1000$ Hz, $\rho_{co} = 0.99$, and $M = 64$, the spectrum width should be larger than 0.9 m s^{-1} $\approx$ 1 m s^{-1}. This can be seen from Fig. 2.8

where calculations are compared with the results of computer simulations: for narrow widths, the difference between calculated and simulated data is larger.

For low SNR and for spectrum widths more than 3 m s^{-1} (S-band), we can neglect the third term in (2.16) and neglecting 1 in comparison with 2SNR, we obtain

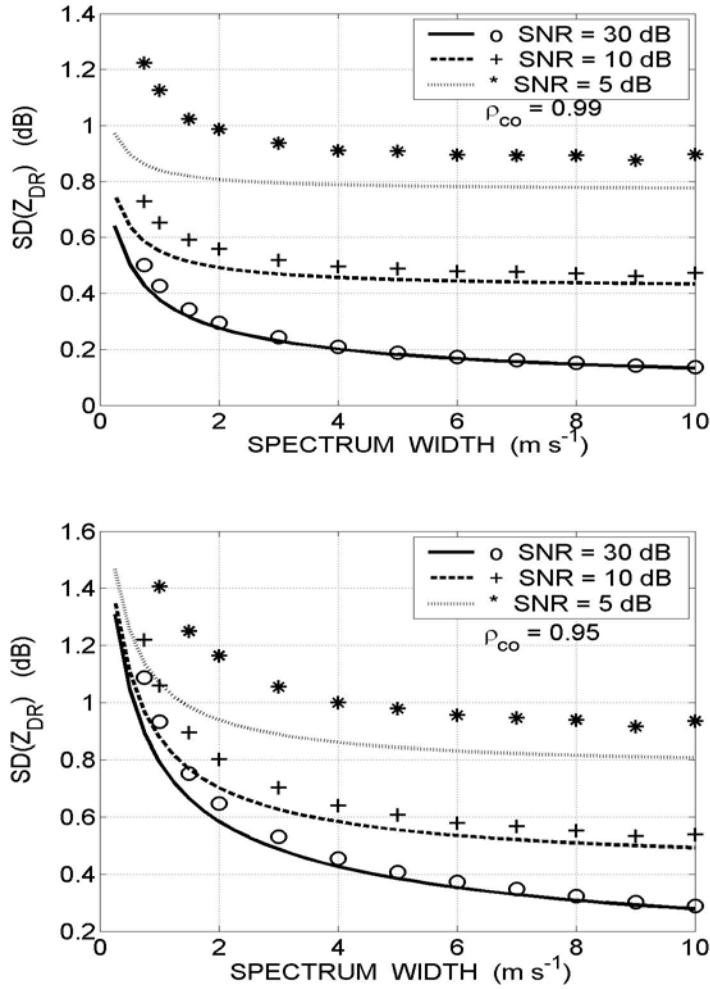$$SNR_v \geq \frac{2(1 + Z_{dr}^{-1})}{0.01M} \ . \tag{2.18}$$

Fig. 2.8. Standard deviations of differential reflectivity calculated via the perturbation analysis (the lines) and the results of simulations (the symbols), $\rho_{co} = 0.99$ (the top figure), $\rho_{co} = 0.95$ (the bottom figure), $Z_{DR} = 3$ dB, $M = 64$.

For Z_{dr} in the interval of $1,\ldots2$, and $M = 64$, SNR_v should be more than $7,\ldots8$ dB. One can see the noise influence in Fig. 2.8. For $SNR_h = 5$ dB, the simulation data is noticeable larger than calculated ones. So the applicability of the perturbation analysis for differential reflectivity can be written as

$$SNR_v \geq 8 \text{ dB}, \qquad \sigma_v \geq 1 \text{ m s}^{-1} \text{ (S-band)} \qquad (2.19)$$

If SNR or the spectrums with are out of bounds (2.19), the actual biases and standard deviations can be significantly larger than ones calculated via the perturbation technique. For the latter cases, the signal simulations can be used to obtain the statistical errors.

3. Differential phase φ_{dp}

Differential phase φ_{dp} between H and V polarized waves is determined as (Doviak and Zrnic 1993)

$$\varphi_{dp} = \arg(R_{co}), \qquad (3.1)$$

where R_{co} is determined by (1.3c). Given finite number of samples in calculations of the estimate, we can consider (3.1) as an equation connecting the estimates. To apply the perturbation method, we represent function R_{co} in the polar form:

$$\hat{R}_{co} = \hat{\rho}_{co} \exp(j\hat{\varphi}_{dp}). \qquad (3.2)$$

From the latter, the phase can be expressed as

$$j\hat{\varphi}_{dp} = \ln \hat{R}_{co} - \ln \hat{\rho}_{co}.$$

The perturbation of this equation is

$$j\delta\hat{\varphi}_{dp} = \frac{\delta\hat{R}_{co}}{\hat{R}_{co}} - \frac{\delta\hat{\rho}_{co}}{\hat{\rho}_{co}}.$$

The second term on the right hand side of the latter equation is a real number so that it can be omitted and in first order of perturbations we write

$$\delta\hat{\varphi}_{dp} = \text{Im} \frac{\delta\hat{R}_{co}}{\hat{R}_{co}} \approx \text{Im} \frac{\delta\hat{R}_{co}}{R_{co}},$$

where Im(x) stands for the imaginary part of x and R_{co} is the mean of the copolar correlation function. Inserting the definition $\delta \hat{R}_{co} = \hat{R}_{co} - R_{co}$ in the latter equation we get

$$\delta \hat{\varphi}_{dp} = \text{Im}\left(\frac{\hat{R}_{co}}{R_{co}} - 1\right) = \text{Im}\frac{\hat{R}_{co}}{R_{co}}. \tag{3.3}$$

Equation (3.3) is a basic perturbation relation and it is in accord with equation (A5.20) by Bringi and Chandrasekar 2001 derived with perturbations of the differential phase expressed as $\tan^{-1}$ function of imaginary and real parts of the correlations.

3.1. *Bias*

In the SHV mode, the differential phase has no bias due to white noise and a finite number of samples. It can be seen from definition (1.3c). In (1.3c) it is assumed that the mean noise and echo voltages are zero, i.e., there is no DC in analog-to-digital conversion and noise in the H and V channels is independent.

When the mean differential phase is close to the boundary of ambiguity, some phase estimates become negative due to statistical fluctuations and phase ambiguity. This is shown in Fig. 3.1 where two distributions of the estimates of the differential phase are shown. The distributions have same width and different mean values. An interval of the phase measurements is -180^0 to 180^0. The first distribution shown with the dotted line has the mean of 50^0 that is far from the boundaries. The second distribution shown with the solid line has the mean of 175^0. Some of the phase estimates are more than 180^0 and appear to be of negative differential phases so that the calculated mean phase has strong negative bias. The width of the phase distribution is controlled with the value of the correlation coefficient ρ_{co}: the lower ρ_{co} the broader the distribution. The negative bias of the differential phase is similar to ambiguity of the Doppler velocity when the mean velocity is close to the Nyquist velocity.
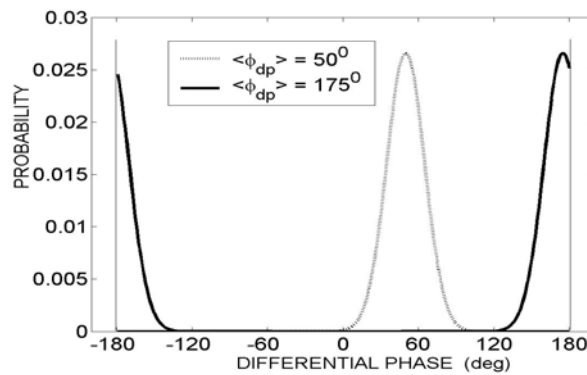

Fig. 3.1. Two distributions of the differential phase
estimates with the mean differential phases of
50^0 (the dotted line) and 175^0 (the solid line)
and for equal widths of the distributions.

24

In Fig. 3.2, simulation results of phase bias are presented. The unambiguous interval for the differential phase is -180° to 180°. Two correlation coefficients have been used for the simulations: 0.99 and 0.95. One can see strong negative bias when the differential phase becomes close to 180°. The similar negative bias is for the left boundary, i.e., -180°. The folding of the differential phase is a well known effect and because of continuity of the differential phase, its unfolding is not a problem.
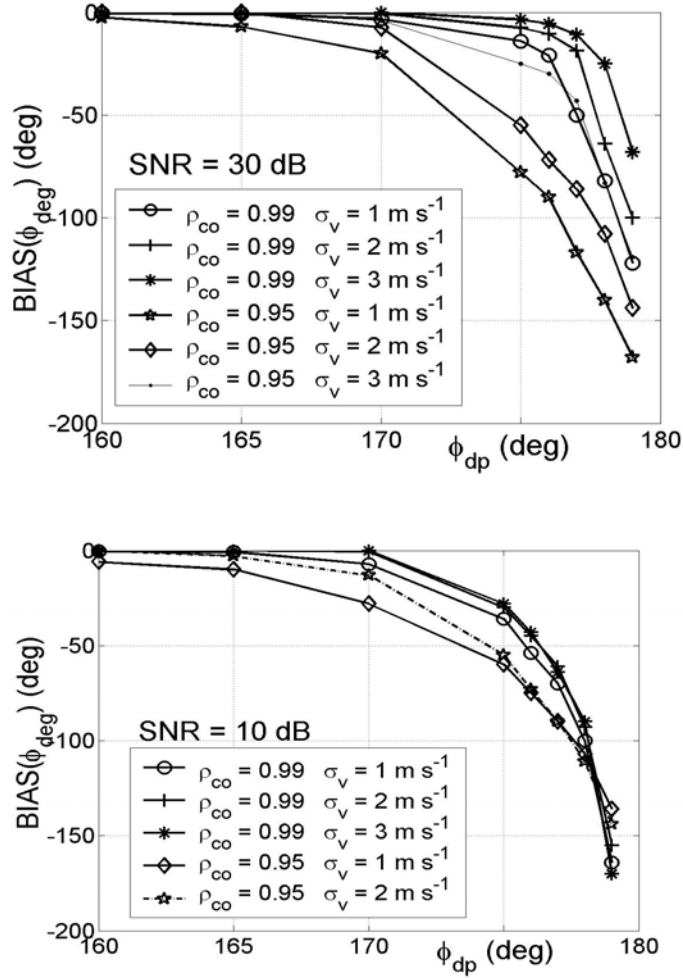

Fig. 3.2. Bias of the differential phase obtained from simulations for SNR = 30 dB (top) and 10 dB (bottom). $M = 64$.

3.2. Standard deviation

The standard deviation of the estimate has been studied by Sachidananda and Zrnic 1986 for alternative transmission of radar pulses and by Ryzhkov and Zrnic 1998c for simultaneous transmission and high SNR. Here we present expressions for finite SNR. For the unfolded differential phase, the variance of the differential phase is the mean value of the perturbations squared, i.e.,

$$<\delta^2\hat{\varphi}_{dp}>=<\text{Im}^2\frac{\hat{R}_{co}}{R_{co}}>=\frac{1}{2}\left[\frac{<|\hat{R}_{co}|^2>}{|\hat{R}_{co}|^2}-\text{Re}\left(\frac{<\hat{R}_{co}^2>}{R_{co}^2}\right)\right]. \tag{3.4}$$

All needed quantities are calculated in Appendix B. Using (B5) and (B7) from the appendix, we obtain the standard deviation in radians

$$SD(\hat{\varphi}_{dp})=<\delta^2\hat{\varphi}_{dp}>^{1/2}=\frac{1}{2^{1/2}\rho_{co}}\left(\frac{SNR_h+SNR_v+1}{M\ SNR_h SNR_v}+\frac{1-\rho_{co}^2}{M_I}\right)^{1/2}\text{(rad).} \tag{3.5}$$

For very large SNR, the latter equation coincides with equation (III.42) given by Doviak and Zrnic 1998, Ryzhkov and Zrnic 1998c, and (6.143) by Bringi and Chandrasekar 2001. Using approximation (A9) for the number of independent samples we can write the latter as

$$SD(\hat{\varphi}_{dp})=\frac{1}{(2M)^{1/2}\rho_{co}}\left[\frac{SNR_h+SNR_v+1}{SNR_h SNR_v}+\frac{0.56(1-\rho_{co}^2)}{\sigma_{vn}}\right]^{1/2}\text{(rad).} \tag{3.6}$$

$$0.04\le\sigma_{vn}\le0.60$$

Convenience of (3.6) is that it is explicitly expressed as a function of signal-to-noise ratios in the channels, ρ_{co}, and the spectral width. In Fig. 3.3, the noise contribution to the standard deviation is plotted, i.e., the first term in (3.5) for equal noise in the channels and Z_{DR} of 0 and 3 dB. We see that for ρ_{co} grater than 0.9, the standard deviation is less than 2° for $SNR\ge14$ dB.
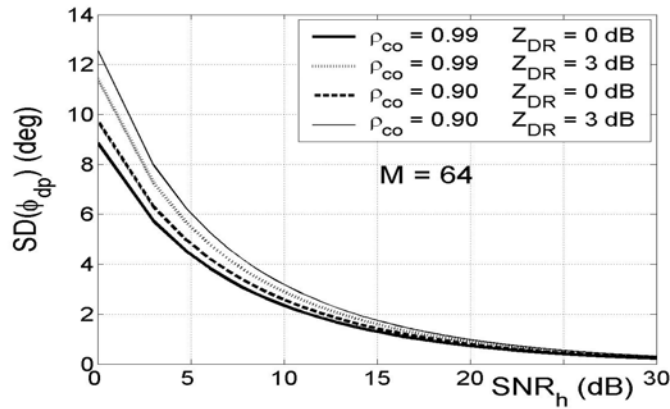

Fig. 3.3. Noise contribution to the standard deviation of the
differential phase for Z_{DR} and ρ_{co} indicated. The
noise levels in the H and V channel are equal. $M=64$.

The spectrum width contribution to the standard deviation, i.e., the second term in (3.5) is plotted in Fig. 3.4. One can see that the standard deviation of 2° is achieved only for very high correlation coefficients, i.e., $\rho_{co} > 0.99$ and for the spectrum widths more than 2 m s[1].
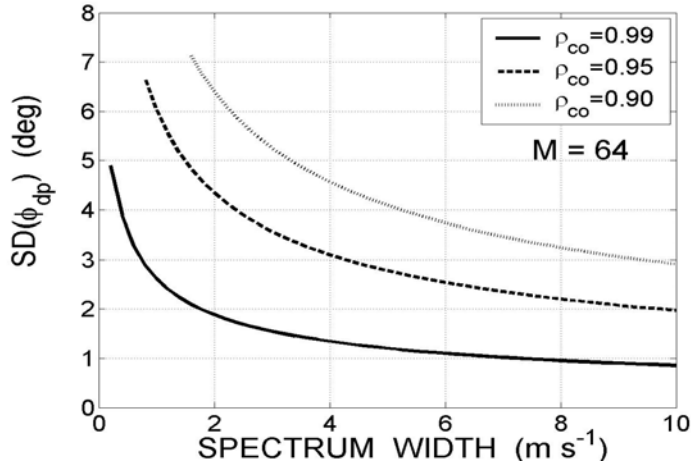

Fig. 3.4. The spectrum width contribution to the standard deviation of the differential phase. $M = 64$.
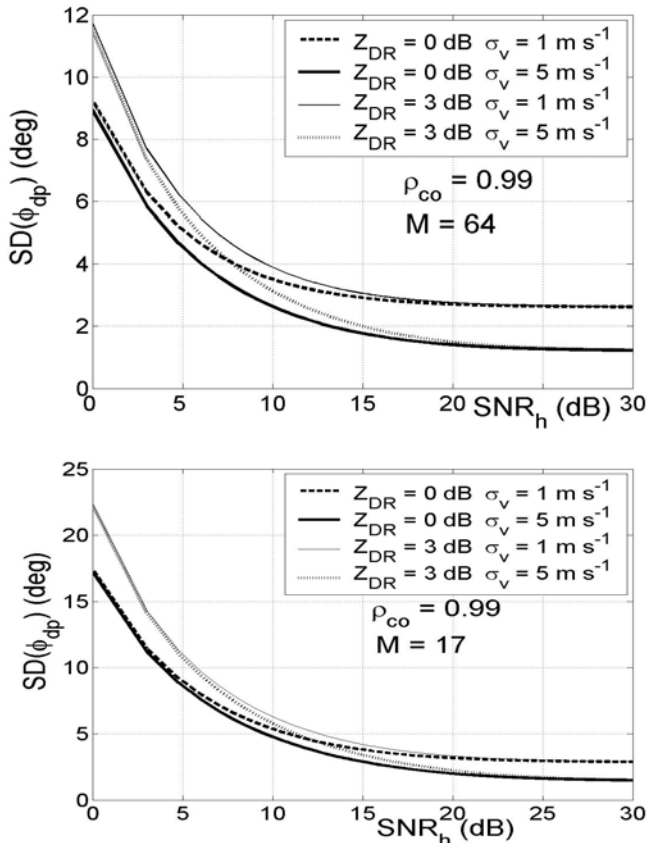

Fig. 3.5. The standard deviation of the differential phase for parameters indicated for $M = 64$, PRF = 1000 Hz (top) and $M = 17$, PRF = 321 Hz (bottom).

The total standard deviation of the differential phase is shown in Fig. 3.5 for spectrum widths of 1 and 5 m s^{-1} and correlation coefficients of 0.99.

The additional thermal noise from a cloud itself influences the differential phase measurements. This noise decreases SNR in the channel and increases the standard deviations of the estimate. The influence of additional noise is shown in Fig. 3.6. We see the effect of additional thermal noise is small for SNR > 10 dB.
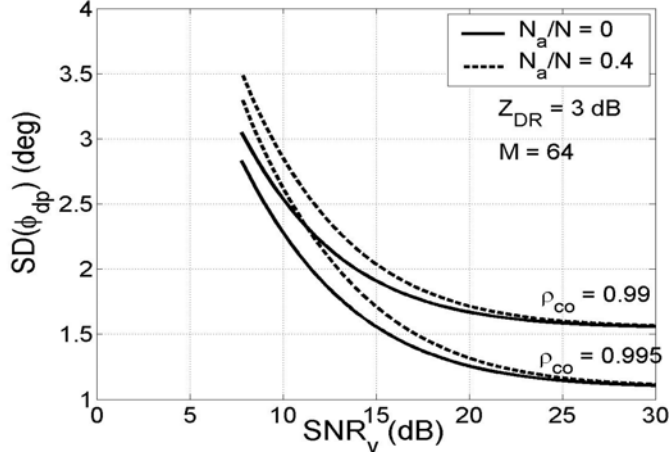

Fig. 3.6. Standard deviation of the differential phase due to additional thermal noise N_a. The spectrum width is 3 m s^{-1}, the wavelength is 10 cm.

The specific differential phase K_{dp} is defined as

$$\hat{K}_{dp} = \frac{\hat{\varphi}_{dp}(r + L/2) - \hat{\varphi}_{dp}(r - L/2)}{2L},$$

where r is the distance to the radar resolution volume and L is the scale of the measurement. Integer 2 in the denominator means that the specific differential phase is measured for 'one way' whereas the differential phase is a 'two way' value. In the nominator, there is a difference of differential phases measured in two radar volumes. Because these two phases are uncorrelated the variance of the difference is a sum of variances of the differential phases. Assuming equal variances of the differential phases, we can write for the standard deviation of K_{dp} (Bringi, Chandrasekar, 2001, section 6.6)

$$SD(\hat{K}_{dp}) = SD(\hat{\varphi}_{dp})/\sqrt{2}L. \tag{3.7}$$

The perturbation analysis used in the calculations has limits of applicability. To obtain the limits, we will compare calculated and simulated data. In Fig. 3.7, we plot the data for $\rho_{co} = 0.99$ and 0.95. We consider the data obtained with the perturbation analysis as a good approximation if it does not deviate from the simulation data more than by 10%. Comparing the data we obtain the limits

$$SNR_v \geq 5 \text{ dB}, \qquad \sigma_v \geq 1.5 \text{ m s}^{-1} \text{ (S-band)} \qquad\qquad (3.8)$$

Comparing with the limits for differential reflectivity (2.19) we see that for the differential phase restriction on SNR is slightly easier.
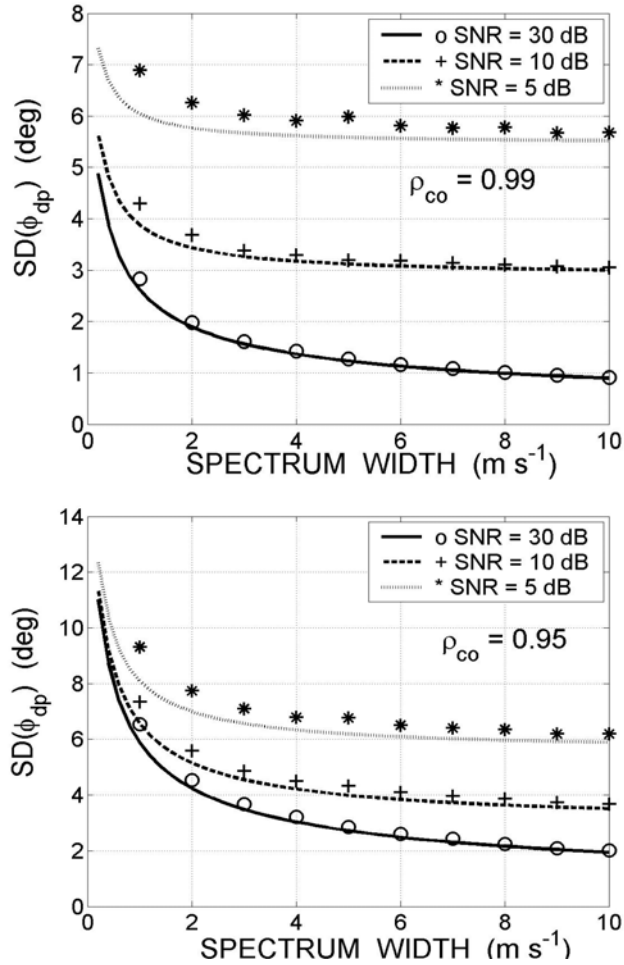

Fig. 3.7. Standard deviations of the differential phase calculated via the perturbation analysis (the lines) and the results of simulations (the symbols), $\rho_{co} = 0.99$ (the top figure), $\rho_{co} = 0.95$ (the bottom figure), $Z_{DR} = 3$ dB, $M = 64$.

4. Modulus of the correlation coefficient ρ_{co}

The modulus of the copolar correlation coefficient ρ_{co} is determined as

$$\hat{\rho}_{co} = \frac{|\hat{R}_{co}|}{[(\hat{P}_h - N_h)(\hat{P}_v - N_v)]^{1/2}} , \qquad (4.1)$$

where the estimates on the right hand side are determined by (1.2). It follows from definition (4.1) that there can be two special cases in the computations. Firstly, in the denominator of (4.1), the estimates of total powers in the channels must be larger than the noise levels. Due to fluctuations of the power estimates the differences in the denominator can be negative. We have to exclude such cases and conclude that we cannot calculate ρ_{co} . Simulations show that this effect takes place for narrow spectra with spectrum widths less than 1 m s^{-1} and probability of such cases is less than 1% for $SNR \geq$ 5 dB. For lesser SNR this probability grows fast. Due to small probability of such cases for $SNR \geq 5$ dB we will not consider this effect further.

Secondly, due to noise subtraction in (4.1) and statistical nature of radar weather signals, estimated ρ_{co} can be more than 1 and we can set $\rho_{co} = 1$ because $\rho_{co} > 1$ has no physical sense. This leads to negative bias that is explained in Fig. 4.1. The bell shaped line in the figure is the distribution of measured ρ_{co}. Some of the estimates are grater than unity that corresponds to the part of the curve that is to the right of the vertical dotted line. The true mean ρ_{co} is shown with the vertical solid line. If we set $\rho_{co} = 1$ for all modulus that are grater than 1, we modify the distribution and move the measured mean modulus to the left that shown with the dash-dot vertical line. So setting $\rho_{co} = 1$ for the estimates that are grater than 1 introduces negative bias. If this negative bias is negligible
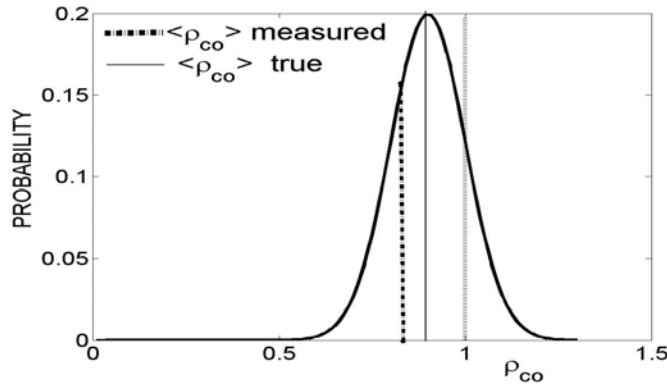

Fig. 4.1. On negative bias of the measured ρ_{co} . The thick solid line is the distribution of $\hat{\rho}_{co}$.

the perturbations approximation can be applied for (4.1) and the deviation of ρ_{co} is written as:

$$\rho_{co} + \delta\hat{\rho}_{co} = \frac{|R_{co} + \delta\hat{R}_{co}|}{[(P_h + \delta\hat{P}_h - N_h)(P_v + \delta\hat{P}_v - N_v)]^{1/2}}$$

In second order of deviations, the latter equation can be represented as (see equations (E4) and (E6) in Appendix E):

$$\rho_{co} + \delta\hat{\rho}_{co} = \hat{\rho}_{co}\left\{1 + \mathrm{Re}\left(\frac{\delta\hat{R}_{co}}{R_{co}}\right) + \frac{1}{2}\frac{|\delta\hat{R}_{co}|^2}{|R_{co}|^2} - \frac{1}{2}\left[\mathrm{Re}\left(\frac{\delta\hat{R}_{co}}{R_{co}}\right)\right]^2\right\} *$$

$$\left[1 - \frac{1}{2}\frac{\delta\hat{P}_h}{S_h} + \frac{3}{8}\frac{\delta P_h^2}{S_h^2}\right]\left[1 - \frac{1}{2}\frac{\delta\hat{P}_v}{S_v} + \frac{3}{8}\frac{\delta P_v^2}{S_v^2}\right].$$

From the latter, in second order of magnitudes, the relative deviation of the correlation coefficient can be written in this form:

$$\frac{\delta\hat{\rho}_{co}}{\rho_{co}} = -\frac{1}{2}\frac{\delta\hat{P}_h}{S_h} - \frac{1}{2}\frac{\delta\hat{P}_v}{S_v} + \frac{3}{8}\frac{\delta\hat{P}_h^2}{S_h^2} + \frac{3}{8}\frac{\delta\hat{P}_v^2}{S_v^2} + \frac{1}{4}\frac{\delta\hat{P}_h\delta\hat{P}_v}{S_h S_v} +$$

$$\mathrm{Re}\left(\frac{\delta\hat{R}_{co}}{R_{co}}\right) + \frac{1}{2}\frac{|\delta\hat{R}_{co}|^2}{|R_{co}|^2} - \frac{1}{2}\left[\mathrm{Re}\left(\frac{\delta\hat{R}_{co}}{R_{co}}\right)\right]^2 - \frac{1}{2}\left(\frac{\delta\hat{P}_h}{S_h} + \frac{\delta\hat{P}_v}{S_v}\right)\mathrm{Re}\left(\frac{\delta\hat{R}_{co}}{R_{co}}\right). \quad (4.2)$$

From (4.2), bias and the variance of the estimate can be found.

4.1. Bias
Taking the expectation on (4.2), bias is obtained:

$$\frac{1}{\rho_{co}}BIAS\,(\rho_{co}) = \frac{3}{8}\frac{<\delta\hat{P}_h^2>}{S_h^2} + \frac{3}{8}\frac{<\delta\hat{P}_v^2>}{S_v^2} + \frac{1}{4}\frac{<\delta\hat{P}_h\delta\hat{P}_v>}{S_h S_v} -$$

$$\frac{1}{2}<\left(\frac{\delta\hat{P}_h}{S_h} + \frac{\delta\hat{P}_v}{S_v}\right)\mathrm{Re}\left(\frac{\delta\hat{R}_{co}}{R_{co}}\right)> + \frac{1}{2}\frac{<|\delta\hat{R}_{co}|^2>}{|R_{co}|^2} - \frac{1}{2}<\left[\mathrm{Re}\left(\frac{\delta\hat{R}_{co}}{R_{co}}\right)\right]^2>. \quad (4.3)$$

The variances in the first three terms on the right hand side of the latter equation can be found in Appendix A (see (A6), (A8), and (A12)). The rest terms are calculated in Appendix B (see (B10), (B11), (B12), and (B13)). Substituting corresponding expressions into (4.3) we obtain

$$\frac{1}{\rho_{co}} BIAS\,(\rho_{co}) = \frac{2\,SNR_h + 3}{8M\;SNR_h^2} + \frac{2\,SNR_v + 3}{8M\;SNR_v^2} +$$

$$\frac{SNR_h + SNR_v + 1}{4M\;SNR_h SNR_v \rho_{co}^2} + \frac{(1 - \rho_{co}^2)^2}{4M_I \rho_{co}^2} \qquad (4.4)$$

One can see that bias is positive and consists of two contributors: the first three terms on the right hand side of (4.4) are noise contribution, and the last term is the contribution from spectral width and ρ_{co}. Using approximation (A9) equation (4.4) can be represented in the form:

$$\frac{M}{\rho_{co}} BIAS\,(\rho_{co}) = \frac{2\,SNR_h + 3}{8\,SNR_h^2} + \frac{2\,SNR_v + 3}{8\,SNR_v^2} +$$

$$\frac{SNR_h + SNR_v + 1}{4\,SNR_h SNR_v \rho_{co}^2} + \frac{0.14\,(1 - \rho_{co}^2)^2}{\sigma_{vn} \rho_{co}^2} \qquad (4.5)$$

$$0.04 \leq \sigma_{vn} \leq 0.60\ .$$

The noise contribution, i.e. the first three terms on the right hand side of (4.4) or (4.5), is shown in Fig. 4.2 for equal noise levels in the channels. We see that this contribution becomes less than 0.005 for SNR > 6 dB.
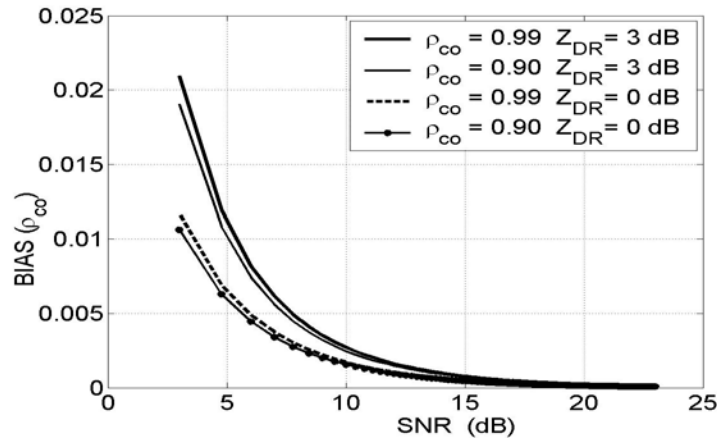

Fig. 4.2. Noise contribution to the bias of the modulus of the correlation coefficient for equal noise levels in the H and V channels. $M = 64$. SNR is for the H channel.

The spectrum width contribution is shown in Fig. 4.3. This contribution increases fast with decrease of the correlation coefficient ρ_{co}. For $\rho_{co} > 0.9$, the contribution is smaller than 0.005. So the main contribution to bias is determined by noise.
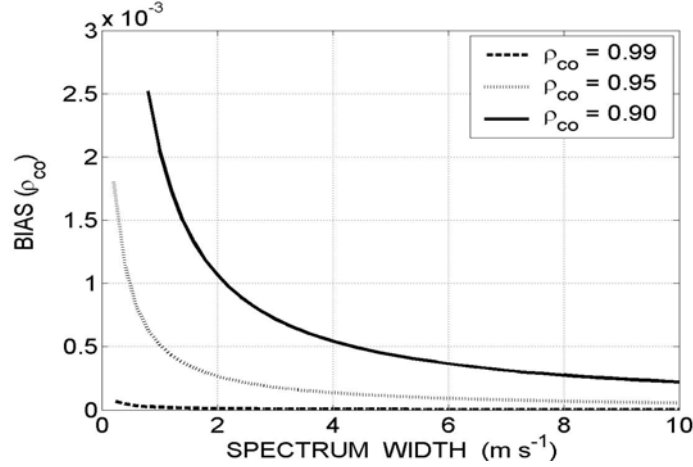
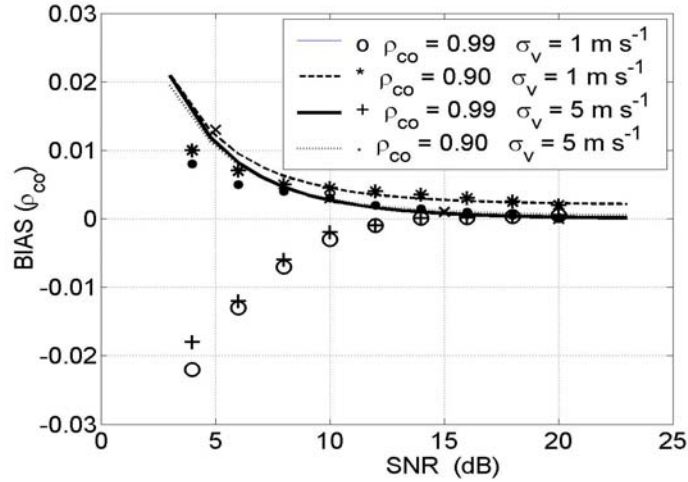Fig. 4.3. Spectrum width contribution to bias of the modulus of the correlation coefficient. $M = 64$.

Fig. 4.4. Bias of the modulus of the correlation coefficient for spectral width of 1 and 5 m s^{-1}. $M = 64$. Results of the simulation are shown with the symbols. Simulation results with setting $\hat{\rho}_{co} = 1$ for $\hat{\rho}_{co} > 1$ are shown with dotes, asterisks, pluses, and circles. Simulation results including $\hat{\rho}_{co} > 1$ are shown with the crosses ($\sigma_v = 5$ m s^{-1}, $\rho_{co} = 0.99$).

Total bias of the modulus of the correlation coefficient according to the perturbation approximation is shown in Fig. 4.4 along with the simulated data. The simulated results shown with the asterisks, stars, circles, and pluses have been obtained setting $\rho_{co} = 1$ if calculated modulus is grater than 1. For high ρ_{co}, bias is negative in accord with our expectations (see Fig. 4.1). For $\rho_{co} \leq 0.90$, negative bias competes with positive bias obtained from the perturbation approximation and one can see the deviation

of biases for SNR less than 7 dB. From the figure, we conclude that the absolute value of bias is les than 0.005 for $SNR \geq 10$ dB. In the figure simulation data for the estimated ρ_{co} without setting $\rho_{co} = 1$ when $\hat{\rho}_{co} > 1$ is shown with crosses, x ($\rho_{co} = 0.99$ and the spectrum width of 5 m s^{-1}). It is seen that bias of the simulated data is positive and is very close to the calculated curve with the same input parameters.

Additional thermal noise (1.7) biases the modulus of the correlation coefficient. Bias of the measured modulus in the presence of uncompensated thermal noise N_a is

$$\frac{1}{\rho_{co}} BIAS\ (\rho_{co}) = \left[\left(1 + N_a\ /\ N_h SNR_h \right)\left(1 + N_a\ /\ N_v SNR_v \right) \right]^{-1/2} - 1 . \qquad (4.6)$$

This bias is negative like in the case of differential reflectivity and can exceed the designated threshold of 0.005 even for very large SNR as seen in Fig. 4.5.
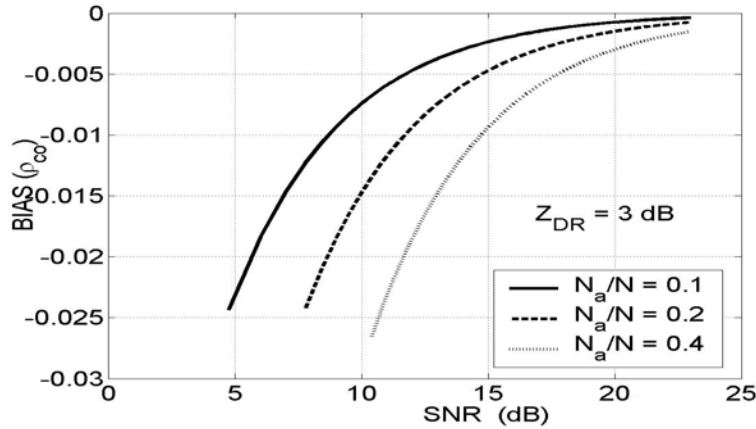

Fig. 4.5. Bias of the modulus of the correlation coefficient due to
additional thermal noise.

Because additional white noise decreases signal-to-noise ratios in the channels there is additional positive statistical bias but for $Na/N < 0.5$, this bias is much less than bias (4.6). Thus, additional white noise biases the estimate according to (4.6).

4.2. Standard deviation
The variance of the estimate of the modulus of the correlation coefficient can be found from (4.2) squaring deviation of the modulus and retaining terms of second order of the deviations:

$$< \delta^2 \hat{\rho}_{co} > \ \approx \ \rho_{co}^2 < \left[\frac{1}{2}\frac{\delta\hat{P}_h}{S_h} + \frac{1}{2}\frac{\delta\hat{P}_v}{S_v} - \text{Re}\left(\frac{\delta\hat{R}_{co}}{R_{co}} \right) \right]^2 > .$$

The standard deviation of the variance above can be written in second order of the deviations as:

$$\frac{1}{\rho_{co}} SD(\hat{\rho}_{co}) \approx \left\{ \frac{1}{4} \frac{<\delta \hat{P}_h^2>}{S_h^2} + \frac{1}{4} \frac{<\delta \hat{P}_v^2>}{S_v^2} + \frac{1}{2} \frac{<\delta \hat{P}_h \delta \hat{P}_v>}{S_h S_v} \right.$$

$$\left. - \left\langle \left(\frac{\delta \hat{P}_h}{S_h} + \frac{\delta \hat{P}_v}{S_v} \right) Re\left(\frac{\delta \hat{R}_{co}}{R_{co}} \right) \right\rangle + \left\langle \left[Re\left(\frac{\delta \hat{R}_{co}}{R_{co}} \right) \right]^2 \right\rangle \right\}^{1/2} . \tag{4.7}$$

All needed values can be found in the appendixes (see (A6), (A8), (A12), (B10), (B11), and (B13) and substitution yields:

$$SD(\hat{\rho}_{co}) = \left\{ \frac{(1 - 2SNR_h)\rho_{co}^2}{4M \ SNR_h^2} + \frac{(1 - 2SNR_v)\rho_{co}^2}{4M \ SNR_v^2} + \right.$$

$$\left. \frac{SNR_h + SNR_v + 1}{2M \ SNR_h SNR_v} + \frac{(1 - \rho_{co}^2)^2}{2M_I} \right\}^{1/2} \tag{4.8}$$

It can be seen from the latter that the sum of the first three terms in (4.8) is positive for all ρ_{co} and *SNR*. For high *SNR*, equation (4.8) deviates from (6.144) by Bringi and Chandrasekar 2001 which reads

$$SD(\hat{\rho}_{co}) = \left[\frac{(1 - \rho_{co}^2)^2}{2M_I \rho_{co}^2} \right]^{1/2}$$

and has ρ_{co} in the denominator; this is a misprint. Equation (4.8) also deviates from Eq.(9) by Torlachi and Gingras 2003 in the noise containing terms which are in error.

Using approximation (A9) for the number of independent samples, (4.8) can be written in the form:

$$SD(\hat{\rho}_{co}) = \frac{1}{M^{1/2}} \left\{ \frac{(1 - 2SNR_h)\rho_{co}^2}{4SNR_h^2} + \frac{(1 - 2SNR_v)\rho_{co}^2}{4SNR_v^2} + \right.$$

$$\left. \frac{SNR_h + SNR_v + 1}{2SNR_h SNR_v} + \frac{0.28(1 - \rho_{co}^2)^2}{\sigma_{vn}} \right\}^{1/2} \tag{4.9}$$

$$0.04 \leq \sigma_{vn} \leq 0.60 .$$

Fig. 4.6 shows the noise contribution to the standard deviation, i.e., the first three terms on the right hand side of (4.8) or (4.9). One can see from the figure that desired accuracy of 0.01 can be achieved only for SNR grater than 15 dB for ρ_{co} grater than 0.9.

In Fig. 4.7, the spectral narrowness contribution is shown. We see that the accuracy of 0.01 can be achieved only for high correlations, i.e., for $\rho_{co} \geq 0.99$.

The calculated total standard deviations are shown in Fig. 4.8 for spectral widths of 1 and 5 m s^{-1}. The results of the simulations are shown with the symbols. One can see that for low SNR, the deviations for the simulated data are smaller than the calculated ones. This is a results of setting $\rho_{co} = 1$ for obtained estimates grater than 1. The statistical uncertainty of 0.01 is achieved only for ρ_{co} equal or grater than 0.99 and SNR ≥ 15 dB.
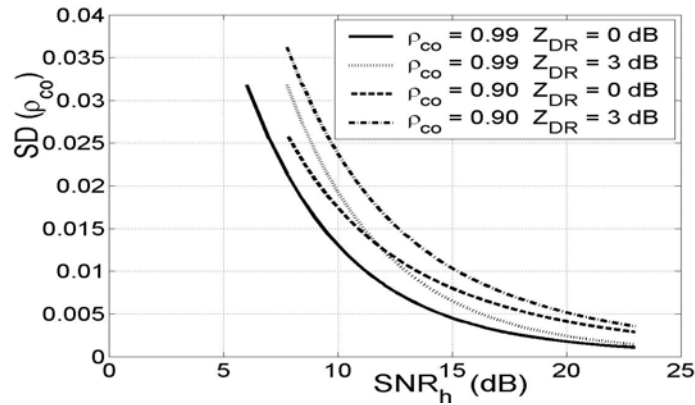

Fig. 4.6. Noise contribution to the standard deviation of ρ_{co} for equal noise levels in the channels. $M = 64$.
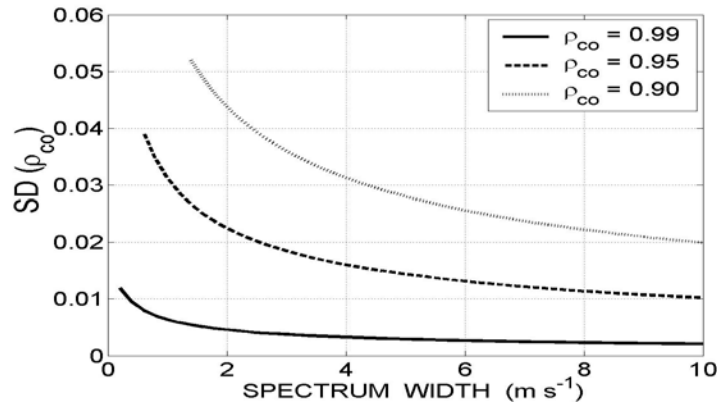

Fig. 4.7. Spectrum width dependence of the standard deviation of ρ_{co} for ρ_{co} indicated and $M = 64$.
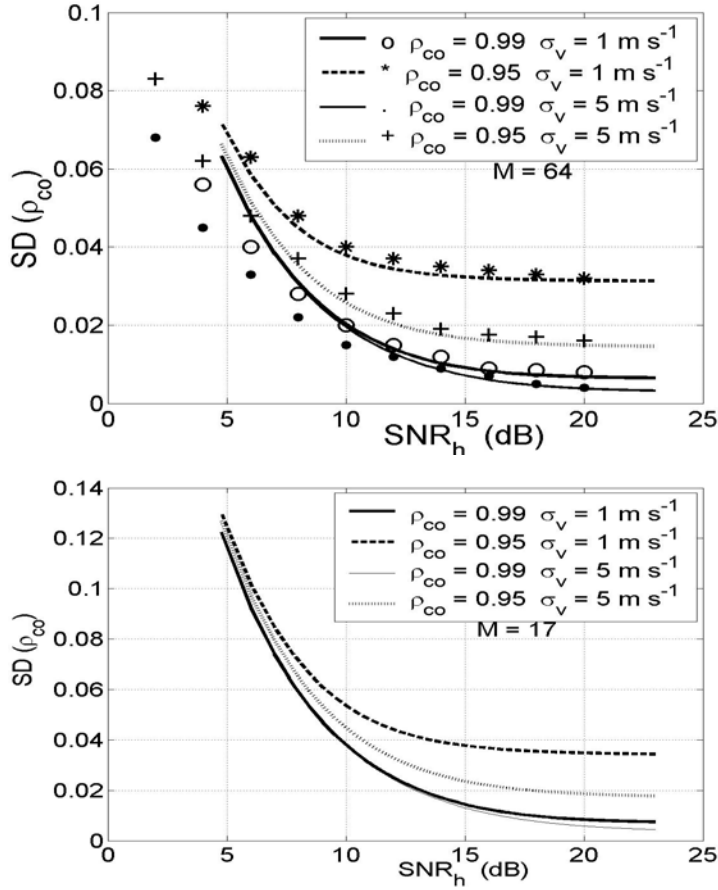
Fig. 4.8. Calculated standard deviation of ρ_{co} for parameters indicated (the lines) and results of the simulations (the symbols). $M = 64$, PRF = 100 Hz (top) and $M = 17$, PRF = 321 Hz (bottom). $Z_{DR} = 3$ dB.
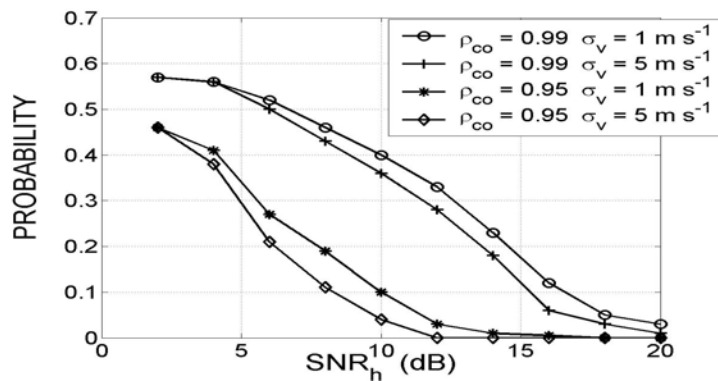

Fig. 4.9. Probability to obtain $\hat{\rho}_{co} > 1$ for S-band radar with PRF of 1000 Hz, $Z_{DR} = 3$ dB, and $M = 64$, simulations.

Fig. 4.9 shows the simulation results for probability of calculated ρ_{co} to be grater than 1. It is seen that for $\rho_{co} \geq 0.99$, this probability is under 10% for SNR > 17 dB but for $\rho_{co} \geq 0.95$, 10% is achieved for SNR $\geq$10 dB.

From Fig. 4.8 we can obtain limits of applicability of the perturbation approximation for ρ_{co}. For $\rho_{co} \geq 0.95$ and spectral widths grater than 1 m s^{-1}, calculated and simulated data differ less by 10% for SNR $\geq$ 9 dB. So these limits are

$$SNR_v \geq 9 \text{ dB}, \qquad \sigma_v \geq 1 \text{ m s}^{-1} \text{ (S-band)} \qquad (4.10)$$

Additional thermal noise (1.7) contributes to the standard deviation of ρ_{co}. The standard deviation consists of two contributions, i.e., the noise contribution that is described with the first three terms on the right hand side of (4.8) or (4.9) and the spectral width contribution, i.e., the fourth term in the equations. Additional white noise affects the noise contribution and the standard deviation SD_a can be written as:

$$SD_a(\hat{\rho}_{co}) = \left\{ \frac{(1 - 2SNR_{ha})\rho_{co}^2}{4M \, SNR_{ha}^2} + \frac{(1 - 2SNR_{va})\rho_{co}^2}{4M \, SNR_{va}^2} + \frac{SNR_{ha} + SNR_{va} + 1}{2M \, SNR_{ha} \, SNR_{va}} + \frac{(1 - \rho_{co}^2)^2}{2M_I} \right\}^{1/2}$$

where SNR_{ha} and SNR_{va} are signal-to-noise ratios in the channels in the presence of the additional noise:

$$SNR_{ha} = \frac{SNR_h}{1 + N_a / N}, \qquad SNR_{va} = \frac{SNR_v}{1 + N_a / N}.$$

Fig. 4.10 shows the effect of additional white noise. For the purposes of assessment, the noise levels in the channels are assumed equal. One can see that this effect is insignificant for $Na/N < 0.5$.
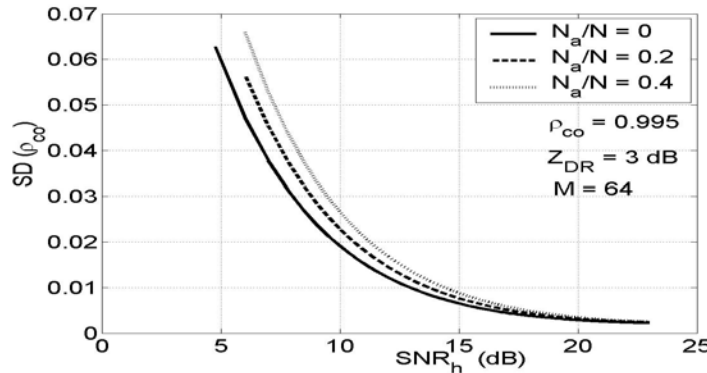

Fig. 4.10. Additional thermal noise contribution to the standard deviation of the ρ_{co} for specified parameters.

5. Radar sensitivity

For the legacy WSR-88D radar, all transmitted power is in one polarization. In the SHV mode of the WSR-88D, the total transmitted power is partitioned in two and the signal to noise ratio per channel is two times smaller than what it is in a single polarization radar. Note, that in alternate transmission via a ferrite switch the loss in power could be even larger! So the SHV scheme leads to the loss of sensitivity of 3 dB in each polarimetric channel and the question is: can the loss be restored? We show here that this can be done to some extend.

We can capitalize on strong correlation between weather signals in the H and V channels. Summing voltages in the channels we can form this signal:

$$e_{sum} = e^{(h)} + e^{(v)} = s^{(h)} + n^{(h)} + s^{(v)} + n^{(v)}, \qquad (5.1)$$

where s and n are weather signals and noise voltages correspondingly in the channels marked with the superscripts. The mean power of the sum signal is

$$P_{sum} = < [e^{(h)} + e^{(v)}][e^{(h)*} + e^{(v)*}] > = S_h + S_v + < s^{(h)} s^{(v)*} > + \\ < s^{(h)} s^{(v)*} > + < n^{(h)} n^{(h)*} > + < n^{(v)} n^{(v)*} > .$$

We used the fact that the mean voltages in the channels are zero and the noise voltages in the channels are uncorrelated so the latter equation can be written as:

$$P_{sum} = S_h + S_v + 2(S_h S_v)^{1/2} \rho_{co} \cos \varphi_{dp} + N_h + N_v .$$

Signal-to-noise ratio for the sum signal is

$$SNR_{sum} = \frac{S_h + S_v + 2(S_h S_v)^{1/2} \rho_{co} \cos \varphi_{dp}}{N_h + N_v} . \qquad (5.2)$$

It follows from the latter that if there is no differential phase between the signals in the channels, SNR_{sum} is

$$SNR_{sum} = \frac{S_h + S_v + 2(S_h S_v)^{1/2} \rho_{co}}{N_h + N_v} = 2 SNR_h \frac{Z_{dr} + 2 Z_{dr}^{1/2} \rho_{co} + 1}{4 Z_{dr}} . \qquad (5.3)$$

Thus to achieve (5.3), we have to measure the differential phase and then must shift the voltages in the vertical channel by this phase. In cases with low reflections where it is difficult to measure φ_{dp}, two alternatives can be applied. If low reflecting echoes are not screened by other parts of echoes, the differential phase is the system differential phase which is known with sufficient accuracy. If low reflecting echoes are screened by other

echoes, the differential phase at low reflecting echoes is phase φ_{dp} at the edge of a screening echo which is known also.

Weather signals have the modulus of the correlation coefficient ρ_{co} very close to 1 and we want to restore weak echoes, i.e., powers reflected from small particles for which differential reflectivity as a ratio is close to 1. It follows from (5.3) that for such regions, we have $SNR_{sum} \approx 2\ SNR_h$. If full energy goes to the H channel, the signal-to noise ratio is $2\ SNR_h$. It means that the summing of the voltages allows almost full restoration of radar sensitivity. Because of the differential phase is measured independently from powers, all we need to do is to shift the vertical voltages by the differential phase and calculate the power of summed voltages.

Another scheme to increase radar sensitivity uses measurements of the cross-correlation function for H and V channels. The function is defined in (1.3c):

$$R_{co} = (S_h S_v)^{1/2} \rho_{co} \exp(j\varphi_{dp}). \tag{5.4}$$

The modulus of this function is

$$|R_{co}| = S_h Z_{dr}^{-1/2} \rho_{co}; \tag{5.5}$$

it is proportional to the weather signal power and is independent on noise levels in the channels. For cloud regions with small particles, the following holds: $Z_{dr} \approx 1$ and $\rho_{co} \approx 1$ so that the modulus (5.5) is close to the power of weather signal.

Let us consider sensitivity of (5.5) in comparison with sensitivity of the power measurement. Sensitivity of power measurements is defined as some signal threshold S_0 so that if the estimate of measured signal power exceeds the threshold, the weather signal is considered to exist. For the WSR-88D radar the threshold is determined as one when $S_0 + N$ exceeds noise by 3.5 dB, i.e., $10\log[(S_0 + N)/N] = 3.5$. This threshold determines corresponding signal-to-noise ratio $SNR_0 = S_0 / N$. Signal S_0 is measured with the accuracy that is determined by a ratio of corresponding standard deviation SD(S_0) and S_0. Using (A6) we can write this ratio:

$$\frac{SD(\hat{P}_0)}{S_0} = \left[\frac{2SNR_0 + 1}{M\ SNR_0^2} + \frac{1}{M_I} \right]^{1/2}. \tag{5.6}$$

Sensitivity of the measurements (5.5) can be defined with a ratio of the standard deviation of the estimate and its mean value, i.e.,

$$\frac{SD(|\hat{R}_{co}|)}{|R_{co}|} = \left[\frac{<\delta|R_{co}|^2>}{|R_{co}|} \right]^{1/2}, \tag{5.7}$$

The ratio on the right side side of (5.7) is calculated in Appendix B (see (B12)), then

$$\frac{SD\,(|\,\hat{R}_{co}\,|)}{|\,R_{co}\,|} = \frac{1}{\rho_{co}}\left[\frac{SNR_{0h}+SNR_{0v}+1}{M\,SNR_{0h}\,SNR_{0v}}+\frac{1}{M_I}\right]^{1/2}. \tag{5.8}$$

For equal noise levels in the channels and Z_{DR} close to zero, the term in the rectangular brackets in (5.8) equals (5.6), then

$$\frac{SD\,(|\,\hat{R}_{co}\,|)}{|\,R_{co}\,|} = \frac{1}{\rho_{co}}\frac{SD\,(\hat{P}_0)}{S_0}. \tag{5.9}$$

Thus the relative accuracy of the measurements of R_{co} is $1/\rho_{co}$ times larger than the accuracy of power measurements. For weather signals, ρ_{co} is close to unity, thus these measurements are almost equivalent. So measuring the correlation function (5.5) we achieve almost the same accuracy that is set for power measurements. Attractiveness of the measurements of the correlation function to restore radar sensitivity is that this function is actually obtained in calculation of the differential phase so it can be determined with no effort.

6. Doppler velocity estimates in both radar channels

Is it possible to increase the accuracy of the Doppler velocity and spectrum width measurements by averaging corresponding estimates from the two channels? One can calculate the Doppler velocities in the H and V channels, v_h and v_v and then form the estimate (Doviak and Zrnic 1998, section III.3.4)

$$v = \frac{v_h + v_v}{2}. \tag{6.1}$$

Is estimate (6.1) better than the estimates of Doppler velocities in each channel? To answer this question we have to compare the standard deviations of the estimates. The variation of (6.1) is

$$\delta v = \frac{1}{2}(\delta v_h + \delta v_v)\,,$$

so that the variance can be written as

$$<\delta v^2> = \frac{1}{4}[<\delta v_h^2> + <\delta v_v^2> + 2<\delta v_h \delta v_v>]. \tag{6.2}$$

We see that there could be a reduction of the variance if the covariance in (6.2) is small. To asses the variance reduction, we can consider signal-to-noise rations to be equal in the channels, then the relative reduction of the variance is

$$\frac{<\delta v^2>}{<\delta v_h^2>} = \frac{1}{2}[1+ <\delta v_h \delta v_v > / <\delta v_h^2 >)].$$

Needed variances and covariance are calculated in Appendix C. Using (C11) and (C17) for equal noise levels in the channels and $Z_{dr} = 1$, we obtain

$$\delta^2 = \frac{<\delta v^2>}{<\delta v_h^2>} = \frac{1}{2}\left\{1+\rho_{co}^2\left[1+\frac{(2SNR[1-\rho^2(1)]+1)M_{I1}}{[1-\rho^2(1)](M-1)SNR^2}\right]^{-1}\right\}. \qquad (6.3)$$

where M_{I1} is the number of independent samples for a sequence of M-1 samples; see (C6) in Appendix 6. For strong signals, the right hand side of (6.3) becomes $(1+\rho_{co}^2)/2$ and is very close to 1 because of the modulus of the correlation coefficient is close to 1. So for strong signals, there is no decrease of the variance of the estimate (6.1) in comparison with the variance of the Doppler velocity measured in one of the channels. This is a manifestation of high correlation of the velocity estimates in the two polarimetric channels. Fig. 6.1 presents square root of the ratio (6.3) as a function of signal-to-noise ratio. One can see that the decrease of the variation of estimate (6.1) is substantial for low signal-to-noise ratios. For uncorrelated estimates, this decrease is $1/\sqrt{2} = 0.71$. So the estimate (6.1) can be applied for SNR less than 5 dB.
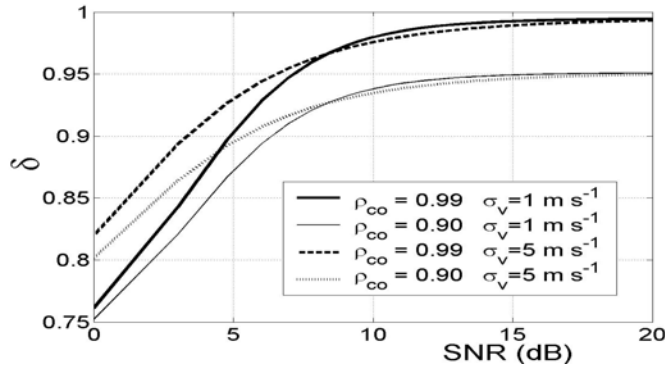

Fig. 6.1. The ratio of standard deviations of estimates (6.3) as
a function of signal-to-noise ratio for the spectrum widths
of 1 and 5 m s^{-1}. $M = 64$.

To measure the Doppler velocity in the H and V channels, one can utilize another estimator. A combined correlation function $R(T)$ can be constructed from the correlation functions for the H and V channels $R_h(T)$ and $R_v(T)$ as

$$R(T) = \frac{1}{2}[R_h(T)+ R_v(T)]. \qquad (6.4)$$

42

Then the Doppler velocity is obtained as the argument of the correlation function: $v = \arg(R(T))$. This estimator is unbiased and its variance can be obtained using (C1), i.e.,

$$< \delta v^2 > = \frac{v_a^2}{\pi^2} < \mathrm{Im}^2 \frac{\hat{R}(T)}{R(T)} > .$$

Substituting (6.4) into the latter equation and using the results of Appendix C we obtain

$$< \delta v^2 > = \frac{v_a^2}{2\pi^2 \rho^2(T)} \left\{ \left(\frac{Z_{dr}}{Z_{dr}+1} \right)^2 \frac{2SNR_h[1-\rho^2(T)]+1}{(M-1)SNR_h^2} + \right.$$

$$\left. \left(\frac{1}{Z_{dr}+1} \right)^2 \frac{2SNR_v[1-\rho^2(T)]+1}{(M-1)SNR_v^2} + \frac{Z_{dr}^2 + 2Z_{dr}\rho_{co}^2 + 1}{(Z_{dr}+1)^2} \frac{[1-\rho^2(T)]}{M_{I1}} \right\} . \qquad (6.5)$$

The variance of the Doppler velocity estimates in the H channel is given by (C10). An improvement to the velocity estimate can be calculated from a ratio of standard deviations obtained from the variances (6.5) and (C10). This ratio is plotted in Fig. 6.2. One can see that there is a substantial improvement in the measurements for SNR less than 5 dB. Comparing Figs. 6.1 and 6.2, we conclude that estimate (6.4) is almost the same as (6.1) in improvement of standard deviation.
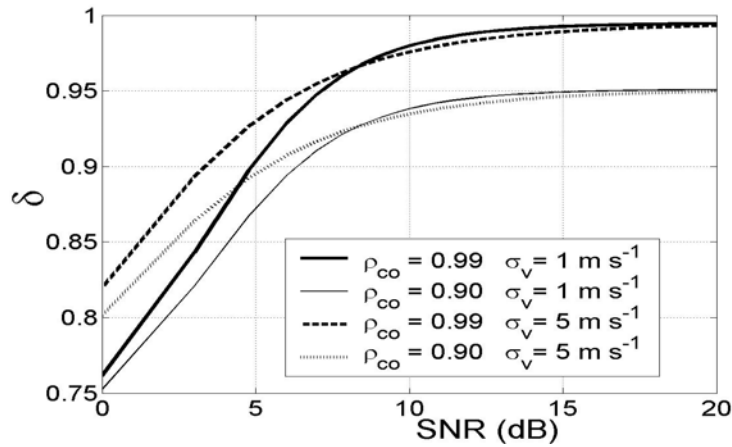

Fig. 6.2. The ratio of standard deviations of estimates (6.5) and (C10) as a function of signal-to-noise ratio for the spectrum widths of 1 and 5 m s^{-1}. $Z_{DR} = 0$ dB, $M = 64$.

It is worth comparing the velocity measurements for three cases: a) the H legacy channel, b) the H channel in the SHV mode, and c) the sum of the correlation functions (6.4) that uses the estimates in the H and V channels. Fig. 6.3 presents the standard deviations of the velocity for those three cases. The accuracy of 1 m s^{-1} has been set for

the velocity measurements with the WSR-88D radars. We see that such accuracy is achieved on the legacy system at SNR $\geq$ 1 dB. For the H channel of the SHV mode this accuracy is achieved at SNR $\geq$ 4 dB, i.e., 3 dB higher because of 3 dB loss of SNR due to power splitting. Calculation the velocity from the sum of the correlation functions according to (6.3) improves the estimate but this improvement depends on differential reflectivity; the closer Z_{dr} is to 1 the larger is possible improvement. This dependence on differential reflectivity is clear because the estimator combines echo powers from the two channels. If one return is very week it would not contribute to the combined aurocovariance. So in time domain, the velocity estimate can not be fully restored to the legacy level summing the correlation functions.

For small particles, Z_{dr} is close to 1 and according to Fig. 6.3, the sum of the correlation functions improves the velocity estimate by 2 dB, it is only 1 dB worse than the estimate for the legacy WSR-88D.
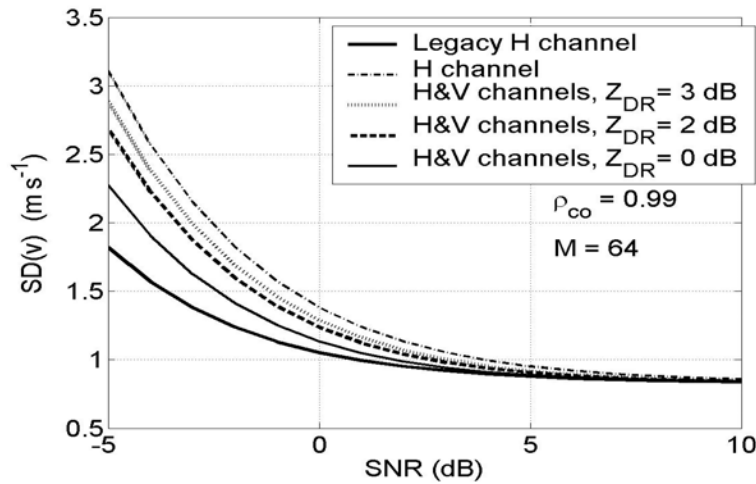

Fig. 6.3. Standard deviations of velocity estimates in the legacy
WSR-88D channel (the thick solid line), in the H channel
of the SHV mode (the dash-and-dott line), and for the sum
of the correlation functions for the H and V channels.

7. Z_{DR} and R_{co} estimates not biased by white noise

The noise level depends on the temperature of receiver and external noise which in turn depends on antenna elevation and precipitation along the radar beam. Measurements with the WSR-88D show that noise level can increase by as much as 1 dB if the beam propagates a significant distance through heavy precipitation. Additional thermal noise biases the estimates of the spectrum width, differential reflectivity, and the modulus of the correlation coefficient. It should be noted also that noise levels on the field WSR-88Ds are set erroneously on about half of inspected radars (Sirmans, et al. 1997). Thus, it is desirable to device estimates that will not be biased by white noise. Such estimates can be obtained using 1-lag correlation and cross-correlation functions in the two polarimetric channels.

The cross-correlation function in the channels for lag 1 is presented in the form (1.5c):

$$R_{co}(1) = (S_h S_v)^{1/2} \rho_{co} \rho(1) \exp(j\pi v / v_a + j\varphi_{dp}),$$
(7.1)

For m = 0, (1.5c) can be written as:

$$R_{co}(0) = (S_h S_v)^{1/2} \rho_{co} \exp(j\varphi_{dp}),$$
(7.2)

Correlation functions (1.5a) and (1.5b) at lag 1 in the H and V channels are:

$$R_h(1) = S_h \rho(1) \exp(j\pi v / v_a),$$
(7.3)

$$R_v(1) = S_v \rho(1) \exp(j\pi v / v_a).$$
(7.4)

We see that the parameters entering equations (7.1) through (7.4) do not depend on noise and we can obtain estimations not biased by white noise. From (7.3) and (7.4) we obtain Z_{dr} as:

$$Z_{dr} = \frac{S_h}{S_v} = \frac{|R_h(1)|}{|R_v(1)|}.$$
(7.5)

Obtaining modulus of (7.1), (7.3), and (7.4) the copolar correlation coefficient is calculated as:

$$\rho_{co} = \frac{|R_{co}(1)|}{(|R_h(1)||R_v(1)|)^{1/2}}.$$
(7.6)

The temporal correlation coefficient $\rho(1)$ can be obtained from the modulus of functions (7.1) and (7.2):

$$\rho(1) = |R_{co}(1)| / |R_{co}(0)|.$$
(7.7)

From the latter, the spectrum width estimate can be obtained assuming the Gaussian spectral shape:

$$\sigma_v = \frac{v_a}{\pi}\left[2\ln|R_{co}(0)|/|R_{co}(1)|\right]^{1/2}. \tag{7.8}$$

So we obtained the estimates of differential reflectivity, the copolar correlation coefficient, and spectrum width which are not biased by white noise. Because of the estimates of the Doppler velocity and the differential phase are not biased by noise, we obtained the full set of radar polarimetric variables immune to white noise. In the next sections, we compare estimates of differential reflectivity (7.5) and the copolar correlation coefficient (7.6) with conventional ones.

7.1. Differential reflectivity
In the SHV mode, the conventional estimate of differential reflectivity is obtained via (2.2). Here we compare bias and the standard deviation of the regular estimate (2.1) with the corresponding statistical properties of estimate (7.5). We can write variation equation for (7.5) as

$$Z_{dr1} + \delta Z_{dr1} = \frac{|R_h(1) + \delta\hat{R}_h(1)|}{|R_v(1) + \delta\hat{R}_v(1)|} = Z_{dr1}\frac{|1 + \delta\hat{R}_h(1)/R_h(1)|}{|1 + \delta\hat{R}_v(1)/R_v(1)|}.$$

Hereafter, we will use the subscript '1' to distinguish this estimate from the conventional one. To obtain bias and the variance of the estimate, we have to represent the latter variation equation to second order terms of the variations. Using approximation (E4) and (E5) from Appendix E we can represent the variation equation as

$$\frac{\delta Z_{dr1}}{Z_{dr1}} = \mathrm{Re}\left(\frac{\hat{R}_h(1)}{R_h(1)}\right) - \mathrm{Re}\left(\frac{\hat{R}_v(1)}{R_v(1)}\right) + \frac{1}{2}\left|\frac{\hat{R}_h(1)}{R_h(1)}\right|^2 - \frac{1}{2}\left|\frac{\hat{R}_v(1)}{R_v(1)}\right|^2 -$$

$$\mathrm{Re}\left(\frac{\hat{R}_h(1)}{R_h(1)}\right)\mathrm{Re}\left(\frac{\hat{R}_v(1)}{R_v(1)}\right) + \frac{3}{2}\mathrm{Re}^2\left(\frac{\hat{R}_v(1)}{R_v(1)}\right) - \frac{1}{2}\mathrm{Re}^2\left(\frac{\hat{R}_h(1)}{R_h(1)}\right). \tag{7.9}$$

Using identity (E1) equation (7.9) can be represented in the following form:

$$\frac{\delta Z_{dr1}}{Z_{dr1}} = \mathrm{Re}\left(\frac{\hat{R}_h(1)}{R_h(1)}\right) - \mathrm{Re}\left(\frac{\hat{R}_v(1)}{R_v(1)}\right) + \frac{1}{4}\left|\frac{\hat{R}_h(1)}{R_h(1)}\right|^2 + \frac{1}{4}\left|\frac{\hat{R}_v(1)}{R_v(1)}\right|^2 - \frac{1}{2}\mathrm{Re}\left(\frac{\hat{R}_h(1)\hat{R}_v(1)}{R_h(1)R_v(1)}\right) -$$

$$-\frac{1}{2}\text{Re}\left(\frac{\hat{R}_h(1)\hat{R}_v^*(1)}{R_h(1)R_v^*(1)}\right)+\frac{3}{4}\text{Re}\left(\frac{\hat{R}_v^2(1)}{R_v^2(1)}\right)-\frac{1}{4}\text{Re}\left(\frac{\hat{R}_h^2(1)}{R_h^2(1)}\right).\tag{7.10}$$

From (7.10), bias and the variance of the estimate is obtained.

7.1.1. Bias of differential reflectivity

To calculate bias, we have to average (7.10):

$$\frac{1}{Z_{dr}}Bias(Z_{dr1})=\frac{1}{4}\frac{<|\hat{R}_h(1)|^2>}{|R_h(1)|^2}+\frac{1}{4}\frac{<|\hat{R}_v(1)|^2>}{|R_v(1)|^2}-\frac{1}{2}\text{Re}\left(\frac{<\hat{R}_h(1)\hat{R}_v(1)>}{R_h(1)R_v(1)}\right)-$$

$$\frac{1}{2}\text{Re}\left(\frac{<\hat{R}_h(1)\hat{R}_v^*(1)>}{R_h(1)R_v^*(1)}\right)+\frac{3}{4}\text{Re}\left(\frac{<\hat{R}_v^2(1)>}{R_v^2(1)}\right)-\frac{1}{4}\text{Re}\left(\frac{<\hat{R}_h^2(1)>}{R_h^2(1)}\right).\tag{7.11}$$

All needed means are calculated in Appendix C (see (C5), (C9), (C15), and (C16)). Substitution of those into (7.11) yields:

$$Bias(Z_{dr1})=\frac{Z_{dr}}{2\rho^2(1)}\left\{\frac{2SNR_h[1-\rho^4(1)]+1}{2(M-1)SNR_h^2}+\frac{2SNR_v[1+3\rho^4(1)]+1}{2(M-1)SNR_v^2}+\frac{(1-\rho_{co}^2)[1+\rho^2(1)]}{M_{I1}}\right\}\tag{7.12}$$

It is seen that bias is positive and at wide spectra, it increases with the spectrum width because of $\rho^2(1)$ in the denominator. For narrow spectra, i.e. $\rho^2(1)\approx 1$, and strong signal, equation (7.12) becomes

$$Bias(Z_{dr1})=Z_{dr}\frac{(1-\rho_{co}^2)}{M_{I1}},\tag{7.13}$$

which is very close to a strong signal limit of conventional estimator's bias (2.5) because M_{II} is very close to M_I: the difference between (2.5) and (7.13) is of order of $1/M$, i.e., negligible. Fig. 7.1 presents biases of the conventional estimator and estimator (7.5). One can see from the figure that for narrow spectra ($\sigma_v\leq 3$ m s^{-1}) and moderate to strong SNR, these two estimators have almost equal biases. For weak signals and the spectrum widths less than 6 m s^{-1}, estimator (7.5) exhibits smaller biases than the conventional estimator. This is advantageous because estimator (7.5) should be applied at low SNR. The limitation $\sigma_v\leq 6$ m s^{-1} is not strong because Fang and Doviak (2001) have shown that more than 80 % of clouds and precipitation have such spectrum width.
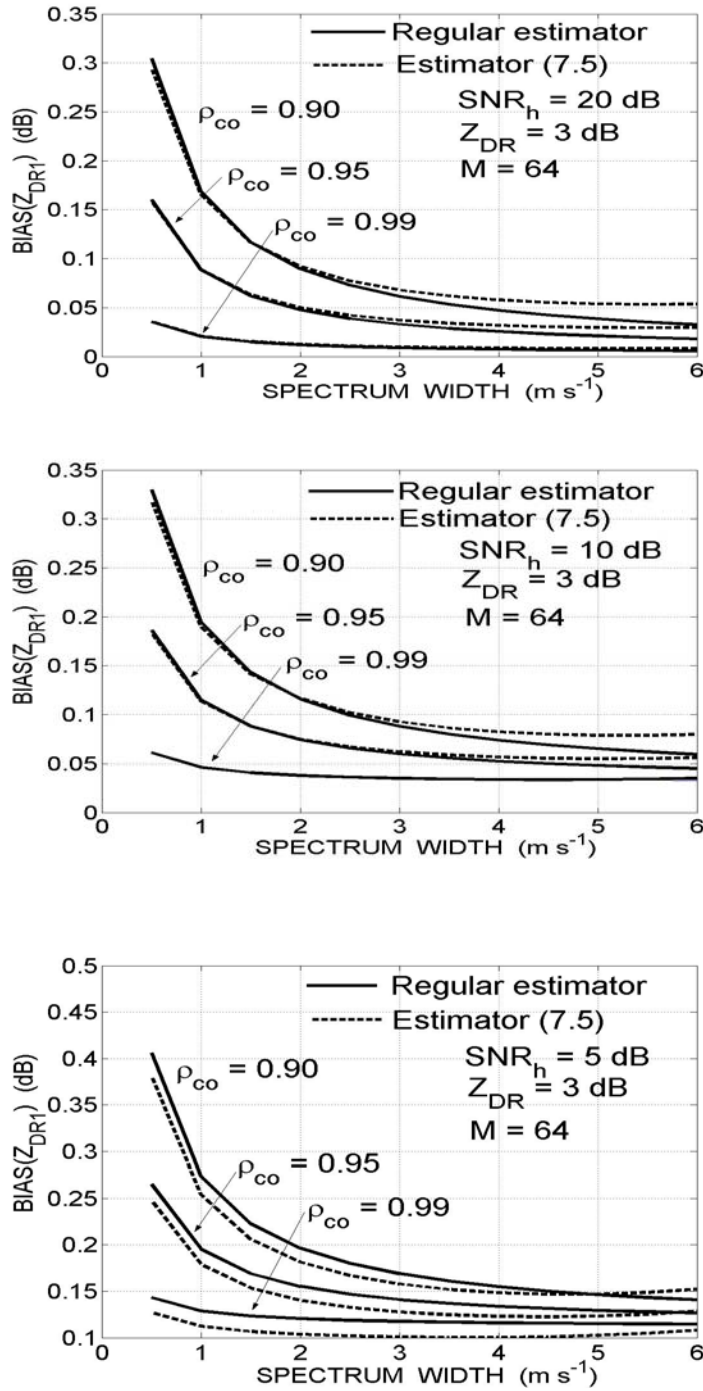
Fig. 7.1. Z_{DR} biases for "regular" estimator (2.6), solid lines, and estimator (7.5), dashed lines, for $SNR_v = 20$, 10, and 5 dB and copolar correlation coefficients indicated.

7.1.2. Standard deviation of differential reflectivity

An expression for the variance follows from the squared and averaged right hand side of (7.10):

$$\frac{1}{Z_{dr}^2} < \delta Z_{dr1}^2 > = < \mathrm{Re}^2\left(\frac{\hat{R}_h(1)}{R_h(1)}\right) > + < \mathrm{Re}^2\left(\frac{\hat{R}_v(1)}{R_v(1)}\right) > -2 < \mathrm{Re}\left(\frac{\hat{R}_h(1)}{R_h(1)}\right)\mathrm{Re}\left(\frac{\hat{R}_v(1)}{R_v(1)}\right) > \quad (7.14)$$

and we retained terms to second order of variations. Using (E4) we can rewrite the latter in the form:

$$\frac{1}{Z_{dr}^2} < \delta Z_{dr1}^2 > = \frac{1}{2}\left[\frac{<|\hat{R}_h(1)|^2>}{|R_h(1)|^2} + \frac{<|\hat{R}_v(1)|^2>}{|R_v(1)|^2} + \mathrm{Re}\left(\frac{<\hat{R}_h^2(1)>}{R_h^2(1)}\right) + \mathrm{Re}\left(\frac{<\hat{R}_v^2(1)>}{R_v^2(1)}\right)\right] -$$

$$\mathrm{Re}\left(\frac{<\hat{R}_h(1)\hat{R}_v(1)>}{R_h(1)R_v(1)}\right) - \mathrm{Re}\left(\frac{<\hat{R}_h(1)\hat{R}_v^*(1)>}{R_h(1)R_v^*(1)}\right). \quad (7.15)$$

All needed means are calculated in Appendix C (see (C5), (C9), (C15), and (C16)). Substitution into (7.15) yields:

$$< \delta Z_{dr1}^2 > = \frac{Z_{dr}^2}{\rho^2(1)}\left[\frac{2SNR_h[1+\rho^4(1)]+1}{2(M-1)SNR_h^2} + \frac{2SNR_v[1+\rho^4(1)]+1}{2(M-1)SNR_v^2} + \frac{(1-\rho_{co}^2)[1+\rho^2(1)]}{M_{I1}}\right]. \quad (7.16)$$

For strong signals and narrow spectra, variance (7.16) becomes

$$< \delta Z_{dr1}^2 > = Z_{dr}^2 \frac{2(1-\rho_{co}^2)}{M_{i1}} \quad (7.17)$$

which is very close to the corresponding limit of conventional estimate (2.10) because difference between $1/M_I$ and $1/M_{II}$ is of order of $1/M$.

Comparing variance (7.16) with the variance of conventional estimate (2.10), one can see that (7.16) has $\rho^2(1)$ in the denominator so that the standard deviation increases with spectrum width for wide spectra. Fig. 7.2 shows the standard deviations of the conventional estimator (2.2) and estimator (7.5). We see that for the spectral widths less than 5 m s^{-1}, both estimators perform equally: increase of the standard deviations for estimator (7.5) becomes visible for wider spectral widths. For low SNR and the spectrum widths less than 4 m s^{-1}, estimator (7.5) has lower standard deviations than the conventional one. According to Fang and Doviak (2001) and Fang et. al (2004) more than 60% of radar measurements have the spectrum widths less than 4 m s^{-1}. We see also that the results of the perturbation theory differ from the simulation results for low SNR and this is due to applicability limitations of the perturbation expansions.
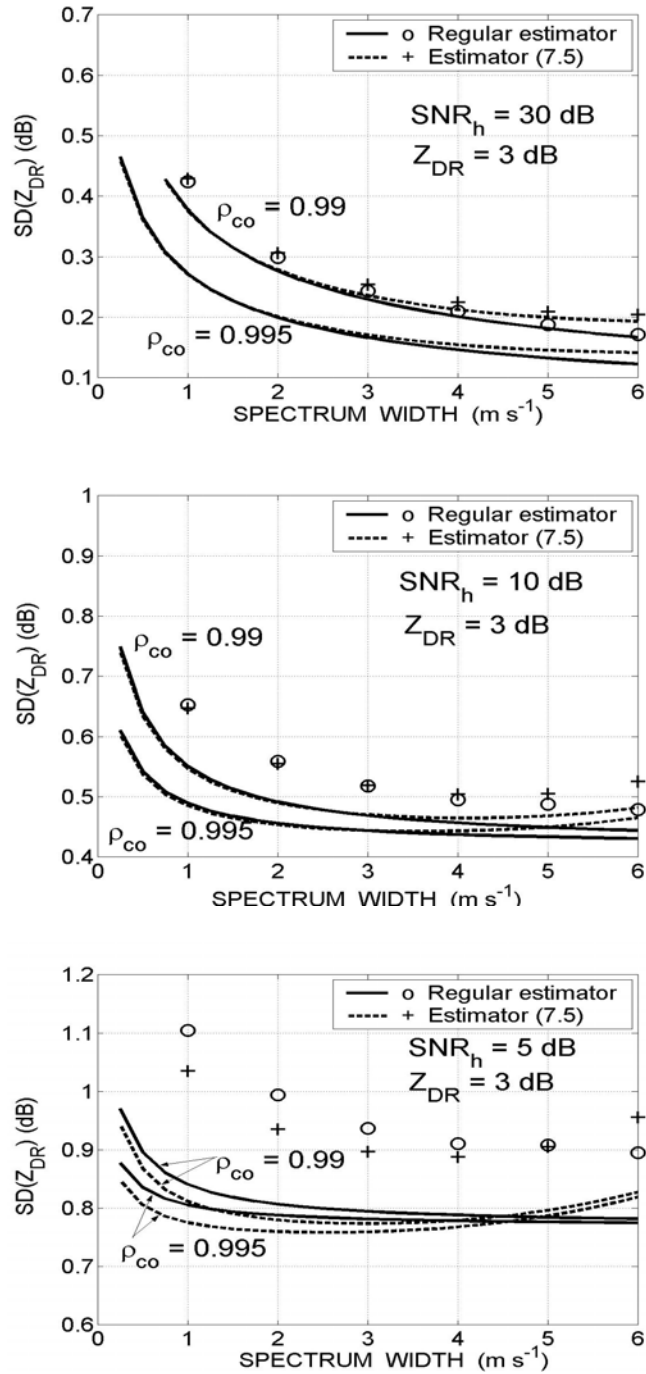
Fig. 7.2. Standard deviations of Z_{DR} for "regular" estimator (2.2), solid lines, and estimator (7.5), dashed lines, for SNR_h = 30, 10, and 5 dB and copolar correlation coefficients indicated. M = 64. Symbols are results of simulations for ρ_{co} = 0.99.

7.2.Modulus of the copolar correlation coefficient

In the SHV mode, the modulus is obtained via (4.1) and its bias and the standard deviation is given by (4.4) and (4.8). Here we calculate the statistical properties of estimate (7.6). To calculate those, we can use two different schemes. According to Fig. 1.1 the estimate of the 1-lag cross-correlation function can be calculated as follows:

$$\hat{R}_{col}(1) = \frac{1}{M-1} \sum_m e_m^{(h)} e_{m+1}^{(v)*}, \tag{7.18}$$

$$\hat{R}_{co2}(1) = \frac{1}{M-1} \sum_m e_{m+1}^{(h)} e_m^{(v)*}. \tag{7.19}$$

The mean values of the functions are different in the Doppler velocity terms:

$$R_{col}(1) = (S_h S_v)^{1/2} \rho(1) \rho_{co} \exp(j\varphi_{dp} + j\pi v/v_a), \tag{7.20}$$

$$R_{co2}(1) = (S_h S_v)^{1/2} \rho(1) \rho_{co} \exp(j\varphi_{dp} - j\pi v/v_a), \tag{7.21}$$

but the modules of the functions are equal so that we can accept the following estimation for the modulus of the correlation function:

$$|\hat{R}_{co}(1)| = \frac{1}{2}(|\hat{R}_{col}(1)| + |\hat{R}_{co2}(1)|). \tag{7.22}$$

Then estimator (7.6) can be represented as:

$$\hat{\rho}_{col} = \frac{|\hat{R}_{col}(1)| + |\hat{R}_{co2}(1)|}{2(|\hat{R}_h(1)| \, |\hat{R}_v(1)|)^{1/2}}. \tag{7.23}$$

We will add the subscript 1 to the estimate of the modulus to distinguish this estimation from the conventional one, i.e., (4.1). The perturbation equation for (7.23) is:

$$\rho_{co} + \delta\hat{\rho}_{col} = \frac{|R_{col}(1) + \delta\hat{R}_{col}(1)| + |R_{co2}(1) + \hat{R}_{co2}(1)|}{2(|R_h(1) + \delta\hat{R}_h(1)| \, |R_v(1) + \delta\hat{R}_v(1)|)^{1/2}}. \tag{7.24}$$

It is follows from (7.20) and (7.21):

$$\hat{\rho}_{col} = \frac{|\hat{R}_{col}(1)|}{(|\hat{R}_h(1)| \, |\hat{R}_v(1)|)^{1/2}} = \frac{|\hat{R}_{co2}(1)|}{(|\hat{R}_h(1)| \, |\hat{R}_v(1)|)^{1/2}}.$$

Then (7.24) can be represented as

$$\frac{\delta\hat{\rho}_{co1}}{\rho_{co}} = \frac{|1+\delta\hat{R}_{co1}(1)/R_{co1}(1)| + |1+\hat{R}_{co2}(1)/R_{co2}(1)|}{2(|1+\delta\hat{R}_h(1)/R_h(1)||1+\delta\hat{R}_v(1)/R_v(1)|)^{1/2}} - 1. \qquad (7.25)$$

Using approximations (E4) and (E7) the latter equation can be written as:

$$\frac{\delta\hat{\rho}_{co1}}{\rho_{co}} = -\frac{1}{2}\mathrm{Re}\left(\frac{\delta\hat{R}_v(1)}{R_v(1)}\right) - \frac{1}{2}\mathrm{Re}\left(\frac{\delta\hat{R}_h(1)}{R_h(1)}\right) + \frac{1}{16}\frac{|\delta\hat{R}_v(1)|^2}{|R_v(1)|^2} + \frac{1}{16}\frac{|\delta\hat{R}_h(1)|^2}{|R_h(1)|^2} + \frac{1}{2}\mathrm{Re}\left(\frac{\delta\hat{R}_{co1}(1)}{R_{co1}(1)}\right)$$

$$+\frac{1}{2}\mathrm{Re}\left(\frac{\delta\hat{R}_{co2}(1)}{R_{co2}(1)}\right) + \frac{1}{4}\mathrm{Re}\left(\frac{\delta\hat{R}_h(1)}{R_h(1)}\right)\mathrm{Re}\left(\frac{\delta\hat{R}_v(1)}{R_v(1)}\right) + \frac{5}{16}\mathrm{Re}\left(\frac{\delta\hat{R}_v^2(1)}{R_v^2(1)}\right) + \frac{5}{16}\mathrm{Re}\left(\frac{\delta\hat{R}_h^2(1)}{R_h^2(1)}\right)$$

$$-\frac{1}{8}\mathrm{Re}\left(\frac{\delta\hat{R}_{co1}(1)\delta\hat{R}_v(1)}{R_{co1}(1)R_v(1)}\right) - \frac{1}{8}\mathrm{Re}\left(\frac{\delta\hat{R}_{co1}(1)\delta\hat{R}_v^*(1)}{R_{co1}(1)R_v^*(1)}\right) - \frac{1}{8}\mathrm{Re}\left(\frac{\delta\hat{R}_{co1}(1)\delta\hat{R}_h(1)}{R_{co1}(1)R_h(1)}\right) - \frac{1}{8}\mathrm{Re}\left(\frac{\delta\hat{R}_{co1}(1)\delta\hat{R}_h^*(1)}{R_{co1}(1)R_h^*(1)}\right)$$

$$+\frac{1}{8}\frac{|\delta\hat{R}_{co1}(1)|^2}{|R_{co1}(1)|^2} + \frac{1}{8}\frac{|\delta\hat{R}_{co2}(1)|^2}{|R_{co2}(1)|^2} - \frac{1}{8}\mathrm{Re}\left(\frac{\delta\hat{R}_{co1}^2(1)}{R_{co1}^2(1)}\right) - \frac{1}{8}\mathrm{Re}\left(\frac{\delta\hat{R}_{co2}^2(1)}{R_{co2}^2(1)}\right) - \frac{1}{8}\mathrm{Re}\left(\frac{\delta\hat{R}_{co2}(1)\delta\hat{R}_v(1)}{R_{co2}(1)R_v(1)}\right)$$

$$-\frac{1}{8}\mathrm{Re}\left(\frac{\delta\hat{R}_{co2}(1)\delta\hat{R}_v^*(1)}{R_{co2}(1)R_v^*(1)}\right) - \frac{1}{8}\mathrm{Re}\left(\frac{\delta\hat{R}_{co2}(1)\delta\hat{R}_h(1)}{R_{co2}(1)R_h(1)}\right) - \frac{1}{8}\mathrm{Re}\left(\frac{\delta\hat{R}_{co2}(1)\delta\hat{R}_h^*(1)}{R_{co2}(1)R_h^*(1)}\right). \qquad (7.26)$$

From (7.26), expressions for bias and the standard deviation follow.

7.2.1. Bias of the estimator
Averaging (7.26), we get an expression for the bias:

$$\frac{Bias(\hat{\rho}_{co1})}{\rho_{co}} = \frac{1}{16}\frac{<|\delta\hat{R}_v(1)|^2>}{|R_v(1)|^2} + \frac{1}{16}\frac{<|\delta\hat{R}_h(1)|^2>}{|R_h(1)|^2} + \frac{1}{8}\mathrm{Re}\left(\frac{<\delta\hat{R}_h(1)\delta\hat{R}_v(1)>}{R_h(1)R_v(1)}\right)$$

$$+\frac{1}{8}\mathrm{Re}\left(\frac{<\delta\hat{R}_h(1)\delta\hat{R}_v^*(1)>}{R_h(1)R_v^*(1)}\right) + \frac{5}{16}\mathrm{Re}\left(\frac{<\delta\hat{R}_v^2(1)>}{R_v^2(1)}\right) + \frac{5}{16}\mathrm{Re}\left(\frac{<\delta\hat{R}_h^2(1)>}{R_h^2(1)}\right) - \frac{1}{8}\mathrm{Re}\left(\frac{<\delta\hat{R}_{co1}(1)\delta\hat{R}_v(1)>}{R_{co1}(1)R_v(1)}\right)$$

$$-\frac{1}{8}\mathrm{Re}\left(\frac{<\delta\hat{R}_{co1}(1)\delta\hat{R}_v^*(1)>}{R_{co1}(1)R_v^*(1)}\right) - \frac{1}{8}\mathrm{Re}\left(\frac{<\delta\hat{R}_{co1}(1)\delta\hat{R}_h(1)>}{R_{co1}(1)R_h(1)}\right) - \frac{1}{8}\mathrm{Re}\left(\frac{<\delta\hat{R}_{co1}(1)\delta\hat{R}_h^*(1)>}{R_{co1}(1)R_h^*(1)}\right)$$

$$+\frac{1}{8}\frac{<|\delta\hat{R}_{co1}(1)|^2>}{|R_{co1}(1)|^2}+\frac{1}{8}\frac{<|\delta\hat{R}_{co2}(1)|^2>}{|R_{co2}(1)|^2}-\frac{1}{8}\mathrm{Re}\left(\frac{<\delta\hat{R}_{co1}^2(1)>}{R_{co1}^2(1)}\right)-\frac{1}{8}\mathrm{Re}\left(\frac{<\delta\hat{R}_{co2}^2(1)>}{R_{co2}^2(1)}\right)$$

$$-\frac{1}{8}\mathrm{Re}\left(\frac{<\delta\hat{R}_{co2}(1)\delta\hat{R}_v(1)>}{R_{co2}(1)R_v(1)}\right)-\frac{1}{8}\mathrm{Re}\left(\frac{<\delta\hat{R}_{co2}(1)\delta\hat{R}_v^*(1)>}{R_{co2}(1)R_v^*(1)}\right)-\frac{1}{8}\mathrm{Re}\left(\frac{<\delta\hat{R}_{co2}(1)\delta\hat{R}_h(1)>}{R_{co2}(1)R_h(1)}\right)$$

$$-\frac{1}{8}\mathrm{Re}\left(\frac{<\delta\hat{R}_{co2}(1)\delta\hat{R}_h^*(1)>}{R_{co2}(1)R_h^*(1)}\right)\quad. \tag{7.27}$$

All needed means are calculated in Appendix D. Using the expressions from the appendix we obtain

$$BIAS(\rho_{co1})=\frac{1}{4\rho_{co}\rho^2(1)}\left\{\frac{\rho_{co}^2+2SNR_h[2-\rho_{co}^2+3\rho_{co}^2\rho^4(1)]}{4(M-1)SNR_h^2}+\frac{\rho_{co}^2+2SNR_v[2-\rho_{co}^2+3\rho_{co}^2\rho^4(1)]}{4(M-1)SNR_v^2}\right.$$

$$\left.+\frac{1}{(M-1)SNR_hSNR_v}+\frac{(1-\rho_{co}^2)[2-\rho_{co}^2(1+\rho^2(1))]}{2M_{I1}}\right\}. \tag{7.28}$$

It can be seen that bias is positive for all SNR, spectral widths, and copolar correlation coefficients. For large SNR and narrow spectra, the latter expression becomes

$$BIAS(\rho_{co1})=\frac{(1-\rho_{co}^2)^2}{4M_{I1}\rho_{co}}$$

that is close to corresponding limit of conventional estimate (4.4) if we neglect difference between $1/M_I$ and $1/M_{II}$. Thus, for strong signals and narrow spectra, estimate (7.6) has the same bias as the conventional one. Due to $\rho^2(1)$ in the denominator of (7.28), the bias of the estimator (7.6) increases with the spectrum width for wide spectra.

Biases of the conventional and 1-lag estimators are compared in Fig. 7.3. It is seen that the 1-lag estimator has less bias than conventional estimator (4.1) at low signal-to-noise ratios. This is advantageous because estimator (7.23) should be applied at low SNR where noise bias of the conventional estimator is prone to bias. For wide spectra, the bias of the 1-lag estimator becomes larger than bias of the conventional estimator because of $\rho(1)$ in the denominator of (7.28). But for spectrum widths less than 6 m s^{-1} this increase is not significant as it is seen in Fig. 7.3.
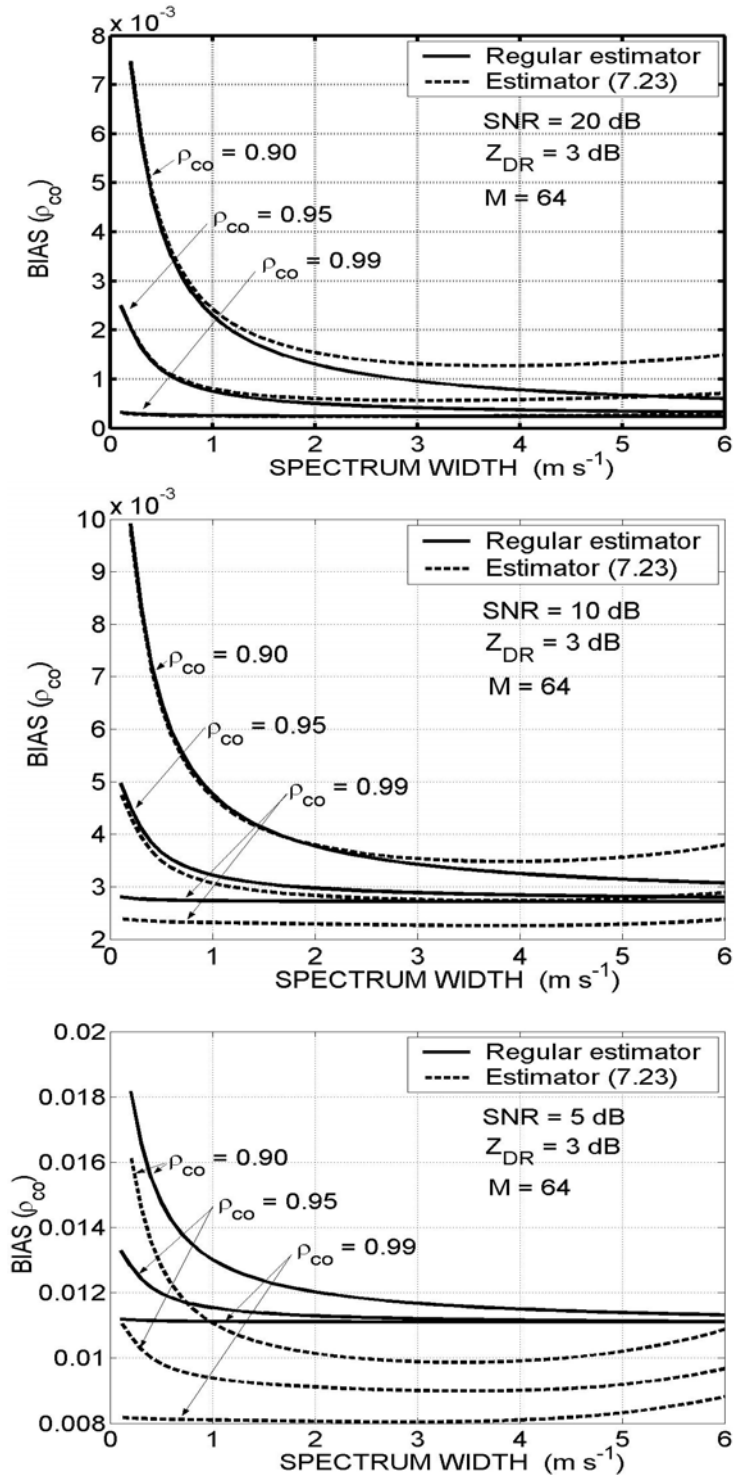
Fig. 7.3. Bias of the modulus of the copolar correlation coefficient calculated via "classical" estimator (4.1) (thick lines) and estimator (7.23) (dashed lines).

7.2.2. Standard deviation of the estimator

To obtain the variance of estimator (7.23), we have to average (7.26) squared, i.e.:

$$\frac{4}{\rho_{co}^2} < \delta^2 \hat{\rho}_{col} > = < \left[-\mathrm{Re}\left(\frac{\delta \hat{R}_v}{R_v}\right) - \mathrm{Re}\left(\frac{\delta \hat{R}_h}{R_h}\right) + \mathrm{Re}\left(\frac{\delta \hat{R}_{col}}{R_{col}}\right) + \mathrm{Re}\left(\frac{\delta \hat{R}_{co2}}{R_{co2}}\right) \right]^2 > .$$

In the latter equation we retained terms to second order of variations. Performing calculations using identities (E1) and (E2) and the means from Appendix D, we obtain

$$SD(\hat{\rho}_{col}) = \frac{1}{\rho(1)} \left\{ \frac{\rho_{co}^2 + 2SNR_h(1-\rho_{co}^2)[1+\rho^4(1)]}{8(M-1)SNR_h^2} + \frac{\rho_{co}^2 + 2SNR_v(1-\rho_{co}^2)[1+\rho^4(1)]}{8(M-1)SNR_v^2} \right. $$

$$\left. + \frac{1}{4(M-1)SNR_h SNR_v} + \frac{(1-\rho_{co}^2)^2[1+\rho^2(1)]}{4M_{I1}} \right\}^{1/2} . \qquad (7.29)$$

For high SNR and narrow spectra, i.e., SNR $\gg 1$ and $\rho(1) \rightarrow 1$, equation (7.29) becomes

$$SD(\hat{\rho}_{col}) = \frac{1-\rho_{co}^2}{2^{1/2} M_{I1}^{1/2}}$$

that is very close to corresponding limit of the standard deviation (4.8) of the conventional estimator; closeness is of order of $1/M$. Thus, for strong signals and narrow spectra, the standard deviations of the conventional estimator and estimator (7.23) are practically equal.

Fig. 7.4 shows the standard deviations of the estimators. It is seen than for low signal-to-noise ratios, estimator (7.23) has low standard deviation than the conventional estimator. This is an advantage because estimator (7.23) should be applied at low SNR. For wide spectra, the standard deviation of estimator (7.23) increases because of $\rho(1)$ in the denominator in (7.29). It is seen from Fig. 7.4 that for spectral widths less than 6 m s^{-1} this increase is not significant. Results of computer simulations are presented in the figure with the symbols. One can see that for high SNR, the simulation results follow the curves very closely, but for low SNR, the standard deviations of the simulations are larger than the calculated ones. It is because for low SNR, the perturbation approximations are not fully applicable. We noticed such deviations earlier for all polarization parameters.
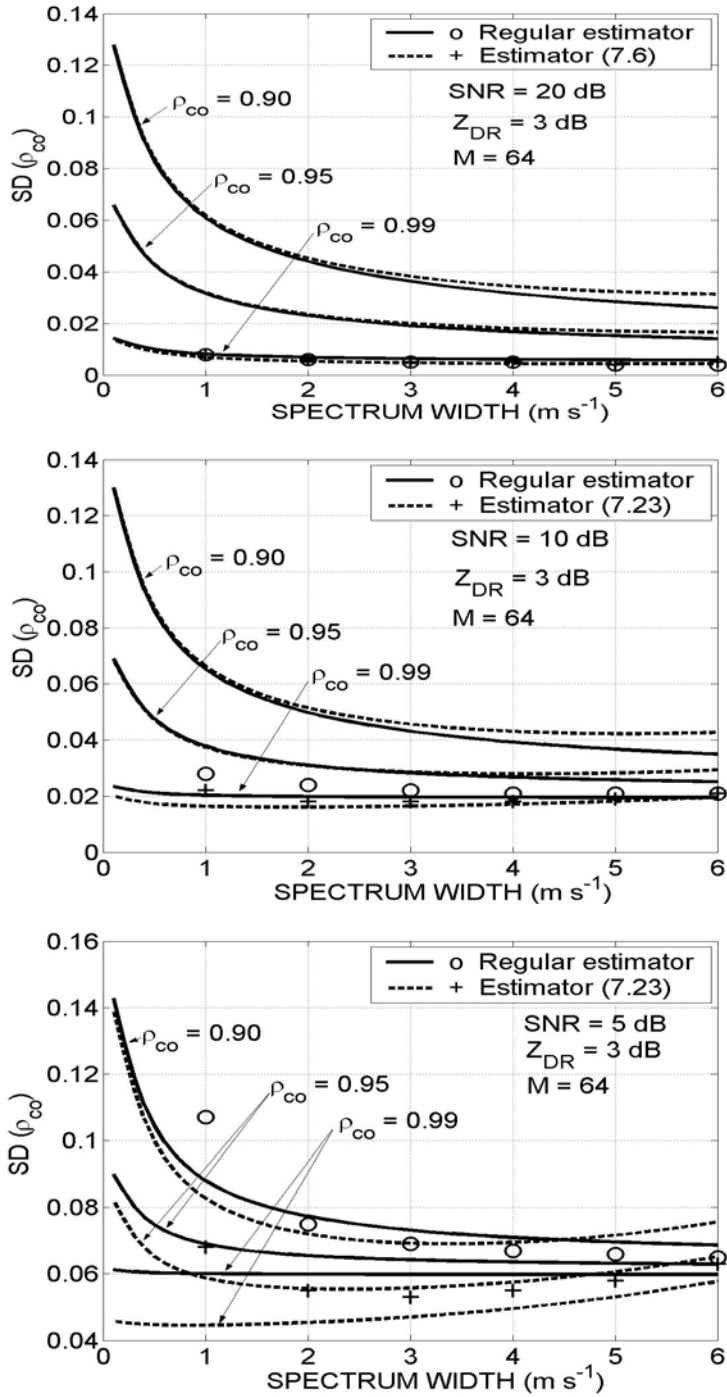
Fig. 7.4. Standard deviations of the modulus of the copolar correlation coefficient calculated via "classical" estimator (4.1) (solid lines) and estimator (7.23) (dashed lines). Results of simulations for $\rho_{co} = 0.99$ are shown with the symbols.

7.3. Performance on radar data

To assess the new estimators of differential reflectivity and the modulus of the copolar correlation coefficient described in this section, time series data, (i.e., I and Q signal samples) from both H and V channels have been recorded. Herein such data obtained during April to August 2002 is used. Recording was made through the RVP-7 processor on seventeen days. The number of samples from each channel (H and V) was 128 per range gate. The ground clutter filter was off, so that some contamination from clutter is expected in the data. Because the elevation angles were larger than 1°, the majority of echoes were weather signals.

Fig. 7.5 shows a scatter plot of difference of differential reflectivities computed via conventional estimator (2.2) (i.e., $\hat{Z}_{DR}$) and estimator (7.5) (i.e., $\hat{Z}_{DR1}$). The figure presents data with SNR > 20 dB. The total number of points in the figure is 17807. The differential reflectivities were calculated with the accuracy of 0.01 dB that is why the data in the figure has a form of horizontal lines. One can see few Z_{DR}s less -4 dB and over 5 dB; these are definitely from ground clutter. The vast majority of the data with negative Z_{DR} is from clutter too. It is seen that there are no points with the difference exceeding 0.1 dB. Therefore estimator (7.5) is applicable to signals form ground clutter as well.
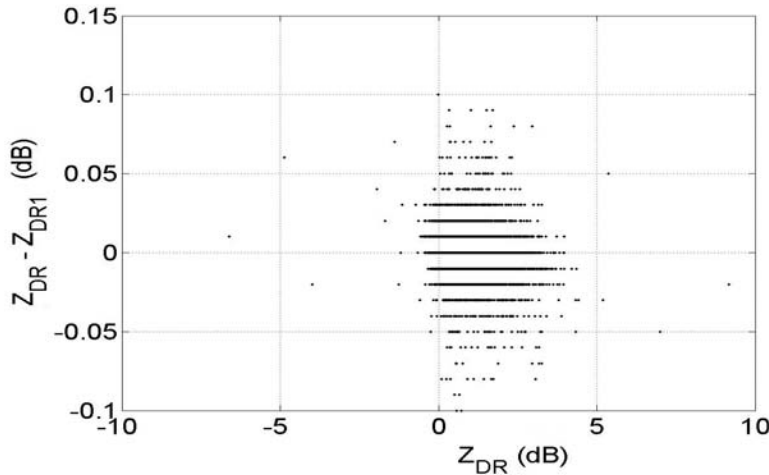

Fig. 7.5. Scatter plot of the difference of $\hat{Z}_{DR}$ calculated via regular
algorithm (2.2) and estimator (7.5) at SNR$_h \geq$ 20 dB.
The number of points is 17807.

Fig. 7.6 presents probability of the difference for the same data. It is seen that 99% of the data have the absolute difference less than 0.03 dB.
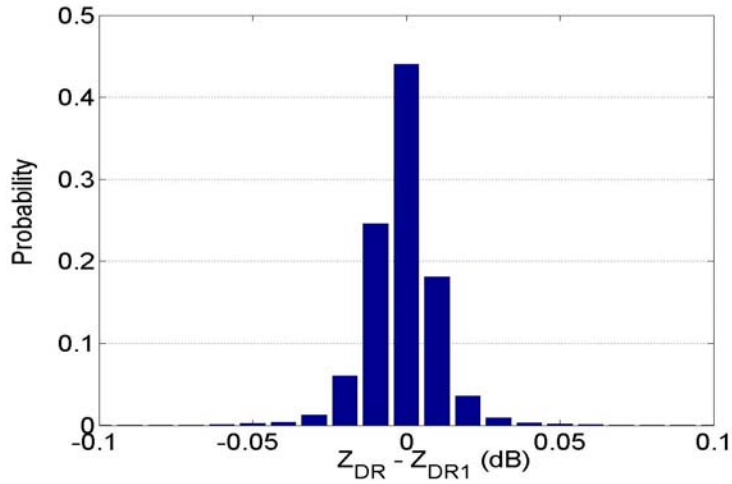
Fig. 7.6. Probability of the difference of differential reflectivities
   obtained via estimators (2.2) and (7.5). WSR-88D KOUN.
   $SNR_h \geq 20$ dB. The number of the measurements is 17807.

In Fig. 7.7, a scatter plot of the difference of Z_{DR} calculated via algorithms (2.2) and (7.5) is shown for SNR in the interval 10 to13 dB. No noise subtraction has been done to algorithm (2.2), so we should expect negative bias in Z_{DR} - Z_{DR1}. Such bias is indeed apparent in Fig. 7.7.
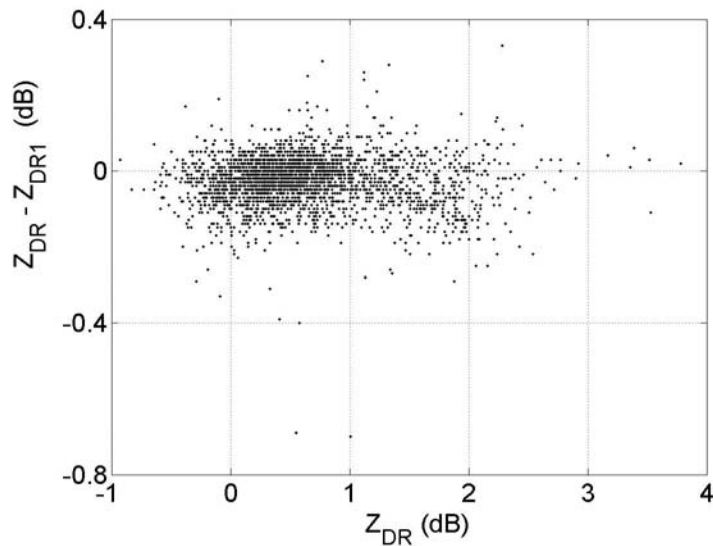

Fig. 7.7. Same as in Fig. 7.5 but for $10 \leq SNR_h \leq 13$ dB.
   The number of points is 2830.

Fig. 7.8 represents a scatter plot of the modulus of the correlation coefficient calculated via conventional algorithms (4.1) designated in the figure as ρ_{co} (lag 0), and algorithm (7.23), designated as ρ_{co} (lag 1). No noise subtraction has been done in the conventional algorithm, SNR is more than 20 dB, and the number of points is 17807. It is seen that the estimate ρ_{co} (lag 1) tends to be closer to one than the conventional estimate. This is caused by slight noise bias (even at large SNR) in the conventional estimate.

In Fig. 7.9, a similar scatter plot is presented but for SNR_h in the interval 10 to 13 dB. Stronger noise bias effect is evident from the figure.
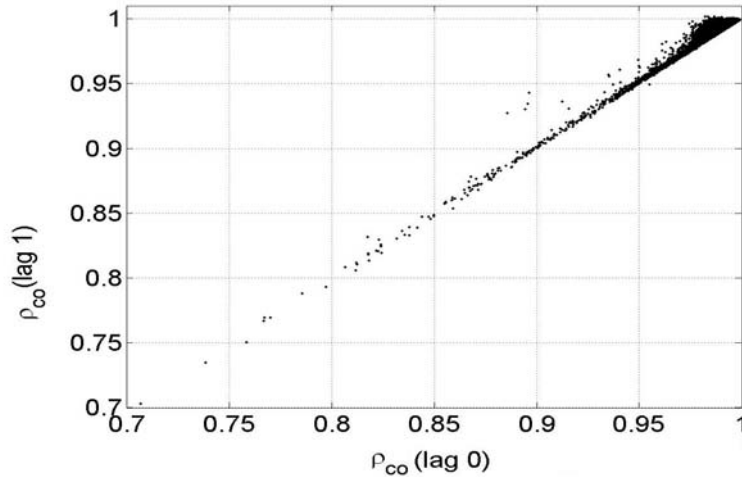

Fig. 7.8. Scatter plot of ρ_{co} obtained via conventional algorithm (4.1) and estimator (7.23) at $SNR_h \geq 20$ dB. The number of points is 17807.
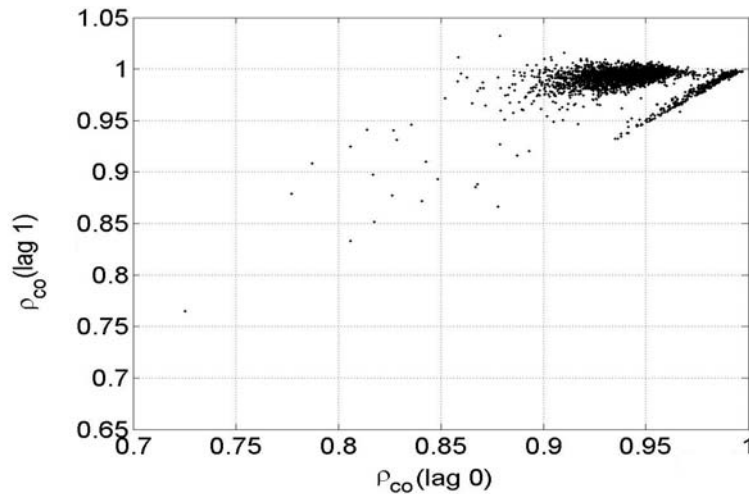

Fig. 7.9. Same as in Fig. 7.8 but for $10 \leq SNR_h \leq 13$ dB. The number of points is 2830.

Conclusions

To measure precipitation with accuracy of 15 to 20 % and to measure polarimetric parameters in snow, desired levels of biases and the standard deviations of the measurements are summarized below.

Desired biases and standard deviations of estimations
of the polarimetric variables

Z_{DR}		φ_{dp}		ρ_{co}	
Bias dB	SD dB	Bias deg	SD deg	Bias	SD
0.1	0.2	1	2	0.005	0.01

Biases and the standard deviations have different impact on the measurements. The standard deviations can be reduced with additional spatial averaging, but biases can not and thus it is important to have biases as low as possible. In the report, the statistical biases and standard deviations are analyzed and main results are as follows.

Differential reflectivity, Z_{DR}
- Statistical biases of Z_{DR} due to finite number of samples in the estimate are less than 0.1 dB if the copolar correlation coefficient $\rho_{co} \geq 0.98$ (i.e., in rain), signal-to-noise ratios are larger than 10 dB, and the spectrum width is over 2 m s^{-1}. In the melting layers, in regions with hail, and at long distances where ρ_{co} drops to 0.7 to 0.9, biases are positive and can exceed 0.2 dB. Such bias has little impact on Z_{DR} in the melting layer because its value is already sufficiently high, but it can slightly bias differential reflectivity in hail.
- Additional noise such as thermal noise of the ground and precipitation, noise from electrically active clouds, and temporal variations of the system gains in the channels cause bias less than 0.1 dB in magnitude if additional noise or variations of the gains are less than 1 dB and SNR is larger than 15 dB. For lower SNR, this bias is negative and rapidly increases in magnitude with decrease of SNR.
- The standard deviation of Z_{DR} estimate in one radar volume (i.e., at a point) is 0.4 dB for $\rho_{co} \geq 0.98$ and SNR > 20 dB. To achieve the desired level of uncertainties of 0.2 dB, four consecutive estimates in range can be used. The standard deviation increases with decrease of ρ_{co} and SNR.
- Additional uncompensated noise of 1 dB has little effect on the standard deviations of the measurements.

Differential phase, φ_{dp}
- In the simultaneous transmission mode, the differential phase can be measured in the 360° unambiguous interval. Due to statistical fluctuations of the φ_{dp} estimate there are jumps of the estimates at the edges of the interval. To avoid the occurrence of these discontinuities, the differential phase offset (break point in the 360° interval) should be set at a value which is about 30° below the system differential phase φ_{dps}. This phase is measured in parts of storms closest to the

radar. Then the measurement interval will start at 30° and end at $360^{\circ} - 30^{\circ} = 330^{\circ}$ which is sufficient for most (but not all) weather events at S-band.

- The standard deviation of φ_{dp} estimate at a point is 2° for $\rho_{co} \geq 0.98$, SNR > 20 dB, and the spectrum width larger than 2 m s^{-1}. For SNR about 10 dB, the standard deviation is 4° and to reduce the uncertainty to 2°, four estimates from consecutive range locations should be averaged. The standard deviation increases rapidly with decrease of ρ_{co}; at $\rho_{co} = 0.8$ it reaches 10° even for strong signals, (SNR = 20 dB and the spectrum width of 3 m s^{-1}).

Modulus of the copolar correlation coefficient, ρ_{co}

- Bias due to a finite number of samples in the estimate is positive and less than 0.005 if the copolar correlation coefficient $\rho_{co} \geq 0.98$, SNR >10 dB, and the spectrum width is larger than 2 m s^{-1}. In the melting layer, in regions with hail, and at long distances where ρ_{co} drops to 0.7 to 0.9, biases are positive and can exceed the desired level of 0.005 but this is not detrimental because ρ_{co} itself is low and out of the range typical for precipitation.
- If ρ_{co} is clipped at 1 (for the estimates that are larger than 1) it will bias statistics of the coefficient. This setting is done for instance in the RVP8 processor. To reduce statistical uncertainties by spatial averaging, it is important to use the actual estimate of ρ_{co} even if it is larger than 1. Otherwise a negative bias will be introduced to the spatial average.
- Additional noise of 1 dB causes negative bias less than 0.005 only if SNR > 15 dB. This bias increases rapidly with decrease of SNR.
- The standard deviations of point estimate is less than 0.01 in rain if $\rho_{co} \geq 0.98$, SNR >15 dB, and the spectrum width is larger than 2 m s^{-1}. The deviations increase rapidly with decreasing SNR and ρ_{co}.
- Additional noise of 1 dB has little effect on the standard deviations of the measurements.

Radar sensitivity

- In the simultaneous transmittion mode, the total transmitted power is split into two channels so that the H channel has two times lower transmitted power than the legacy WSR-88D. Because the noise level of the receivers is same as for the legacy WSR-88D, the total loss of sensitivity is two times or 3 dB. To recover sensitivity, two approaches have been considered.
- The first approach is based on coherent summation of the voltages in the H and V channels with V voltage shifted by the differential phase. In this case, the equivalent SNR is a product of the legacy SNR with this number: $(Z_{dr} + 2Z_{dr}^{1/2}\rho_{co} + 1)/4Z_{dr}$, where differential reflectivity is in linear units. For small particles $Z_{dr} \approx 1$ and $\rho_{co} \approx 1$, and this number is close to 1, i.e., it is possible to achieve legacy sensitivity. For Zdr = 2 (3 dB), the ratio is 0.75 which is still better than 0.5 that is obtained without coherent summation, i.e., in the H channel in the SHV mode.

- The second approach utilizes the measurements of the copolar correlation function R_{co}. This function is routinely calculated in order to obtain the differential phase and the modulus of the correlation coefficient. The modulus of the function is $|R_{co}| = S_h \rho_{co}/Z_{dr}^{1/2}$, where S_h is weather signal power in the H channel. This modulus is not biased by white noise and is proportional to the weather signal power. For small particles ($Z_{dr} \approx 1$ and $\rho_{co} \approx 1$), this function is close to S_h. It is shown in the report, that the standard deviation of $|R_{co}|$ estimate is same as the standard deviation of the regular power estimate in the legacy channel so that measurements of $|R_{co}|$ should show same weak reflectivity regions like the legacy channel does. This approach requires further study.

Velocity estimates in both channels

- WSR-88D KOUN has two almost identical radar channels, i.e., H and V channels. The signals in both channels can be used to increase the accuracy of the base radar moments. The Doppler velocity measurements have been considered in the report. It is shown that calculations of two temporal correlation functions for the channels increases the accuracy of the velocity estimate for low SNR. For small particles with Z_{dr} close to 1, the sum of the correlation functions improves the velocity estimate by 2 dB, it is only 1 dB worse than the estimate for the legacy WSR-88D. For larger Z_{dr}, these improvements are between 2 dB and 1 dB.

Z_{DR} and ρ_{co} estimates immune to noise bias

- Z_{DR} and ρ_{co} estimates are prone to bias due to uncompensated noise. The noise levels in the radar channels are hard to control with the accuracy better than 1 dB. Additional thermal noise from ground and precipitation, wideband electrical signals from thunderstorms, and fluctuations of system gains make this control almost impossible. It is shown in the report that additional noise of 1 dB can bias estimates of differential reflectivity and the modulus of the copolar correlation coefficient.

- A method to calculate Z_{DR} and ρ_{co} estimates that has no noise bias was proposed. The method is based on calculation of cross correlation coefficients that are immune to bias from white noise. In comparison with the conventional estimators, it was shown that the method has lower bias and standard deviations for spectral width lower than 6 m s^{-1}, which is sufficient for vast majority of meteorological situations.

Appendix A. The variances and covariance of the powers in the H and V channels

To calculate the bias and the variance of differential reflectivity, the variance of the powers in the channels and theirs covariance are needed. Here we calculate relevant parameters. The estimate of the power in the H channel is

$$\hat{P}_h = \frac{1}{M}\sum_{m=1}^{M} e_m^{(h)} e_m^{(h)*} , \qquad (A1)$$

The deviation of the power is introduced as

$$\delta\hat{P}_h = \hat{P}_h - P_h, \qquad (A2)$$

where P_h is the mean power. We need to calculate the mean value of this deviation squared, i.e., $<\delta\hat{P}_h^2>$. From (A2) and (A1) we obtain

$$<\delta\hat{P}_h^2> = \frac{1}{M^2}\sum_{m,n=1}^{M} <e_m^{(h)} e_m^{(h)*} e_n^{(h)} e_n^{(h)*}> - P_h^2, \qquad (A3)$$

The voltages are complex Gaussian signals and therefore the fourth order moments reduce to sums of products of second order moments (see e.g., Whalen 1971, section 4.1):

$$<e_m^{(h)} e_m^{(h)*} e_n^{(h)} e_n^{(h)*}> = <e_m^{(h)} e_m^{(h)*}><e_n^{(h)} e_n^{(h)*}> + <e_m^{(h)} e_n^{(h)*}><e_m^{(h)*} e_n^{(h)}> +$$
$$<e_m^{(h)} e_n^{(h)}><e_m^{(h)*} e_n^{(h)*}> \qquad (A4)$$

Using (1.5), the pertinent second moment that enter in (A4) are

$$<e_n^{(h)} e_m^{(h)*}> = S_h \rho[(m-n)T]\exp[j\pi v_n(m-n)] + N_h\delta_{nm} , \qquad (A5)$$
$$<e_n^{(h)} e_m^{(h)}> = <e_n^{(h)*} e_m^{(h)*}> = 0.$$

Substitution (A5) into (A4) and then into (A3) yields

$$<\delta P_h^2> = \frac{(S_h+N_h)^2}{M} + \frac{2S_h^2}{M^2}\sum_{m=1}^{M-1}(M-m)|\rho(mT)|^2 .$$

In (A5), we assume that the Doppler velocity and the spectrum width are equal for the H and V polarizations. We can rewrite the latter expression using the number of independent samples M_{I} (see e.g., Doviak and Zrnic 1993, section 6.3.1.2) as:

$$\frac{<\delta P_h^2>}{S_h^2} = \frac{2SNR_h + 1}{M\ SNR_h^2} + \frac{1}{M_I}, \qquad\qquad (A6)$$

$$M_I = M\left(1 + 2\sum_{m=1}^{M-1}(1 - m/M)\,|\,\rho(mT)\,|^2\right)^{-1}. \qquad\qquad (A7)$$

Representation (A6) is very useful because its first term does not depend on the spectrum width and depends only on signal-to-noise ratio. The second term in (A6) depends on the spectrum width and does not depend on noise.

For the vertical channel, we can write a similar equation:

$$\frac{<\delta P_v^2>}{S_v^2} = \frac{2SNR_v + 1}{M\ SNR_v^2} + \frac{1}{M_I}, \qquad\qquad (A8)$$

Replacing summation in (A7) with integration (Doviak and Zrnic 1993, section 6.3.1.2) one obtains

$$M_I \approx M\,\pi^{1/2}\,\sigma_{vn} = 4MT\,\pi^{1/2}\,\sigma_v/\lambda, \qquad\qquad (A9)$$

where σ_{vn} is the normalized spectrum width, $\sigma_{vn} = \sigma_v/v_a$ and v_a is the unambiguous velocity: $v_a = \lambda/4T$. The product MT in (A9) is the dwell time so that for a given spectral width, M_I depends on the dwell time only and therefore M_I is nearly same for high PRF and low PRF modes of the WSR-88D. Thus, the accuracy of polarimetric measurements will be nearly same for high and low PRF for sufficiently high SNR (more than 20 dB) to eliminate influence of noise contribution which is inversely proportional to the number of samples. In Fig. A1, a ratio of $M_I/M\,\pi^{1/2}\,\sigma_{vn}$ is plotted for $M = 32$, 48, and 64 and $v_a = 25$ m s^{-1}. We see that for $M = 64$ and the spectrum width in the interval of 1..15 m s^{-1}, the deviation of this ratio from 1 is less than 10%. Thus we will consider approximation (A9) as good for $0.04 \leq \sigma_{vn} \leq 0.60$
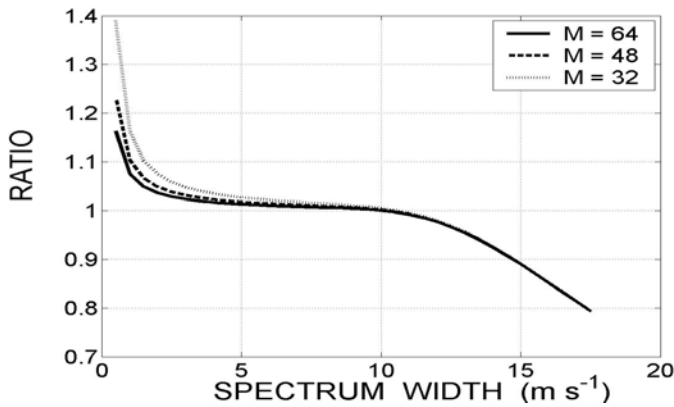

Fig. A1. Ratio $M_I/M\,\pi^{1/2}\,\sigma_{vn}$ for S-band radar with $T = 1$ ms.

Using approximation (A9) we can write the variance of the power estimates for the H or V channels as

$$\frac{<\delta P^2>}{S^2} = \frac{2SNR+1}{M\ SNR^2} + \frac{0.56}{M\sigma_{vn}},$$ (A10)

$$0.04 \leq \sigma_{vn} \leq 0.60 \ .$$

Representation (A10) is an explicit dependence of the variance on noise and narrowness of the spectrum.

The covariance $<\delta\hat{P}_h\delta\hat{P}_v>$ of the power perturbations is:

$$<\delta\hat{P}_h\delta\hat{P}_v>=<(\frac{1}{M}\sum e_m^{(h)}e_m^{(h)*}-P_h)(\frac{1}{M}\sum e_m^{(v)}e_m^{(v)*}-P_v)>=$$

$$<\frac{1}{M^2}\sum_{m,n=1}^{M} e_m^{(h)}e_m^{(h)*}e_n^{(v)}e_n^{(v)*}>-P_hP_v=\frac{1}{M^2}\sum_{m,n=1}^{M}<e_m^{(h)}e_m^{(h)*}><e_n^{(v)}e_n^{(v)*}>+$$

$$\frac{1}{M^2}\sum_{m,n=1}^{M}<e_m^{(h)}e_n^{(v)*}><e_m^{(h)*}e_n^{(v)}>-P_hP_v=\frac{1}{M^2}\sum_{m,n=1}^{M}<e_m^{(h)}e_n^{(v)*}><e_m^{(h)*}e_n^{(v)}>$$

For different polarizations, equation (A5) is written as

$$<e_n^{(h)}e_m^{(v)*}>=(S_hS_v)^{1/2}\rho_{co}\rho[(m-n)T]\exp[j\varphi_{dp}+j\pi v_n(m-n)],$$ (A11)

$$<e_n^{(h)}e_m^{(v)}>=<e_n^{(h)*}e_m^{(v)*}>=0,$$

where ρ_{co} is the copolar correlation coefficient and φ_{dp} is the differential phase. Using (A7) we obtain

$$\frac{<\delta\hat{P}_h\delta\hat{P}_v>}{S_hS_v}=\frac{\rho_{co}^2}{M_I}.$$ (A12)

We see that in contrast to the variance of the power, the covariance of the powers does not depend on noise and is a function of the spectrum width and ρ_{co} . Using approximation (A9) we can write the latter equation as

$$\frac{<\delta P_h\delta P_v>}{S_hS_v}=\frac{0.56\ \rho_{co}^2}{M\sigma_{vn}}.$$ (A13)

$$0.04 \leq \sigma_{vn} \leq 0.60.$$

The perturbation analysis has applicability limits. In this section, we have not used any assumption on values of power variations $\delta\hat{P}_h$ and $\delta\hat{P}_v$ so that equations (A6), (A8), and (A12) are exact expressions. In Fig. A2, the standard deviations of power (A6) are presented for different signal-to-noise ratios along with the simulation results, $SD(P)$ $= <\delta\hat{P}>^{1/2}$. One can see there are no discrepancies between calculated data and simulated results. For polarimetric variables which contain nonlinear dependences on the powers, we can expect deviations of calculated variances from simulation results because of the use of the perturbation approximations. As an example consider an estimate of a value that is reciprocal to the signal power, i.e., $\hat{y} = 1/(\hat{P} - N) = 1/\hat{S}$. Using the perturbation approximation we obtain for the standard deviation of the estimate

$$S < \delta\hat{y}^2 >^{1/2} = S\ SD(1/\hat{S}) = \frac{2SNR+1}{M\ SNR^2} + \frac{1}{M_I}, \qquad (A14)$$

which is similar to (A8). In Fig. A3, this standard deviations are shown for different SNR. We see deviations of the calculated data from the simulated results especially for narrow spectra. For $SNR = 5$ dB, these deviations exceed 10% so that if we want to obtain statistical properties with such accuracy we should be careful in interpreting results of the perturbation analysis for narrow spectra and/or for low SNR. In such cases, results of computer simulations are preferable because we usually use the perturbation expansions to second order of deviations and this limits applicability of the results. The main polarimetric variables are determined as ratios of the estimates; so we should expect deviations of calculated biases and standard deviations from simulation results especially for low SNR and for narrow spectra.
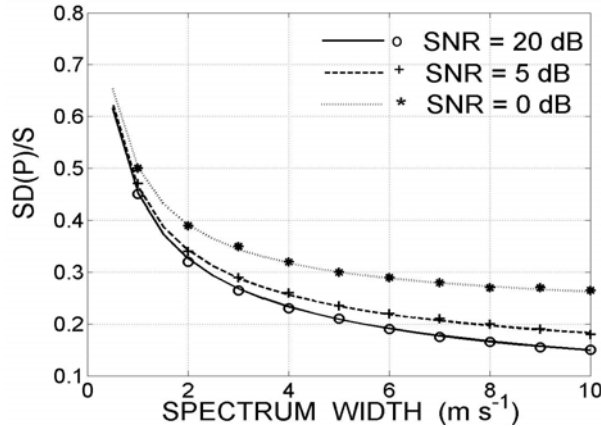

Fig. A2. Standard deviations of the power calculated
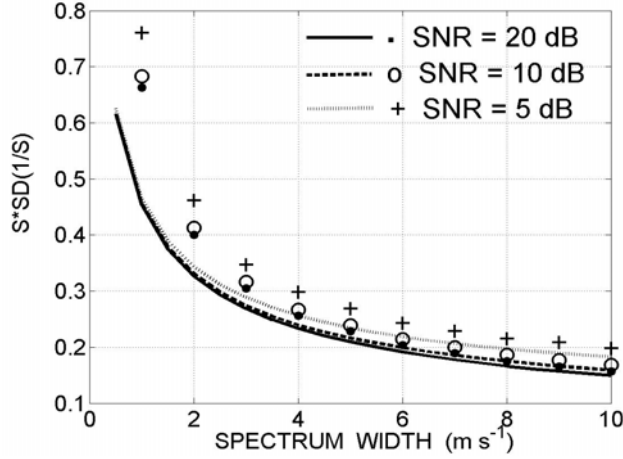via (A6) or (A8), the lines, and results of
computer simulations, the symbols.

Fig. A3. Standard deviations of the reciprocal signal power calculated via (A14), the lines, and the simulation results, the symbols.

Appendix B. Variances of correlations at lag 0

To calculate the variance of the differential phase (3.4), we consider the mean of the correlation function of the voltages in the H and V channels:

$$< \hat{R}_{co} > = \frac{1}{M} \sum_{m=1}^{M} < e_m^{(h)} e_m^{(v)*} > .$$ (B1)

Using (A11) we obtain

$$R_{co} = (S_h S_v)^{1/2} \rho_{co} \exp(j\varphi_{dp}) .$$ (B2)

The modulus of (B2) is

$$| R_{co} | = (S_h S_v)^{1/2} \rho_{co} .$$ (B3)

Now we have to calculate the mean of the modulus squared, i.e.,

$$< | \hat{R}_{co} |^2 > = \frac{1}{M^2} \sum_{m,n=1}^{M} < e_m^{(h)} e_m^{(v)*} e_n^{(h)*} e_n^{(v)} > =$$

$$\frac{1}{M^2} \sum_{m,n=1}^{M} [< e_m^{(h)} e_m^{(v)*} > < e_n^{(h)*} e_n^{(v)} > + < e_m^{(h)} e_n^{(h)*} > < e_m^{(v)*} e_n^{(v)} >]$$

67

Using (B2) and (A5) we obtain

$$<|\hat{R}_{co}|^2> = S_h S_v \rho_{co}^2 + \frac{(S_h + N_h)(S_v + N_v)}{M} + \frac{2 S_h S_v}{M^2} \sum_{n=1}^{M-1} (M-n) |\rho(nT)|^2 .$$

Expressing the latter sum via the number of independent samples (A9) we can write:

$$<|\hat{R}_{co}|^2> = S_h S_v \rho_{co}^2 + \frac{S_h N_v + S_v N_h + N_h N_v}{M} + \frac{S_h S_v}{M_I} , \quad (B4)$$

and the ratio of (B4) and (B3) squared is

$$\frac{<|\hat{R}_{co}|^2>}{|R_{co}|^2} = 1 + \frac{SNR_h + SNR_v + 1}{M \rho_{co}^2 SNR_h SNR_v} + \frac{1}{M_I \rho_{co}^2} . \quad (B5)$$

The mean of the correlation function squared that enters (3.4) is

$$< \hat{R}_{co}^2 > = \frac{1}{M^2} \sum_{m,n=1}^{M} < e_m^{(h)} e_m^{(v)*} e_n^{(h)} e_n^{(v)*} > =$$

$$\frac{1}{M^2} \sum_{m,n=1}^{M} [< e_m^{(h)} e_m^{(v)*} >< e_n^{(h)} e_n^{(v)*} > + < e_m^{(h)} e_n^{(v)*} >< e_m^{(v)*} e_n^{(h)} >]$$

Using (B2) and (A12) we obtain

$$< \hat{R}_{co}^2 > = S_h S_v \rho_{co}^2 \exp(j2\varphi_{dp}) + \frac{S_h S_v \rho_{co}^2 \exp(j2\varphi_{dp})}{M}$$

$$\frac{2 S_h S_v \rho_{co}^2 \exp(j2\varphi_{dp})}{M^2} \sum_{n=1}^{M-1} (M-n) |\rho(nT)|^2 \quad (B6)$$

The latter can be expressed via the number of independent samples M_I as

$$< \hat{R}_{co}^2 > = S_h S_v \rho_{co}^2 \exp(j2\varphi_{dp}) + \frac{S_h S_v \rho_{co}^2 \exp(j2\varphi_{dp})}{M_I}$$

and the needed ratio of this function over (B2) squared is

$$\frac{< \hat{R}_{co}^2 >}{R_{co}^2} = 1 + \frac{1}{M_I} . \quad (B7)$$

To calculate bias and standard deviations of the modulus of the correlation coefficient, the following values are needed:

$$\left(\frac{\delta\hat{P}_h}{S_h} + \frac{\delta\hat{P}_v}{S_v} \right) \mathrm{Re}\left(\frac{\delta\hat{R}_{co}}{R_{co}} \right) >, \qquad \frac{<|\delta\hat{R}_{co}|^2>}{|R_{co}|^2}, \qquad < \left[\mathrm{Re}\left(\frac{\delta\hat{R}_{co}}{R_{co}} \right) \right]^2 > . \qquad \text{(B8)}$$

We begin with the first term:

$$< \frac{\delta\hat{P}_h}{S_h} \mathrm{Re}\left(\frac{\delta\hat{R}_{co}}{R_{co}} \right) >=< \frac{\hat{P}_h - P_h}{S_h} \mathrm{Re}\left(\frac{\hat{R}_{co} - R_{co}}{R_{co}} \right) >=< \frac{\hat{P}_h}{S_h} \mathrm{Re}\left(\frac{\hat{R}_{co}}{R_{co}} \right) > -\frac{P_h}{S_h} =$$

$$\mathrm{Re}\frac{< \hat{P}_h \hat{R}_{co} >}{S_h R_{co}} - \frac{P_h}{S_h} . \qquad \text{(B9)}$$

From definitions (1.3), we write

$$< \hat{P}_h \hat{R}_{co} >= \frac{1}{M^2} \sum_{m,n=1}^{M} < e_m^{(h)} e_m^{(h)*} e_n^{(h)} e_n^{(v)*} >= .$$

$$\frac{1}{M^2} \sum_{m,n=1}^{M} [< e_m^{(h)} e_m^{(h)*} >< e_n^{(h)} e_n^{(v)*} > + < e_m^{(h)} e_n^{(v)*} >< e_m^{(h)*} e_n^{(h)} >] .$$

Using (A5) we can simplify the latter as

$$< \hat{P}_h \hat{R}_{co} >= P_h R_{co} + \frac{(S_h S_v)^{1/2} S_h \rho_{co} \exp(j\varphi_{dp})}{M^2} \sum_{m,n=1}^{M} | \rho(m-n) |^2 =$$

$$P_h R_{co} + \frac{(S_h S_v)^{1/2} (S_h + N_h) R_{co}}{M} + \frac{(S_h S_v)^{1/2} S_h R_{co}}{M^2} \sum_{m \neq n}^{M} | \rho(m-n) |^2 .$$

Using the definition of the number of independent samples (A9) we can simplify the latter further

$$< \hat{P}_h \hat{R}_{co} >= P_h R_{co} + \frac{1}{M \; SNR_h} + \frac{1}{M_I} .$$

For the denominator of (B9), we have

$$S_h R_{co} = S_h (S_h S_v)^{1/2} \rho_{co} \exp(j\varphi_{dp}) .$$

Substitution of the latter two equations into (B9) yields:

$$< \frac{\delta \hat{P}_h}{S_h} \mathrm{Re}\left(\frac{\delta \hat{R}_{co}}{R_{co}} \right) >= \frac{1}{M \; SNR_h} + \frac{1}{M_I}. \tag{B10}$$

For the vertical channel, we can write similarly:

$$< \frac{\delta \hat{P}_v}{S_v} \mathrm{Re}\left(\frac{\delta \hat{R}_{hv}}{R_{hv}} \right) >= \frac{1}{M \; SNR_v} + \frac{1}{M_I}. \tag{B11}$$

Now we calculate $< | \delta \hat{R}_{co} |^2 >$ that enters the second term in (B8). By definition, we write:

$$<| \delta \hat{R}_{co} |^2 > = < | \hat{R}_{co} - R_{co} |^2 > = < (\hat{R}_{co} - R_{co})(\hat{R}_{co}^* - R_{co}^*) > = < | \hat{R}_{co} |^2 > - | R_{co} |^2 .$$

The latter two terms were calculated earlier (see (B3) and (B4)). Substitution of those yields:

$$\frac{<| \delta \hat{R}_{co} |^2 >}{| R_{co} |^2} = \frac{SNR_h + SNR_v + 1}{M \; SNR_h \; SNR_v \rho_{co}^2} + \frac{1}{M_I \rho_{co}^2}. \tag{B12}$$

Now we calculate the third term in (B8), i.e.,

$$< \left[\mathrm{Re}\left(\frac{\delta \hat{R}_{co}}{R_{co}} \right) \right]^2 > = < \left[\mathrm{Re}\left(\frac{\hat{R}_{co} - R_{co}}{R_{co}} \right) \right]^2 > = < \left[\mathrm{Re}\left(\frac{\hat{R}_{co}}{R_{co}} \right) - 1 \right]^2 >$$

$$= < \left[\mathrm{Re}\left(\frac{\hat{R}_{co}}{R_{co}} \right) \right]^2 > - 1 .$$

Using identity (E2) we write

$$< \left[\mathrm{Re}\left(\frac{\hat{R}_{co}}{R_{co}} \right) \right]^2 > - 1 = \frac{1}{2} \mathrm{Re}\left(< \left| \frac{\hat{R}_{co}}{R_{co}} \right|^2 > + \frac{< \hat{R}_{co}^2 >}{R_{co}^2} \right) - 1 .$$

All needed terms in the latter equation were already calculated (see (B5) and (B7)) and substitution yields

$$< \left[\mathrm{Re}\left(\frac{\delta \hat{R}_{co}}{R_{co}} \right) \right]^2 >= \frac{SNR_h + SNR_v + 1}{2 M \rho_{co}^2 SNR_h SNR_v} + \frac{1 + \rho_{co}^2}{2 M_I \rho_{co}^2}. \tag{B13}$$

70

Appendix C. The variance and covariance of Doppler velocities
The Doppler velocity is calculated in one of the radar polarimetric channels, usually in the horizontal one. The Doppler velocity is obtained from the phase shift of the correlation function at lag 1 (Zrnic 1977) so that we can use (3.3) to calculate the variance of the velocity in say the horizontal channel,

$$< \delta V_h^2 > = \frac{v_a^2}{\pi^2} < \mathrm{Im}^2 \frac{\hat{R}_h(1)}{R_h(1)} >, \tag{C1}$$

where $\hat{R}_h(1)$ is the estimate of the correlation function at lag 1 in the H channel and $R_h(1)$ is its mean. By definition

$$\hat{R}_h(1) = \frac{1}{M-1} \sum_{m=1}^{M-1} e_m^{(h)} e_{m+1}^{(h)*} . \tag{C2}$$

Calculating the expectation of (C2), we obtain the mean value of the correlation function:

$$R_h(1) = S_h \rho(1) \exp(j\pi v_n) . \tag{C3}$$

We can represent (C1) as

$$< \delta V_h^2 > = \frac{v_a^2}{2\pi^2} \left[\frac{<|\hat{R}_h^2(1)|>}{|R_h(1)|^2} - \frac{<\hat{R}_h^2(1)>}{R_h(1)^2} \right]. \tag{C4}$$

Using definition (C2) we write

$$<|\hat{R}_h(1)|^2> = \frac{1}{(M-1)^2} \sum_{m,n=1}^{M-1} < e_m^{(h)} e_{m+1}^{(h)*} e_n^{(h)*} e_{n+1}^{(h)} > =$$

$$\frac{1}{(M-1)^2} \sum_{m,n=1}^{M-1} [< e_m^{(h)} e_{m+1}^{(h)*} >< e_n^{(h)*} e_{n+1}^{(h)} > + < e_m^{(h)} e_n^{(h)*} >< e_{m+1}^{(h)*} e_{n+1}^{(h)} >] =$$

$$|R_h(1)|^2 + \frac{2S_h N_h + N_h^2}{M-1} + \frac{S_h^2}{M_{I1}} =$$

$$S_h^2 \rho^2(1) \left[1 + \frac{2SNR_h + 1}{(M-1)\rho^2(1)SNR_h^2} + \frac{1}{M_{I1}\rho^2(1)} \right].$$

Then the needed ratio is

$$\frac{<|R_h(1)|^2>}{|R_h(1)|^2} = 1 + \frac{2SNR_h + 1}{(M-1)\rho^2(1)SNR_h^2} + \frac{1}{M_{I1}\rho^2(1)}, \tag{C5}$$

where M_{I1} is the number of independent samples (A7) for M-1 samples, i.e.,

$$M_{I1} = (M-1)\left(1 + 2\sum_{m=1}^{M-2}(1-m/M)|\rho(mT)|^2\right)^{-1}. \tag{C6}$$

To calculate the second term on the right hand side of (C4), we need to obtain

$$< \hat{R}_h^2(1) > = \frac{1}{(M-1)^2}\sum_{m,n=1}^{M-1}< e_m^{(h)}e_{m+1}^{(h)*}e_n^{(h)}e_{n+1}^{(h)*} > =$$

$$\frac{1}{(M-1)^2}\sum_{m,n=1}^{M-1}[< e_m^{(h)}e_{m+1}^{(h)*} >< e_n^{(h)}e_{n+1}^{(h)*} > + < e_m^{(h)}e_{n+1}^{(h)*} >< e_{m+1}^{(h)*}e_n^{(h)} >] =$$

$$R_h^2(1) + \frac{2S_h N_h \rho(2)}{M-1}\exp(2j\pi v / v_a) +$$

$$\frac{S_h^2}{(M-1)^2}\exp(2j\pi v / v_a)\sum_{m,n=1}^{M-1}\rho(m-n-1)\rho^*(m-n+1) =$$

$$R_h^2(1) + \frac{2S_h N_h \rho(2)}{M-1}\exp(2j\pi v_n) + \frac{S_h^2 \rho^2(1)}{M_{I1}}\exp(2j\pi v_n). \tag{C7}$$

The mean correlation coefficient squared is

$$R_h^2(1) = S_h^2 \rho^2(1)\exp(2j\pi v_n). \tag{C8}$$

For Gaussian spectra, we have $\rho(2) = \rho^4(1)$, and the ratio can be written as:

$$\frac{< \hat{R}_h^2(1) >}{R_h^2(1)} = 1 + \frac{2\rho^2(1)}{(M-1)SNR_h} + \frac{1}{M_{I1}}. \tag{C9}$$

Using (C3), (C5), and (C9) we obtain for the variance of the Doppler velocity

$$< \delta V_h^2 > = \frac{v_a^2}{2\pi^2\rho^2(1)}\left[\frac{2SNR_h[1-\rho^2(1)]+1}{(M-1)SNR_h^2} + \frac{1-\rho^2(1)}{M_{I1}}\right]. \tag{C10}$$

A similar expression holds for the variance of the Doppler velocity in the vertical channel

$$< \delta V_v^2 >= \frac{v_a^2}{2\pi^2\rho^2(1)}\left[\frac{2SNR_v[1-\rho^2(1)]+1}{(M-1)SNR_v^2}+\frac{1-\rho^2(1)}{M_{I1}}\right]. \qquad (C11)$$

Equations (C10) and (C11) are in accord with equation (9) by Zrnic 1977 if we replace M-1 pairs in (C10) with M and neglect the $\rho(2)/M^2$ term in equation (9) as $(1/M)^2$ value.

Now let's calculate the covariance of the Doppler velocities measured in the H and V channels:

$$< \delta V_h \delta V_v >= \frac{v_a^2}{\pi_2} < \operatorname{Im}\frac{\hat{R}_h(1)}{R_h(1)}\operatorname{Im}\frac{\hat{R}_v(1)}{R_v(1)}>=$$

$$-\frac{v_a^2}{4\pi^2} < \left(\frac{\hat{R}_h(1)}{R_h(1)}-\frac{\hat{R}_h^*(1)}{R_h^*(1)}\right)\left(\frac{\hat{R}_v(1)}{R_v(1)}-\frac{\hat{R}_v^*(1)}{R_v^*(1)}\right)> . \qquad (C12)$$

It follows from (C12) that we have to calculate the following correlations:

$$\frac{< \hat{R}_h(1)}{R_h(1)}\frac{\hat{R}_v(1) >}{R_v(1)}, \qquad \frac{< \hat{R}_h(1)}{R_h(1)}\frac{\hat{R}_v^*(1) >}{R_v^*(1)}. \qquad (C13)$$

We calculate the first one:

$$< \hat{R}_h(1)\hat{R}_v(1) >= \frac{1}{(M-1)^2}\sum_{m,n=1}^{M-1}< e_m^{(h)}e_{m+1}^{(h)*}e_n^{(v)}e_{n+1}^{(v)*} >=$$

$$R_h(1)R_v(1)+\frac{1}{(M-1)^2}\sum_{m,n=1}^{M-1}< e_m^{(h)}e_{n+1}^{(v)*} >< e_{m+1}^{(h)*}e_n^{(v)} >=$$

$$R_h(1)R_v(1)+\frac{S_hS_v\rho_{co}^2\exp(2j\pi v/v_a)}{(M-1)^2}\sum_{m,n=1}^{M-1}\rho(m-n-1)\rho(m-n+1)$$

The corresponding mean values are

$$R_h(1) = S_h\exp(j\pi v/v_a)\rho(1), \quad R_v(1) = S_v\exp(j\pi v/v_a)\rho(1). \qquad (C14)$$

Using the latter three equations, we obtain the first term in (C13):

$$\frac{< \hat{R}_h(1)}{R_h(1)}\frac{\hat{R}_v(1) >}{R_v(1)} = 1+\frac{\rho_{co}^2}{(M-1)^2\rho^2(1)}\sum_{m,n=1}^{M-1}\rho(m-n-1)\rho(m-n+1) = 1+\frac{\rho_{co}^2}{M_{I1}}. \quad (C15)$$

For the second term in (C13), we write

$$< \hat{R}_h(1) \hat{R}_v^*(1) > = \frac{1}{(M-1)^2} \sum_{m,n=1}^{M-1} < e_m^{(h)} e_{m+1}^{(h)*} e_n^{(v)*} e_{n+1}^{(v)} > =$$

$$R_h(1) R_v^*(1) + \frac{1}{(M-1)^2} \sum_{m,n=1}^{M-1} < e_m^{(h)} e_n^{(v)*} > < e_{m+1}^{(h)*} e_{n+1}^{(v)} > =$$

$$R_h(1) R_v^*(1) + \frac{S_h S_v \rho_{co}^2}{(M-1)^2} \sum_{m,n=1}^{M-1} \rho^2(m-n) = R_h(1) R_v^*(1) + \frac{S_h S_v \rho_{co}^2}{M_{I1}}.$$

Using (C14) we obtain:

$$\frac{< \hat{R}_h(1)}{R_h(1)} \frac{\hat{R}_v^*(1) >}{R_v^*(1)} = 1 + \frac{\rho_{co}^2}{M_{I1} \rho^2(1)}. \tag{C16}$$

Substitution (C15) and (C16) into (C12) yields

$$< \delta V_h \, \delta V_v > = \frac{v_a^2}{\pi^2} \frac{\rho_{co}^2[1-\rho^2(1)]}{2 M_{I1} \rho^2(1)}. \tag{C17}$$

where M_{II} is determined by (C6).

Appendix D. Variances of correlations at lag 1

To calculate the standard deviation of the modulus of the correlation coefficient ρ_{co} determined as a ratio of the correlation functions at lags 0 and 1, we need the following mean values

$$\mathrm{Re}\frac{<|\hat{R}_{co1}(1)|^2>}{|R_{co1}(1)|^2}, \quad \mathrm{Re}\frac{<\hat{R}_{co1}^2(1)>}{R_{co1}^2(1)}, \quad \mathrm{Re}\frac{<\hat{R}_{co1}(1)\hat{R}_h(1)>}{R_{co1}(1)R_h(1)}, \quad \mathrm{Re}\frac{<\hat{R}_{co1}(1)\hat{R}_h^*(1)>}{R_{co1}(1)R_h^*(1)},$$

$$\mathrm{Re}\frac{<\hat{R}_{co1}(1)\hat{R}_v(1)>}{R_{co1}(1)R_v(1)}, \quad \mathrm{Re}\frac{<\hat{R}_{co1}(1)\hat{R}_v^*(1)>}{R_{co1}(1)R_v^*(1)}, \quad \mathrm{Re}\frac{<\hat{R}_{co2}(1)\hat{R}_h(1)>}{R_{co2}(1)R_h(1)}, \quad \mathrm{Re}\frac{<\hat{R}_{co2}(1)\hat{R}_h^*(1)>}{R_{co2}(1)R_h^*(1)},$$

$$\mathrm{Re}\frac{<|\hat{R}_{co2}(1)|^2>}{|R_{co2}(1)|^2}, \quad \mathrm{Re}\frac{<\hat{R}_{co2}^2(1)>}{R_{co2}^2(1)}, \quad \mathrm{Re}\frac{<\hat{R}_{co2}(1)\hat{R}_v(1)>}{R_{co2}(1)R_v(1)}, \quad \mathrm{Re}\frac{<\hat{R}_{co2}(1)\hat{R}_v^*(1)>}{R_{co2}(1)R_v^*(1)},$$

$$\mathrm{Re}\frac{<\hat{R}_{co1}(1)\hat{R}_{co2}(1)>}{R_{co1}(1)R_{co2}(1)}, \quad \mathrm{Re}\frac{<\hat{R}_{co1}(1)\hat{R}_{co2}^*(1)>}{R_{co1}(1)R_{co2}^*(1)}. \tag{D1}$$

The first term in (D1) can be calculated as follows:

$$< | \hat{R}_{col}(1) |^2 > = \frac{1}{(M-1)^2} \sum < e_m^{(h)} e_{m+1}^{(v)*} e_n^{(h)*} e_{n+1}^{(v)} > =$$

$$| R_{col}(1) |^2 + \frac{1}{(M-1)^2} \sum < e_m^{(h)} e_n^{(h)*} > < e_{m+1}^{(v)*} e_{n+1}^{(v)} > =$$

$$| R_{col}(1) |^2 + \frac{S_h N_v + S_v N_h + N_h N_v}{M-1} + \frac{S_h S_v}{(M-1)^2} \sum_{m,n=1}^{M-1} | \rho(m-n) |^2 =$$

$$| R_{col}(1) |^2 + \frac{S_h N_v + S_v N_h + N_h N_v}{M-1} + \frac{S_h S_v}{M_{I1}} . \tag{D2}$$

Corresponding mean value of the module is

$$| R_{col}(1) |^2 = S_h S_v \rho_{co}^2 \rho^2(1) \tag{D3}$$

and we obtain needed ratio:

$$\frac{< | R_{col}(1) |^2 >}{| R_{col}(1) |^2} = 1 + \frac{SNR_h + SNR_v + 1}{(M-1)SNR_h SNR_v \rho_{co}^2 \rho^2(1)} + \frac{1}{M_{I1} \rho_{co}^2 \rho^2(1)} . \tag{D4}$$

The second mean in (D1) can be obtained calculating the following:

$$< \hat{R}_{col}(1)^2 > = \frac{1}{(M-1)^2} \sum < e_m^{(h)} e_{m+1}^{(v)*} e_n^{(h)} e_{n+1}^{(v)*} > =$$

$$R_{col}^2(1) + \frac{1}{(M-1)^2} \sum < e_m^{(h)} e_{n+1}^{(v)*} > < e_{m+1}^{(v)*} e_n^{(h)} > =$$

$$R_{col}^2(1) + \frac{S_h S_v \rho_{co}^2 \exp(2j\varphi_{dp} + 2j\pi v/v_a)}{(M-1)^2} \sum_{m,n=1}^{M-1} \rho(m-n-1)\rho(m-n+1) =$$

$$R_{col}^2(1) + \frac{S_h S_v \rho_{co}^2 \exp(2j\varphi_{dp} + 2j\pi v/v_a)\rho^2(1)}{M_{I1}} . \tag{D5}$$

The mean correlation function in the latter equation is

$$R_{col}^2(1) = S_h S_v \rho_{co}^2 \rho^2(1) \exp(2j\varphi_{dp} + 2j\pi v/v_a) \tag{D6}$$

and needed ratio is

$$\frac{<R_{col}^2(1)>}{R_{col}^2(1)} = 1 + \frac{1}{M_{I1}} . \tag{D7}$$

Now we calculate the third mean in (D1):

$$< \hat{R}_{col}(1)\hat{R}_h(1) >= \frac{1}{(M-1)^2} \sum_{m,n=1}^{M-1} < e_m^{(h)} e_{m+1}^{(v)*} e_n^{(h)} e_{n+1}^{(h)*} >=$$

$$R_{col}(1)R_h(1) + \frac{1}{(M-1)^2} \sum_{m,n=1}^{M-1} < e_m^{(h)} e_{n+1}^{(h)*} >< e_{m+1}^{(v)*} e_n^{(h)} >=$$

$$R_{col}(1)R_h(1) + \frac{(S_h S_v)^{1/2} N_h \rho_{co} \exp(j\varphi_{dp} + 2j\pi v/v_a)\rho^2(1)}{(M-1)} +$$

$$+ \frac{S_h (S_h S_v)^{1/2} \exp(j\varphi_{dp} + 2j\pi v/v_a)\rho(2)\rho_{co}\rho^2(1)}{M_{I1}} . \tag{D8}$$

The product of the mean correlation functions in the latter equation is

$$R_{col}(1)R_h(1) = S_h (S_h S_v)^{1/2} \exp(j\varphi_{dp} + 2j\pi v/v_a)\rho^2(1)\rho_{co} \tag{D9}$$

and we obtain

$$\frac{<\hat{R}_{col}(1)\hat{R}_h(1)>}{R_{co}1(1)R_h(1)} = 1 + \frac{\rho^2(1)}{(M-1)SNR_h} + \frac{1}{M_{I1}} . \tag{D10}$$

The fourth term in (D1) is calculated as

$$< \hat{R}_{col}(1)\hat{R}_h^*(1) >= \frac{1}{(M-1)^2} \sum_{m,n=1}^{M-1} < e_m^{(h)} e_{m+1}^{(v)*} e_n^{(h)*} e_{n+1}^{(h)} >=$$

$$R_{col}(1)R_h^*(1) + \frac{1}{(M-1)^2} \sum_{m,n=1}^{M-1} < e_m^{(h)} e_n^{(h)*} >< e_{m+1}^{(v)*} e_{n+1}^{(h)} >=$$

$$R_{co1}(1)R_h^*(1) + \frac{(S_h S_v)^{1/2} N_h \rho_{co} \exp(j\varphi_{dp})}{M-1} + \frac{S_h (S_h S_v)^{1/2} \exp(j\varphi_{dp}) \rho_{co}}{M_{I1}}.$$

The product of the mean correlation functions in the latter equation is

$$R_{co1}(1)R_h^*(1) = S_h (S_h S_v)^{1/2} \exp(j\varphi_{dp}) \rho^2(1) \rho_{co}, \qquad (D11)$$

and we obtain needed ratio as

$$\frac{< \hat{R}_{co1}(1)\hat{R}_h^*(1) >}{R_{co1}(1)R_h^*(1)} = 1 + \frac{1}{(M-1)SNR_h \rho^2(1)} + \frac{1}{M_{I1} \rho^2(1)}. \qquad (D12)$$

Fifth and sixth terms in (D1) can be calculated similarly and we write the final expressions:

$$\frac{< \hat{R}_{co1}(1)\hat{R}_v(1) >}{R_{co1}(1)R_v(1)} = 1 + \frac{\rho^2(1)}{(M-1)SNR_v} + \frac{1}{M_{I1}}. \qquad (D13)$$

$$\frac{< \hat{R}_{co1}(1)\hat{R}_v^*(1) >}{R_{co1}(1)R_v(1)} = 1 + \frac{1}{(M-1)SNR_v \rho^2(1)} + \frac{1}{M_{I1} \rho^2(1)}. \qquad (D14)$$

To obtain the seventh term in (D1), we have to calculate the following:

$$< \hat{R}_{co2}(1)\hat{R}_h(1) > = \frac{1}{(M-1)^2} \sum_{m,n=1}^{M-1} < e_{m+1}^{(h)} e_m^{(v)*} e_n^{(h)} e_{n+1}^{(h)*} > =$$

$$R_{co2}(1)R_h(1) + \frac{1}{(M-1)^2} \sum_{m,n=1}^{M-1} < e_{m+1}^{(h)} e_{n+1}^{(h)*} > < e_m^{(v)*} e_n^{(h)} > =$$

$$R_{co2}(1)R_h(1) + \frac{(S_h S_v)^{1/2} N_h \rho_{co} \exp(j\varphi_{dp})}{M-1} + \frac{S_h (S_h S_v)^{1/2} \exp(j\varphi_{dp}) \rho_{co}}{M_{I1}}.$$

The mean product is:

$$R_{co2}(1)R_h(1) = S_h (S_h S_v)^{1/2} \exp(j\varphi_{dp}) \rho^2(1) \rho_{co}. \qquad (D15)$$

Thus needed ratio is:

$$\frac{<\hat{R}_{co2}(1)\hat{R}_h(1)>}{R_{co2}(1)R_h(1)} = 1 + \frac{1}{(M-1)SNR_h\rho^2(1)} + \frac{1}{M_{I1}\rho^2(1)}. \tag{D16}$$

The eighth term in (D1) can be calculated as

$$<\hat{R}_{co2}(1)\hat{R}_h^*(1)> = \frac{1}{(M-1)^2}\sum_{m,n=1}^{M-1}<e_{m+1}^{(h)}e_m^{(v)*}e_n^{(h)*}e_{n+1}^{(h)}> =$$

$$R_{co2}(1)R_h^*(1) + \frac{1}{(M-1)^2}\sum_{m,n=1}^{M-1}<e_{m+1}^{(h)}e_n^{(h)*}><e_m^{(v)*}e_{n+1}^{(h)}> = R_{co2}(1)R_h^*(1) +$$

$$\frac{(S_hS_v)^{1/2}N_h\rho_{co}\rho(2)\exp(j\varphi_{dp}-2j\pi v/v_a)}{M-1} + \frac{S_h(S_hS_v)^{1/2}\exp(j\varphi_{dp}-2j\pi v/v_a)\rho_{co}\rho^2(1)}{M_{I1}}.$$

The mean product is:

$$R_{co2}(1)R_h^*(1) = S_h(S_hS_v)^{1/2}\exp(j\varphi_{dp}-2j\pi v/v_a)\rho^2(1)\rho_{co}, \tag{D17}$$

and needed ratio becomes:

$$\frac{<\hat{R}_{co2}(1)\hat{R}_h^*(1)>}{R_{co2}(1)R_h^*(1)} = 1 + \frac{\rho^2(1)}{(M-1)SNR_h} + \frac{1}{M_{I1}}. \tag{D18}$$

In the latter equation, we used $\rho(2) = \rho^4(1)$ for the Gaussian spectral shape.

The twelfth and thirteenth terms in (D1) can be calculated like (D16) and (D17), and the result is:

$$\frac{<\hat{R}_{co2}(1)\hat{R}_v(1)>}{R_{co2}(1)R_v(1)} = 1 + \frac{1}{(M-1)SNR_v\rho^2(1)} + \frac{1}{M_{I1}\rho^2(1)}. \tag{D19}$$

$$\frac{<\hat{R}_{co2}(1)\hat{R}_v^*(1)>}{R_{co2}(1)R_v^*(1)} = 1 + \frac{\rho^2(1)}{(M-1)SNR_v} + \frac{1}{M_{I1}}. \tag{D20}$$

The ninth and tenth terms in (D1) can be obtained similarly to (D4) and (D7):

$$\frac{<|R_{co2}(1)|^2>}{|R_{co2}(1)|^2} = 1 + \frac{SNR_h + SNR_v + 1}{(M-1)SNR_hSNR_v\rho_{co}^2\rho^2(1)} + \frac{1}{M_{I1}\rho_{co}^2\rho^2(1)}, \tag{D21}$$

$$\frac{< R^2_{co2}(1) >}{R^2_{co2}(1)} = 1 + \frac{1}{M_{I1}}. \qquad (D22)$$

The rest two terms in (D1) can be obtained calculating the following:

$$< \hat{R}_{co1}(1)\hat{R}_{co2}(1) >= \frac{1}{(M-1)^2} \sum < e^{(h)}_m e^{(v)*}_{m+1} e^{(h)}_{n+1} e^{(v)*}_n >=$$

$$R_{co1}(1)R_{co2}(1) + \frac{1}{(M-1)^2} \sum < e^{(h)}_m e^{(v)*}_n >< e^{(h)}_{m+1} e^{(v)*}_{n+1} >=$$

$$R_{co1}(1)R_{co2}(1) + \frac{S_h S_v \rho^2_{co} \exp(2j\varphi_{dp})}{M_{I1}}$$

The mean product in the latter equation is:

$$R_{co1}(1)R_{co2}(1) = S_h S_v \rho^2_{co} \rho^2(1) \exp(2j\varphi_{dp}),$$

and needed ratio can be represented as:

$$\frac{< \hat{R}_{co1}(1)\hat{R}_{co2}(1) >}{R_{co1}(1)R_{co2}(1)} = 1 + \frac{1}{M_{I1}\rho^2(1)}. \qquad (D23)$$

The last ratio in (D1) is obtained by calculating the following:

$$< \hat{R}_{co1}(1)\hat{R}^*_{co2}(1) >= \frac{1}{(M-1)^2} \sum < e^{(h)}_m e^{(v)*}_{m+1} e^{(h)*}_{n+1} e^{(v)}_n >=$$

$$R_{co1}(1)R^*_{co2}(1) + \frac{1}{(M-1)^2} \sum < e^{(h)}_m e^{(h)*}_{n+1} >< e^{(v)*}_{m+1} e^{(v)}_n >=$$

$$R_{co1}(1)R^*_{co2}(1) + \frac{S_v N_h \rho(2)\exp(2j\pi v/v_a)}{M-1} + \frac{S_h N_v \rho(2)\exp(2j\pi v/v_a)}{M-1} + \frac{S_h S_v \rho^2(1)\exp(2j\pi v/v_a)}{M_{I1}}.$$

The mean product in the latter equation is:

$$R_{co1}(1)R^*_{co2}(1) = S_h S_v \rho^2_{co} \rho^2(1) \exp(2j\pi v/v_a), \qquad (D24)$$

and needed ratio can be represented as:

$$\frac{<\hat{R}_{co1}(1)\hat{R}_{co2}^{*}(1)>}{R_{co1}(1)R_{co2}^{*}(1)} = 1 + \frac{\rho^{2}(1)}{(M-1)SNR_{h}\rho_{co}^{2}} + \frac{\rho^{2}(1)}{(M-1)SNR_{v}\rho_{co}^{2}} + \frac{1}{M_{I1}\rho_{co}^{2}}. \quad \text{(D25)}$$

To arrive to the latter expression, we used the following equation: $\rho(2) = \rho^{4}(1)$ that holds for Gaussian shaped spectra.

Appendix E. Identities and approximations

For any complex a and b the following holds:

$$\operatorname{Re}(a)\operatorname{Re}(b) = \frac{1}{2}\operatorname{Re}(ab) + \frac{1}{2}\operatorname{Re}(ab^{*}), \quad \text{(E1)}$$

and from the latter we obtain:

$$\operatorname{Re}^{2}(a) = \frac{1}{2}\operatorname{Re}(a^{2}) + \frac{1}{2}|a|^{2}. \quad \text{(E2)}$$

For $x \ll 1$, the following representations were used in the report in applications of the perturbation analysis:

$$\frac{1}{1+x} \approx 1 - x + x^{2}, \quad \text{(E3)}$$

$$|1+x| \approx 1 + \operatorname{Re}(x) + \frac{1}{4}|x|^{2} - \frac{1}{4}\operatorname{Re}(x^{2}). \quad \text{(E4)}$$

$$\frac{1}{|1+x|} \approx 1 - \operatorname{Re}(x) + \frac{1}{4}|x|^{2} + \frac{3}{4}\operatorname{Re}(x^{2}). \quad \text{(E5)}$$

$$\frac{1}{\sqrt{1+x}} \approx 1 - \frac{1}{2}x + \frac{3}{8}x^{2}. \quad \text{(E6)}$$

$$\frac{1}{\sqrt{|1+x|}} \approx 1 - \frac{1}{2}\operatorname{Re}(x) + \frac{1}{16}|x|^{2} + \frac{5}{16}\operatorname{Re}(x^{2}). \quad \text{(E7)}$$

References

Bringi, V. N. and V. Chandrasekar, 2001: *Polarimetric Doppler Weather Radar. Principles and Applications.* Cambridge University Press. 636 pp.

Bringi, V. N. T.A. Seliga, and S.M. Cherry, 1983: Statistical properties of the dual-polarization differential reflectivity (Zdr) radar signals. *IEEE Trans. Geosci. Remote Sens.*, **21**, 215-220.

Chandrasekar, V., V. N. Bringi, P.J. Brockwell 1986: Statistical properties of dual-polarized radar signals. 23-rd Conf. Radar Meteorol., AMS, Boston, 193-196.

Chandrasekar, V., and V. N. Bringi, 1988: Error structure of multiparameter radar and surface measurements of rainfall. Part I: Differential reflectivity. *J. Atmos. Oceanic Technol,* **5**, 783-795.

Doviak, R.J., V. Bringi, A. Ryzhkov, A. Zahrai, D. Zrnic. 2000. Considerations for polarimetric upgrades to operational WSR-88D radars. J. Atmos. Oceanic Technol. **17**, 257 – 278.

Doviak, R. J. and D. S. Zrnic, 1993: *Doppler radar and weather observations*, 2nd ed., Academic Press, 562 pp.

Doviak, R. J. and D. S. Zrnic, 1998: NOAA/NSSL WSR-88D radar for research and enhancement of operations: Polarimetric upgrade to improve rainfall measurements. NSSL interim report. 110 pp.

Fabry, F. 2001: Using radars as radiometers: promises and pitfalls. 30-th Conf. Radar Meteorol., AMS, Boston, 197-198.

Fang, M. and R. J. Doviak, 2001: Spectrum width statistics of various weather phenomena. *NSSL report*. 62 pp.

Fang, M., R. J. Doviak, and V. Melnikov, 2004: Spectrum width measured by WSR-88D radar. . *J. Atmos. Oceanic Technol*. **21.**

Illingworth, A., 2004. Improved precipitation rates and data quality by using polarimetric measurements. In "*Weather Radar. Principles and Advanced Applications*". Springer. 337 pp.

Papoulis, A. 1965: *Probability, Random Variables, and Stochastic Processes*. McGrow-Hill, 583 pp.

Ryzhkov, A., and D. Zrnic, 1995: Precipitation and attenuation measurements at a 10-cm wavelength. J. Applied Meteorol**., 34**, 2121 -2134.

Ryzhkov, A.**,** and D. Zrnic, 1998a: Discrimination between rain and snow with a polarimetric radar. *Journal of Applied Meteorology*, **37**, 1228-1240.

Ryzhkov, A., D. Zrnic and B. Gordon, 1998b: Polarimetric method for ice water content determination. *Journal of Applied Meteorology,* **37**, 125-134.

Ryzhkov, A.**,** and D. Zrnic, 1998c: Polarimetric rainfall estimation in the presence of anomalous propagation. J. Atmos. Oceanic Technol. **15**, 1320 – 1330.

Sachidananda, M. and D. S. Zrnic. 1985: Z measurement considerations for a fast scan capability radar. *Radio Science*. **20**, 907 - 922.

Sachidananda, M. and D. S. Zrnic, 1986: Differential propagation phase shift and rainfall estimation. *Radio Science*. **21**, 235-247.

Sirmans D., R. Guenter, J. Winds. Engineering study of spectrum width anomaly. NEXRAD, Report of the Operational Support Facility, 1997, 11 pp.

Torlachi E. and Y. Gingras, 2003: Standard deviation of the copolar correlation

coefficient for simultaneous transmission and reception of vertical and horizontal polarized weather radar signals. *J. Atmos. Oceanic Technol*. **20**, 760 – 766.

Torlachi E. and I. Zawadzki, 2003: The effect of mean and differential attenuation on the precision and accuracy of the estimates of reflectivity and differential reflectivity. *J. Atmos. Oceanic Technol*. **20**, 362 – 371.

Unal C.M.H., D.N. Moiseev, F.J.Yanovsky, H.W.J. Russchenberg 2001: Radar Doppler polarimetry applied to precipitation measurements: Introduction of the spectral differential reflectivity 30-th Conf. Radar Meteorol. AMS, Boston, 316-318.

Whalen, A.D., 1971. *Detection of signals in noise*. Academic Press. 411 pp.

Zrnic D.S., 1977. Spectral moment estimates from correlated pulse pairs. *IEEE Trans. on Aerospace and Elctron. Systems*, **AES-13**, 344 – 354.

LIST OF NSSL REPORTS FOCUSED ON POSSIBLE UPGRADES
TO THE WSR-88D RADARS

Bachman S., 2004: Analysis of Doppler spectra obtained with WSR-88D radar from, non-stormy environment. NOAA/NSSL Report, 86 pp.

Torres S., D. Zrnic, and Y. Dubel, 2003: Signal Design and Processing Techniques for WSR-88D Ambiguity Resolution: Phase coding and staggered PRT, implementation, data collection, and processing. NOAA/NSSL Report, Part 7, 128 pp.

Schuur, T., P. Heinselman, and K. Scharfenberg, 2003: Overview of the Joint Polarization Experiment (JPOLE), NOAA/NSSL Report, 38 pp.

Ryzhkov, A, 2003: Rainfall Measurements with the Polarimetric WSR-88D Radar, NOAA/NSSL Report, 99 pp.

Schuur, T., A. Ryzhkov, and P. Heinselman, 2003: Observations and Classification of echoes with the Polarimetric WSR-88D radar, NOAA/NSSL Report, 45 pp.

Melnikov, V. M, D. S. Zrnic, R. J. Doviak, and J. K. Carter, 2003: Calibration and Performance Analysis of NSSL's Polarimetric WSR-88D, NOAA/NSSL Report, 77 pp.

NCAR-NSSL Interim Report, 2003: NEXRAD Range-Velocity Ambiguity Mitigation SZ(8/64) Phase Coding Algorithm Recommendations.

Sachidananda, M., 2002: Signal Design and Processing Techniques for WSR-88D Ambiguity Resolution, NOAA/NSSL Report, Part 6, 57 pp.

Doviak, R. J., J. Carter, V. Melnikov, and D.S. Zrnic, 2002: Modifications to the Research WSR-88D to obtain Polarimetric Data, NOAA/NSSL Report, 49 pp.

Fang, M., and R. J. Doviak, 2001: Spectrum width statistics of various weather phenomena, NOAA/NSSL Report, 62 pp.

Sachidananda, M., 2001: Signal Design and Processing Techniques for WSR-88D Ambiguity Resolution, NOAA/NSSL Report, Part 5, 75 pp.

Sachidananda, M., 2000: Signal Design and Processing Techniques for WSR-88D Ambiguity Resolution, NOAA/NSSL Report, Part 4, 99 pp.

Sachidananda, M., 1999: Signal Design and Processing Techniques for WSR-88D Ambiguity Resolution, NOAA/NSSL Report, Part 3, 81 pp.

Sachidananda, M., 1998: Signal Design and Processing Techniques for WSR-88D Ambiguity Resolution, NOAA/NSSL Report, Part 2, 105 pp.

Torres, S., 1998: Ground Clutter Canceling with a Regression Filter, NOAA/NSSL Report, 37 pp.

Doviak, R. J. and D. S. Zrnic, 1998**:** WSR-88D Radar for Research and Enhancement of Operations: Polarimetric Upgrades to Improve Rainfall Measurements, NOAA/NSSL Report, 110 pp.

Sachidananda, M., 1997**:** Signal Design and Processing Techniques for WSR-88D Ambiguity Resolution, NOAA/NSSL Report, Part 1, 100 pp.

Sirmans, D., D. S. Zrnic, and M. Sachidananda, 1986**:** Doppler radar dual polarization considerations for NEXRAD, NOAA/NSSL Report, Part I, 109 pp.

Sirmans, D., D. S. Zrnic, and N. Balakrishnan, 1986**:** Doppler radar dual polarization considerations for NEXRAD, NOAA/NSSL Report, Part II, 70 pp.